Editorial Team

JAEHR
Journal of Advances in Environmental Health Research
Environmental Health Research Center
دارای امتیاز علمی- پژوهشی از کمیسیون نشریات علوم پزشکی کشور
Kurdistan University of Medical Sciences
eISSN: 2345-3990

Information for Authors

AIM AND SCOPE

*Journal of Advances in Environmental Health Research (JAEHR)*is a quarterly peer-reviewed scientific journal published by Kurdistan University of Medical Sciences. The manuscripts on the topic of environmental science and engineering will be published in this journal. This contains all aspects of solid waste management, air pollution, water and wastewater, environmental monitoring and modeling, innovative technologies and studies related to the environmental science.

Instruction to Authors

MANUSCRIPTS

Manuscripts containing original material are accepted for consideration if neither the article nor any part of its essential substance, tables, or figures has been or will be published or submitted elsewhere before appearing in the *Journal of Advances in Environmental Health Research*. This restriction does not apply to abstracts or press reports published in connection with scientific meetings. Copies of any closely related manuscripts must be submitted along with the manuscript that is to be considered by the *Journal of Advances in Environmental Health Research*. Authors of all types of articles should follow the general instructions given below.

HUMAN AND ANIMAL RIGHTS

The research involves human beings or animals must adhere to the principles of the Declaration of Helsinki (http://www.wma.net/e/ethicsunit/helsinki.htm).

Types of Articles

- *Original article* which reports the results of an original scientific research should be less than 4000 words.
- *Review article* which represents the researches and works on a particular topic.
- *Brief communication* is a short research article and should be limited to 1500 words. This article contains all sections of an original article.
- *Case report* is a detailed report of an individual patient that may represent a previously non-described condition and contains new information about different aspects of a disease. It should be less than 2000 words.
- *Letter to the Editor* must be less than 400 words in all cases.
- *Book Review* must be less than 1000 words on any book topics related to the scope of *Journal of Advances in Environmental Health Research*.

SUBMISSION

- Only online submission is acceptable. Please submit online at: http://www.jaehr.muk.ac.ir
- This manuscripts should be divided into the following sections: (1) Title page, (2) Abstract and Keywords, (3) Introduction, (4) Materials and Methods, (5) Results and Discussion, (6) Acknowledgements, (7) Author contribution, (8) References, (9) Figure legends, (10) Tables and (11) Figures (figures should be submitted in separate files if the file size exceeds 2 Mb).
- Please supply a word count in title page.
- Use normal page margins (2.5 cm), and double-space throughout the manuscript.
- Use Times New Roman (12) font throughout the manuscript.
- Prepare your manuscript text using a Word processing package (save in .doc or .rtf format). Submissions of text in the form of PDF files are not permitted.

COVER LETTER

A covering letter signed by all authors should identify the corresponding author (include the address, telephone number, fax number, and e-mail address). Please make clear that the final manuscript has been seen and approved by all authors, and that the authors accept full responsibility for the design and conduct of the study, had access to the data, and controlled the decision to publish.
Authors are also asked to provide the names and contact information for three potential reviewers in their cover letter. However, the journal is not obliged to use the suggested reviewers. Final selection of reviewers will be determined by the editors.

AUTHORSHIP

As stated in the Uniform Requirements for Manuscripts Submitted to Biomedical Journals (http://www.icmje.org/icmje-recommendations.pdf), credit for authorship requires substantial contributions to: 1. Substantial contributions to the conception or design of the work; or the acquisition, analysis, or interpretation of data for the work; AND 2. Drafting the work or revising it critically for important intellectual content; AND 3. Final approval of the version to be published; AND 4. Agreement to be accountable for all aspects of the work in ensuring that questions related to the accuracy or integrity of any part of the work are appropriately investigated and resolved. Each author must sign authorship form attesting that he or she fulfills the authorship criteria. There should be a statement in manuscript explaining contribution of each author to the work. Acknowledgments will be limited to one page of *Journal of Advances in Environmental Health Research*, and those acknowledged will be listed only once.

Any change in authorship after submission must be approved in writing by all authors.

ASSURANCES

In appropriate places in the manuscript please provide the following items:

- If applicable, a statement that the research protocol was approved by the relevant institutional review boards or ethics committees and that all human participants gave written informed consent
- The source of funding for the study
- The identity of those who analyzed the data
- Financial disclosure, or a statement that none is necessary

TITLE PAGE

With the manuscript, provide a page giving the title of the paper; titles should be concise and descriptive (not declarative). Title page should include an abbreviated running title of 40 characters, the names of the authors, including the complete first names, the name of the department and institution in which the work was done, the institutional affiliation of each author. The name, post address, telephone number, fax number, and e-mail address of the corresponding author should be separately addressed. Any grant support that requires acknowledgment should be mentioned on this page. Word count of abstract and main text as well as number of tables and figures and references should be mentioned on title page. If the work was derived from a project or dissertation, its code should also be stated.

Affiliation model: Department, Institute, City, Country.
Example: Department of Environmental Health Engineering, School of Health, Kurdistan University of Medical Sciences, Sanandaj, Iran.

ABSTRACT

Provide on a separate page an abstract of not more than 250 words. This abstract should consist of ONE paragraph (Non-structured Abstract). It should briefly describe the problem being addressed in the study, how the study was performed, the salient results, and what the authors conclude from the results respectively. Three to seven keywords may be included. Keywords are preferred to be in accordance with MeSH (http://www.ncbi.nlm.nih.gov/mesh) terms.

CONFLICT OF INTEREST

Authors of research articles should disclose at the time of submission any financial arrangement they may have with a company whose product is pertinent to the submitted manuscript or with a company making a competing product. Such information will be held in confidence while the paper is under review and will not influence the editorial decision, but if the article is accepted for publication, a disclosure will appear with the article.
Because the essence of reviews and editorials is selection and interpretation of the literature, the *Journal of Advances in Environmental Health Research* expects that authors of such articles will not have any significant financial interest in a company (or its competitor) that makes a product discussed in the article.

REVIEW AND ACTION

Submitted papers will be examined for the evidence of plagiarism using some automated plagiarism detection service. Manuscripts are examined by members of the editorial staff, and two thirds are sent to external reviewers. Communications about manuscripts will be sent after the review and editorial decision-making process is complete within **3-6 weeks** after receiving the manuscript. After acceptance, editorial system makes a final language and scientific edition. No substantial change is permitted by authors after acceptance. It is the responsibility of corresponding author to answer probable questions and approve final version.

COPYRIGHT

Journal of Advances in Environmental Health Research is the owner of all copyright to any original work published by the

JAEHR. Authors agree to execute copyright transfer forms as requested with respect to their *Journal of Advances in Environmental Health Research* has the right to use, reproduce, transmit, derive works from, publish, and distribute the contribution, in the *Journal* or otherwise, in any form or medium. Authors will not use or authorize the use of the contribution without the Journal Office' written consent

JOURNAL STYLE

Tables

Double-space tables and provide a title for each.

Figures

Figures should be no larger than 125 (height) x 180 (width) mm (5 x 7 inches) and should be submitted in a separate file from that of the manuscript. The name of images or figures files should be the same as the order that was used in manuscript (fig1, fig2, etc.). Only JPEG, tif, gif and eps image formats are acceptable with CMYK model for colored image at a resolution of at least 300 dpi. Graphs must have the minimum quality: clear text, proportionate, not 3 dimensional and without disharmonic language. Electron photomicrographs should have internal scale markers.

If photographs of patients are used, either the subjects should not be identifiable or the photographs should be accompanied by written permission to use them. Permission forms are available from the Editorial Office.

Scientific illustrations will be created or recreated in-house. If an outside illustrator creates the figure, the *Journal of Advances in Environmental Health Research* reserves the right to modify or redraw it to meet our specifications for publication. The author must explicitly acquire all rights to the illustration from the artist in order for us to publish the illustration. Legends for figures should be an editable text as caption and should not appear on the figures.

References

The Vancouver style of referencing should be used. References must be double-spaced and numbered as **superscripts** consecutively as they are cited. References first cited in a table or figure legend should be numbered so that they will be in sequence with references cited in the text at the point where the table or figure is first mentioned. List all authors when there are six or fewer; when there are seven or more, list the first six, then "et al." The following are sample references:

1. Maleki A, Shahmoradi B, Daraei H, Kalantar E. Assessment of ultrasound irradiation on inactivation of gram negative and positive bacteria isolated from hospital in aqueous solution. J Adv Environ Health Res 2013; 1(1): 9-14.

2. Buckwalter JA, Marsh JL, Brown T, Amendola A, Martin JA. Articular cartilage injury. In: Robert L, Robert L, Joseph V, editors. Principles of Tissue Engineering. 3rd ed. Burlington, MA: Academic Press; 2007. p. 897-907.

3. Kuczmarski RJ, Ogden CL, Grammer-Strawn LM, Flegal KM, Guo SS, Wei R, et al. CDC growth charts: United States. Advance data from vital and health statistics. No. 314. Hyattsville, Md: National Center for Health Statistics, 2000. (DHHS publication no. (PHS) 2000-1250 0-0431)

4. World Health organization. Strategic directions for strengthening nursing and midwifery services [online]. Available from: URL:http://www.wpro.who.int/themesfocuses/theme3/focus2/nursingmidwifery.pdf2002

Units of Measurement

Authors should express all measurements in conventional units, with Système International (SI) units given in parentheses throughout the text. Figures and tables should use conventional units, with conversion factors given in legends or footnotes. In accordance with the Uniform Requirements, however, manuscripts containing only SI units will not be returned for that reason.

Abbreviations

Except for units of measurement, abbreviations are discouraged. Consult Scientific Style and Format: The CBE Manual for Authors, Editors, and Publishers (Sixth edition. New York: Cambridge University Press, 1994) for lists of standard abbreviations. Except for units of measurement, the first time an abbreviation appears, it should be preceded by the words for which it stands.

Chemical Structure

Structures should be produced with a chemical drawing program, preferably ChemDraw 4.5 or higher, and submitted in TIFF format to allow use of electronic files in production. Structures should also be submitted in native file formats, e.g., RDX.

For any more detail about the writing style for your manuscripts refer to:

http://www.jaehr.muk.ac.ir

Authorship Form

Title of the manuscript:

.....

.....

We, the undersigned, certify that we take responsibility for the conduct of this study and for the analysis and interpretation of the data. We wrote this manuscript and are responsible for the decisions about it. Each of us meets the definition of an author as stated by the International Committee of Medical Journal Editors (see http://www.icmje.org/icmje-recommendations.pdf). We have seen and approved the final manuscript. Neither the article nor any essential part of it, including tables and figures, will be published or submitted elsewhere before appearing in the *Journal of Advances in Environmental Health Research* [All authors must sign this form or an equivalent letter.]

Name of Author	**Contribution**	**Signature**

Please scan this form and upload it as a supplementary file in "Step 4" of submitting articles.

Table of Contents

Original Article(s)

JAEHR Journal of Advances in Environmental Health Research

A survey on the performance of moving bed biofilm reactor and rapid sand filter in wastewater treatment

Mostafa Hadei[1], Mohammadreza Aalipour[1], Nezameddin Mengelizadeh[2], Amirhossein Fatemifar[3], Samad Hasanpour-Barijany[4]

1 Department of Environmental Health Engineering, School of Public Health, Isfahan University of Medical Sciences, Isfahan, Iran
2 Department of Environmental Health Engineering, Student Research Committee, School of Public Health, Isfahan University of Medical Sciences, Isfahan, Iran
3 Department of Civil Engineering, School of Engineering and Technology, Islamic Azad University, Parand Branch, Tehran, Iran
4 Department of Water Resources, Islamic Azad University, Science and Research Branch, Tehran, Iran

Original Article

Abstract

Moving bed biofilm reactor (MBBR) is a process in which attached growth is utilized for wastewater treatment. This process does not require sludge recycling or backwash. Activated sludge processes can be promoted to an MBBR by adding media to an aeration tank. Rapid sand filter is a physical method for the removal of total suspended solids (TSS) in advanced wastewater treatment. The purpose of this study was the evaluation of effluent reuse feasibility of MBBR and rapid sand filter in agricultural irrigation. Results showed TSS, biochemical oxygen demand (BOD_5), and chemical oxygen demand (COD) concentrations in effluent were 10, 7.7, and 85.75 mg/l, respectively. Removal efficiency of TSS, BOD_5, and COD was 98%, 98.8%, and 94.6%, respectively. Furthermore, the value of chemical parameters was less than the standard limitations. Average removal efficiency of total coliform, fecal coliform, and nematode was 100%. Total dissolved solids (TDS) and electrical conductivity (EC) in effluent were 960.5 mg/l and 1200.63 µs/cm, respectively. The Wilcox diagram showed that effluent was in the C3-S1 class, which means effluent quality was appropriate for irrigation. The results showed that effluent quality was completely compatible with the national standards in agricultural irrigation.

KEYWORDS: Wastewater, Rapid Sand Filter, Moving Bed Biofilm Reactor (MBBR)

Date of submission: 15 Apr 2015, ***Date of acceptance:*** 15 Jun 2015

Citation: Hadei M, Aalipour M, Mengelizadeh N, Fatemifar A, Hasanpour-Barijany S. **A survey on the performance of moving bed biofilm reactor and rapid sand filter in wastewater treatment.** J Adv Environ Health Res 2015; 3(3): 147-53.

Introduction

Activated sludge process is widely used for wastewater treatment. However, it has some disadvantages that affect its efficiency and can decrease the quality of effluent, such as sensitivity to hydraulic and organic shock, sludge bulking, and sludge rising. Due to these disadvantages, in recent years, the use of processes such as membrane bioreactor (MBR) and moving bed biofilm reactor (MBBR) has increased.[1,2]

MBBR is a process in which attached growth is utilized for conducting wastewater treatment. Media may fill 25-50% of the volume of the aeration tank. Specific area of media is about 500 m^2/m^3. The process does

Corresponding Author:
Nezameddin Mengelizadeh
Email: nezam_m2008@yahoo.com

not require sludge recycling or backwash. Activated sludge processes can be promoted to an MBBR by adding media to an aeration tank. Other advantages of MBBR include the capability to handle organic and hydraulic shock. Furthermore, through attached growth, sludge bulking cannot occur in the process.[2]

In the case of MBBR, in the study by Qdegaard, the removal efficiency of organic matters was reported as higher than 99%, but in most studies it was 94%.[3] However, in an experimental comparison between MBBR and activated sludge system in the treatment of municipal wastewater, the efficiency of activated sludge in chemical oxygen demand (COD) removal was higher than MBBR. The average efficiencies for total COD removal were 76% for MBBR and 84% for activated sludge. The difference between the efficiency of the two systems is related to the difference in biomass concentration. Biomass concentration in activated sludge system was higher than MBBR. The average efficiencies for soluble COD were 71% for both systems.[4]

Another study was conducted on the performance of MBBR in the treatment of anaerobic reactor biowaste effluent.[5] The total COD removal achieved was 53%. The limited COD removal achieved was in agreement with the high COD to biochemical oxygen demand (BOD_5) ratio (1:3) of the influent wastewater. Furthermore, in comparison to a sequencing batch reactor (SBR) system (30%), MBBR offered a higher dissolved COD removal (40%).[5]

Deep filtration is a physical method for removing total suspended solids (TSS) in water treatment plants and advanced wastewater treatment. Rapid sand filters, in comparison to slow sand filters, are more stable during quality variations in wastewater. Moreover, these filters have a longer lifespan.[6,7] The application of these filters in wastewater treatment is for the removal of TSS and suspended BOD (by straining mechanism). Furthermore, considering future upgrading of plants by membrane processes, the application of multi-bed filters before those units are proposed.[2,6]

The quality of water used in agricultural irrigation has short-term and long-term effects on the soil. Continuous irrigation with low quality water places the land at risk of becoming non-arable.[8] High TSS levels also cause blockage of soil pores and reduce its permeability.[9] Moreover, high TSS reduces the efficiency of the disinfection process and can increase the possibility of nuzzle clogging in drip irrigation.[2] The presence of large amounts of organic matters (BOD and COD) in the soil has adverse effects on soil quality, including an increase in partial pressure of carbon dioxide and temperature, and formation of organic acids during decomposition that can stabilize nutrients.[10,11] In a study on effluent from treatment plants in Tehran, Iran, during 2005 to 2007, only in 68% of samples, TSS amount in the effluent was compatible to Iranian national standard levels.[12]

In another study on conventional activated sludge process of Tabriz treatment plant, values of BOD, COD, and TSS were 22.5 mg/l, 34 mg/l, and 16.5 mg/l, respectively.[13] Another study on Owlang treatment plant effluent showed that average BOD_5, COD, and TSS levels were 69 mg/l, 139 mg/l, and 89 mg/l, respectively.[14] The process used in Owlang treatment plant was stabilization ponds. Moreover, a research was conducted on the upgrading of a full-scale overloaded activated sludge treatment plant by MBBR technology.[15] The results showed a relevant increase of up to 60% in the treated flow rate, acceptable efficiency in organic carbon removal and nitrification (equal to 88% and 90%, respectively), and the prevention of the hydraulic overload of the secondary settler.[15]

The purpose of this study was the evaluation of reuse feasibility of MBBR and rapid sand filter effluent in agricultural irrigation. These two processes can easily be included in existing plants to improve

performance. We expected that parameters related to organic compounds and suspended solids would be reduced by these units.

Materials and Methods

The present study was conducted on the City Center treatment plant, a commercial-recreational complex in Isfahan, Iran. The plant uses a MBBR unit for secondary treatment of wastewater. Its tertiary treatment units consist of a rapid sand filter and a granular activated carbon filter.

Wastewater retention time in MBBR is 5 hours at peak flow. Specific area of media is 494 m^2/m^3. Filling percentage of first aeration stage and second aeration stage by media are 50% and 25%, respectively. The diameter of the rapid sand filter vessel is 1.2 m and the height is 2.2 m. Filtration rate of the rapid sand filter is 10 m^3/m^2/hour. In addition, 60 cm of filter height includes two types of sand with grain size of 0.7-1.18 mm and 1.18-2 mm. The effluent did not pass through the activated carbon filter (bypass mode) and final disinfection was performed using sodium hypochlorite. The flow diagram of the treatment plant process is shown in figure 1.

Figure 1. Flow diagram of treatment plant

Sampling was performed 4 times during 6 months in the year 2013. BOD_5, COD, TSS, EC, pH, and sodium, calcium, magnesium, potassium, chloride, sulfate, total coliform, fecal coliform, and nematode content of samples were analyzed according to standard methods.[16] Method ID for BOD, COD, and TSS analyses was 5210 B, 5220 C, and 2540 D, respectively. Other method IDs are presented in table 1. In this study, mixed samples were used to analyze the process. The samples were collected during 8 hours. Although in order to undertake a more accurate investigation of process efficiency, effluent sampling was started about 6-8 hours after the beginning of influent sampling. This time is almost equal to wastewater retention time within the system.[17] It is noteworthy that the data used in this study was obtained from operational records of the City Center wastewater treatment plant. The sampling and analyses were a part of routine monitoring of the plant. Thus, no study was designed for this manuscript.

Sodium adsorption ratio (SAR) was calculated according to the following equation:

$$(1)\ SAR = \frac{Na^+}{\sqrt{\frac{Ca^+ + Mg^+}{2}}}$$

This equation is based on the integrated effect of EC (salinity hazard) and SAR (alkalinity hazard), and has been used to assess water suitability for irrigation.[18] When analytical data of EC and SAR are plotted on the US salinity diagram, it is illustrated that most treated wastewater samples fall into the class of C3-S1 indicating high salinity with low sodium water, which can be used for irrigation on almost all types of soil, with only a minimum risk of exchangeable sodium. This type of water can be suitable for plants with acceptable salt tolerance, but its suitability for irrigation is restricted, especially in soils with restricted drainage.

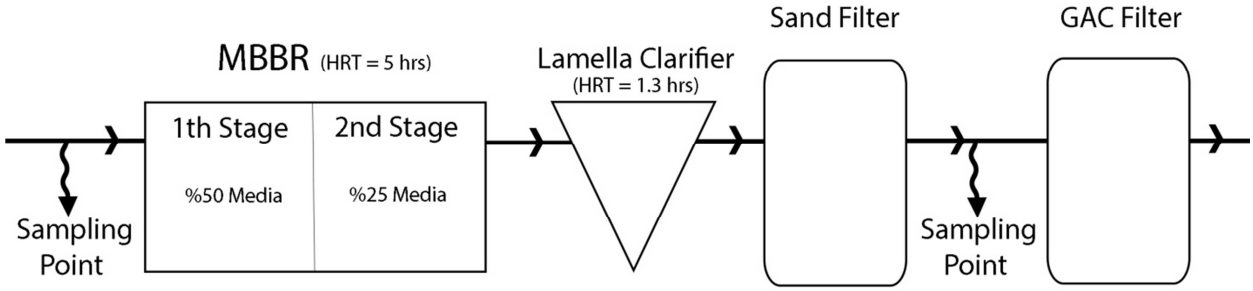

Figure 1. Flow diagram of the treatment plant
MBBR: Moving bed biofilm reactor

Table 1. Results of analyses and standards of the Iranian Environmental Protection Agency

	Unit	Raw wastewater	Effluent	Standard	Method No.
pH	-	7.65	7.55	6.5-8.5	pH Meter-Metrohm 827
TDS	mg/l	940.00	960.50	-	2540 C
EC	µs/cm	1120.00	1200.63	-	D1125A
Sodium	mg/l	108.00	104.00	-	3500-Na B
Calcium	mg/l	80.00	78.00	-	3500-Ca B
Magnesium	mg/l	10.78	10.52	100	3500-Mg B
Potassium	mg/l	12.10	12.00	-	3500-K B
Chloride	mg/l	-	203.00	600	4500-Cl^- B
Sulphate	mg/l	-	13.00	500	4500-SO_4^{2-} A
Total coliform	MPN/100ml	-	0	1000	9221C
Fecal coliform	MPN/100ml	-	0	400	9221E
Nematode	-	-	0	1	10750

TDS: Total dissolved solids; EC: Electrical conductivity; MPN: Most probable number

The Wilcox diagram or US salinity diagram was used to evaluate the chemical quality of effluent. The Wilcox diagram, which is based on the integrated effect of EC (salinity hazard) and SAR (alkalinity hazard), was used to assess the suitability of water for irrigation. The diagram is not presented in this manuscript, but it is available in various references.[18,19]

The results were analyzed in SPSS software (version 16, SPSS Inc., Chicago, IL, USA) using one-sample t-test, with P-value of 0.05 and confidence level of 0.95.

Results and Discussion

One of the parameters for assessing the quality of effluent is hydrogen ion concentration that is presented as pH. In this study, average pH of raw wastewater and effluent was 7.65 and 7.55, respectively, that is within the permitted range for discharge into the environment (pH = 6.5-8.5). This finding is compatible with the results of the study by Altin et al.[20]

TSS, BOD_5, and COD are among the main parameters for evaluation of the performance a treatment plant. According to figure 2, average values for BOD_5 and COD in the effluent were 7.7 mg/l and 85.75 mg/l, respectively. These values are much lower than the standard limitations for wastewater reuse. In addition, as seen in figure 2, TSS removal efficiency with respect to the inlet value (495 mg/l) was very high. TSS concentration of effluent was 10 mg/l. The results indicate that MBBR and rapid sand filter are efficient in the removal of high levels of suspended solids and organic matters.[21] Delnavaz et al. used MBBR for treating wastewater containing different COD levels (1000-3500 mg/l).[22] The results showed 75-90% efficiency for a COD of 750-1000 mg/l.[22] In a study on municipal wastewater reuse in Jubail treatment plant, Saudi Arabia, the biological process and filtration could achieve the values of 4.4 and 2.7 mg/l for TSS and BOD, respectively.[23]

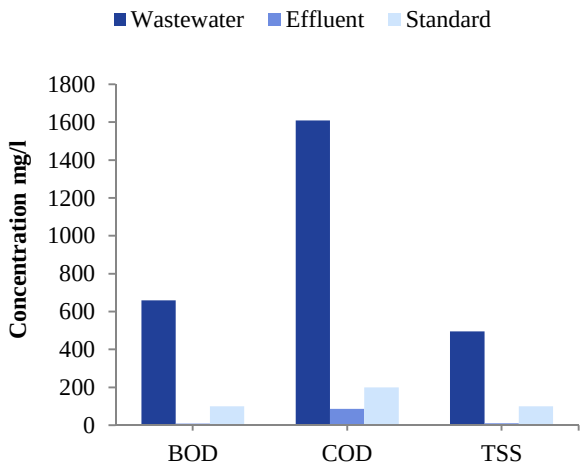

Figure 2. Comparison of total suspended solids, biochemical oxygen demand, and chemical oxygen demand levels of the effluent and standard levels

BOD: biochemical oxygen demand; COD: Chemical oxygen demand; TSS: Total suspended solids

Microorganisms and pathogens are another important issue related to wastewater effluent discharged into the environment and surface water. The presence of microorganisms in water can cause various diseases in animals and humans. Hence, the analysis of the microbial quality of raw wastewater and effluent is essential. Average removal efficiency of total coliform, fecal coliform, and nematode was 100% (Table 1). This result is not in agreement with the results of other studies on processes such as conventional activated sludge and extended activated sludge.[24,25] This may be due to attached growth in MBBR that is supplemented for the application of rapid sand filter and chlorine disinfection. Wilen et al. in a study of sludge particle removal from wastewater through disc filtration concluded that the removal efficiency of COD and indicator microorganisms increased.[26] In a study by Lubello et al., through the application of filtration, peracetic acid, and UV disinfection for tertiary treatment, the most probable number (MPN) value of total coliform was 2 in 100 ml.[27] These results indicate the important role of sand filter and appropriate disinfection in achieving a high microbial quality.[27]

Table 1 shows that average levels of sulphate, chloride, and magnesium are much lower than the related standards for reuse. In addition, a SAR value of 2.39 was obtained. Binavapour et al. reported the average concentration of chloride, sulphate, SAR, and magnesium as lower than the standard values.[28] In a study on Owlang city treatment plant, Mashhad, Iran, Pirsaheb et al. concluded that the effluent was suitable for irrigation, because SAR and (residual sodium carbonate) RSC were low.[14] Hashemi et al. studied the possibility of the reuse of effluent from treatment plants in Isfahan, Iran, and concluded that boron concentration and SAR in the northern treatment plant were within the permitted range for irrigation.[29] The northern treatment plant of Isfahan uses a two-stage activated sludge process. In the study by Al-A'ama and Nakhla, using a biological process and filtration, the obtained total dissolved solids (TDS) and SAR values of effluent were 936 mg/l and 7.4, respectively.[23]

The Willcox diagram illustrated that the studied effluent was in the C3-S1 class, which means the effluent quality is appropriate for irrigation. Considering the results of previous studies, it is evident that most treated wastewater samples fall within the C3-S1 class, indicating high salinity with low sodium water. Thus, they can be used for irrigation on almost all types of soil with only a minimum risk of exchangeable sodium. This type of water is suitable for plants with acceptable salt tolerance, but its suitability for irrigation is restricted, especially in soils with restricted drainage.[19]

The comparison of TDS and EC of wastewater and effluent showed that the value of the effluent had increased, which was due to the use of sodium hypochlorite for the disinfection of effluent. A way to control EC and TDS is the application of chlorine gas instead of sodium hypochlorite. Chlorine gas does not cause an increase in dissolved solids and EC. Finally, through the comparison of the results with the Iran national standards, it became clear that the effluent characteristics had complete compliance with standard values and it was suitable for reuse.

Conclusion

Results of analyses indicate that MBBR and rapid sand filter have acceptable efficiency in parameters such as BOD, COD, and TSS (98.8%, 94.6%, and 98%, respectively). Furthermore, the results showed that effluent quality in term of EC, TDS, total and fecal coliform, and nematode was completely compatible with the national standards for discharge into surface and groundwater resources and agricultural irrigation. By using the Willcox diagram, it was found that effluent

was in the C3-S1 class, indicating high salinity with low sodium water. Therefore, it can be used for irrigation on almost all types of soil with only a minimum risk of exchangeable sodium. Thus, it can be concluded that MBBR and rapid sand filter have a significant impact on treatment performance and existing plants can be upgraded using these units.

Conflict of Interests

Authors have no conflict of interests.

Acknowledgements

The authors are grateful for the financial support of this project by the Student Research Committee of the School of Health of Isfahan University of Medical Sciences.

References

1. Madoni P, Davoli D, Gibin G. Survey of filamentous microorganisms from bulking and foaming activated-sludge plants in Italy. Water Research 2000; 34(6): 1767-72.
2. Tchobanoglous G, Burton FL, Stensel D. Wastewater Engineering: Treatment and Reuse. New York, NY: McGraw-Hill Education; 2003. p. 4.
3. Qdegaard H. The moving bed biofilm reactor [Online]. [cited 1999]; Available from: URL: http://netedu.xauat.edu.cn/jpkc/netedu/jpkc2009/szylybh/content/wlzy/7/3/The%20Moving%20Bed%20Biofilm%20Reactor.pdf
4. Andreottola G, Foladori R, Ragazzi M, Tatàno F. Experimental comparison between MBBR and activated sludge system for the treatment of municipal wastewater. Water Sci Technol 2000; 41(4): 375-82.
5. Comett-Ambriz I, Gonzalez-Martinez S, Wilderer P. Comparison of the performance of MBBR and SBR systems for the treatment of anaerobic reactor biowaste effluent. Water Sci Technol 2003; 47(12): 155-61.
6. Cao X, Liu J, Meng X. Evaluation of a slow sand filter in advanced wastewater treatment. Proceedings of the International Conference on Mechanic Automation and Control Engineering (MACE); 2010 Jun 26-38; Wuhan, China.
7. Deboch B, Faris K. Evaluation of the efficiency of rapid sand filtration. Proceedings of the 25th Conference WEDC; 1999; Addis Ababa, Ethiopia.
8. Danesh S, Amin A. The use of wastewater in agriculture, opportunities and challenges. Proceedings of the 1st National Conference on the Role of Water Recycling and Wastewater Management; 2008 May 24; Mashhad, Iran. [In Persian].
9. Aiello R, Cirelli GL, Consoli S. Effects of reclaimed wastewater irrigation on soil and tomato fruits: A case study in Sicily (Italy). Agricultural Water Management 2007; 93(1-2): 65-72.
10. Chhonkar PK, Datta SP, Joshi HC, Pathak H. Impact of Industrial Effluents on Soil Health and Agriculture - Indian Experience: Part I - Distillery and Paper Mill Effluents. Journal of Scientific and Industrial Research 2000; 59(5): 350-61.
11. Fatta D, Kythreotou N. Wastewater as valuable water resource-concerns, constraints and requirements related to reclamation, recycling and reuse. Proceedings of the IWA International Conference on Water Economics, Statistics and Finance; Water Economics, Statistics and Finance; Rethymno, Greece; 2005 Jul 8-10; London, UK.
12. Taleb Bidokhti A, Dehghani MH, Azam K. Evaluation of the effluent quality of wastewater treatment plants in Tehran. Proceedings of the 12th National Conference on Environmental Health; 2009 Nov 10-12; Tehran, Iran. [In Persian].
13. Asghari Moghaddam A. Feasibility of agricultural and industrial reuse for effluent of wastewater treatment plant of Tabriz. Proceedings of the 32nd National & the 1st International Geosciences Congress; 2014 Feb 16-19; Tehran, Iran. [In Persian].
14. Pirsaheb M, Khodadadi T, Sharafi K, Dogohar K. Feasibility of Owlang Mashhad reuse of effluent for agricultural irrigation. Proceedings of the 3rd National Conference on Water and Wastewater approach to Operation; 2010 Feb 23-24; Tehran, Iran. [In Persian].
15. Andreottola G, Foladori P, Gatti G, Nardelli P, Pettena M, Ragazzi M. Upgrading of a small overloaded activated sludge plant using a MBBR system. J Environ Sci Health A Tox Hazard Subst Environ Eng 2003; 38(10): 2317-28.
16. Eaton AD, Franson MA. Standard Methods for the Examination of Water & Wastewater. Washington, DC: American Public Health Association; 2005.
17. Sawyer C, McCarty P, Parkin G. Chemistry for Environmental Engineering and Science. New York, NY: McGraw-Hill Education; 2003.
18. Richards LA. Diagnosis and improvement of saline and alkali soils. Washington, DC: U.S. Dept. of Agriculture; 1954.
19. Alobaidy A, Al-Sameraiy M, Kadhem A, Majeed A. Evaluation of treated municipal wastewater quality for irrigation. J Environ Prot 2010; 1(3): 216-25.
20. Altin A, Altin S, Degirmenci M. Characteristics and

treatability of hospital (medical) wastewaters. Fresen Environ Bull 2003; 12(9): 1098-108.
21. Borkar RP, Gulhane ML, Kotangale AJ. Moving bed biofilm reactor - a new perspective in wastewater treatment. IOSR Journal of Environmental Science, Toxicology and Food Technology 2013; 6(6): 15-21.
22. Delnavaz M, Ayati B, Ganjidoust H. Prediction of moving bed biofilm reactor (MBBR) performance for the treatment of aniline using artificial neural networks (ANN). Journal of Hazardous Materials 2010; 179(1-3): 769-75.
23. Al-A'ama MS, Nakhla GF. Wastewater reuse in Jubail, Saudi Arabia. Water Research 1995; 29(6): 1579-84.
24. Mahmoudi M, Khamootian R, Dargahi A. Evaluation of Kermanshah city effluent for reuse in agriculture. Proceedings of the 1st National student Conference on Social Determinants of Health; 2010 Oct 13-14; Tehran, Iran. [In Persian].
25. Amouei A, Ghanbari N, Kazemitabar M. Study of wastewater Treatment System in The Educational Hospitals of Babol University of Medical Sciences (2009). J Mazandaran Univ Med Sci 2010; 20(77): 78-86. [In Persian].
26. Wilen BM, Johansen A, Mattsson A. Assessment of sludge particle removal from wastewater by disc filtration. Water Practice & Technology 2012; 7(2).
27. Lubello C, Gori R, Nicese FP, Ferrini F. Municipal-treated wastewater reuse for plant nurseries irrigation. Water Res 2004; 38(12): 2939-47.
28. Binavapour Esforoushani M, Koulivand A, Sabzevari A, Farzadkia M, Mohammad Taheri A, Zafari Pour H, et al. Investigation of irrigation reuse potential of wastewater treatment effluent from Hamedan Atieh-sazan general hospital. Water and Wastewater 2008; 18(4): 83-7. [In Persian].
29. Hashemi H, Ebrahimi A, Khodabakhshi A. Survey on reuse of Isfahan wastewater treatment plants effluent in restricted irrigation. J Health Syst Res 2014; 10(2): 326-34. [In Persian].

JAEHR Journal of Advances in Environmental Health Research

Application of experimental design approach for optimization of the photocatalytic degradation of humic substances in aqueous solution using immobilized ZnO nanoparticles

Hooshyar Hossini[1], Mahdi Safari[2], Reza Rezaee[2], Reza Darvishi Cheshmeh Soltani[3], Omid Giahi[2], Yahya Zandsalimi[2]

1 Department of Environmental Health Engineering, School of Health, Kermanshah University of Medical Sciences, Kermanshah, Iran
2 Environmental Health Research Center, Kurdistan University of Medical Sciences, Sanandaj, Iran
3 Department of Environmental Health, School of Health, Arak University of Medical Sciences, Arak, Iran

Original Article

Abstract

Degradation of humic substances in water is important due to its adverse effects on the environment and human health. The aim of this study was modeling and investigating the degradation of humic substances in water using immobilized ZnO as a catalyst. ZnO nanoparticles were synthesized through simple coprecipitation (CPT) method and immobilized on glass plates. The immobilized ZnO nanocatalyst was characterized through scanning electron microscopy (SEM) and X-ray diffraction (XRD). Response surface methodology (RSM) and central composite design (CCD) were used to create an experimental design for humic degradation and color removal efficiency. The most important parameters including initial concentration, pH, and contact time were optimized. The optimum conditions were initial concentration of 7.68 mg/l, pH of 4.42, and contact time of about 125.6 minutes. Under optimal conditions, maximum humic substances and color removal of about 100 and 82.37% were obtained, respectively. These results illustrate that an immobilized form of ZnO can be used as an efficient nanocatalyst for effective degradation of humic substances in water.

KEYWORDS: Humic Substances, Catalyst, Immobilization, Zinc Oxide, Nanoparticles, Modeling

Date of submission: 12 Apr 2015, ***Date of acceptance:*** 22 Jun 2015

Citation: Hossini H, Safari M, Rezaee R, Darvishi Cheshmeh Soltani R, Giahi O, Zandsalimi Y. **Application of experimental design approach for optimization of the photocatalytic degradation of humic substances in aqueous solution using immobilized ZnO nanoparticles.** J Adv Environ Health Res 2015; 3(3): 154-63.

Introduction

Humic substances are complex macromolecules of natural organic matter (NOM) derived from the decomposition of plants, algal and animal tissues, and microbial activity.[1,2] The undesirable effects of HS on drinking water include color and taste, ability to form complex compositions with heavy metals, and absorption of organic pollutants.[3-5] Moreover, humic substances are the principal precursors in the formation of carcinogenic disinfection byproducts (DBPs) such as trihalomethanes (THMs) and haloacetic acids (HAAs) during the chlorination process in water treatment.[6,7] In addition, many operational problems such as membrane fouling in water treatment processes, increase potential of microbial regrowth in distribution systems, and biological corrosion of pipelines are associated with the presence of these

Corresponding Author:
Mahdi Safari
Email: safari.m.eng@gmail.com

compounds in water recourses.[8,9] Therefore, the removal of undesirable HS from raw water before reaching water treatment plants and distribution systems is necessary.

Different treatment techniques such as enhanced coagulation,[10] membrane technology,[11] electrocoagulation (EC),[12] adsorption process,[13] and advanced oxidation processes (AOPs)[2,14]are considered for the removal of HS from water. Recently, photocatalysis technologies, due to their high potential for generation of reactive hydroxyl radicals (OH), have emerged as an efficient AOP for degradation of HS in aquatic environments.[2,15] In the past decades, zinc oxide (ZnO) as a semiconductor has attracted much interest due to its photocatalytic properties (wide band gap, high potential to adsorb UV irradiation, and large volume-area ratio) and low cost.[16,17]

According to the literature, immobilization of the catalyst on a suitable surface can be an efficient way for catalyst recovery and photocatalytic activity improvement.[16,18] Recently, photocatalytic removal of HS using different catalysts has been investigated.[2,15,19] However, to the best of our knowledge, the effect of immobilized ZnO as a catalyst on the degradation of HS in water has not been explored. To better evaluate the effect of operational factors and achieve valuable photocatalytic degradation results, response surface methodology (RSM) based on central composite design (CCD) was used as statistical approach.[20] The application of experimental design approach has many advantages, such as reduction of the number of experimental runs, evaluation of interactive effects of the operational parameters, optimization of the operational parameters for achieving maximum efficiency, compared to the conventional "one-factor-at-a-time" statistical method.[21,22]

Materials and Methods

In this study, all of the chemicals purchased were analytical grade and were used without further purification. Commercial humic acid (HA) was purchased from Fluka Company (USA). Zinc chloride ($ZnCl_2$), sodium hydroxide (NaOH), and ethanol were purchased from Merck Company (Germany).

The photocatalytic degradation experiments were performed in a Plexiglas reactor with a working volume of 400 ml. UV light irradiation was applied using 3 low-pressure 6 W UVC lamps (Philips, Netherlands) placed above the reactor. The distance between the UV lamps and surface of immobilized ZnO nanocatalyst was 1 cm. A magnetic stirrer (Heidolph, Germany) was used for mixing in the reactor.

ZnO nanoparticles were synthesized through simple coprecipitation method. For the preparation of ZnO nanoparticles, 1.362 g $ZnCl_2$ was added to 50 ml of deionized water. Then, 1 M NaOH solution was dropwise added to the above solution under magnetic stirring until the pH reached 10. The suspension was filtered, washed with absolute deionized water and ethanol, and dried in an oven at 80 °C for 2 days. A 3% suspension of ZnO nanoparticles was prepared. The resulting suspension was mixed with a magnetic stirrer. Then, it was sonicated in an ultrasonic bath at a temperature of 50 °C for 90 minutes. To avoid detachment of the ZnO nanoparticles, glass plates were immersed in concentrated NaOH (50%) for the functionalization of the glass surfaces with hydroxyl groups. The surface of glass plates were then coated with the resulting suspension using a pipette. The ZnO nanoparticle coating of the glass plates were dried at room temperature for 24 hours and then calcined at 400 °C for 3 hours in an electric furnace.[23]

The experiment was conducted to investigate the effect of the 3 variables of initial concentrations, pH, and contact time on process efficiency. Each factor in the experimental designs, based on the CCD, was varied at 5 different levels while the other parameters were kept constant. The coefficients of the response

functions for different independent variables were determined in correlation to the actual experimental results with the response functions using a design-expert regression program.[24] CCD was utilized to introduce the model as a specific design. CCD of the main parameters [x_1: initial concentration (2-30 mg/l), x_2: pH (3-10), and x_3: contact time (30-50 minutes)] is presented in table 1.

The morphology of immobilized ZnO nanoparticles was evaluated through scanning electron microscopy (SEM) (TESCAN, MIRA3). The XRD pattern of synthesized ZnO nanoparticles was studied using X-ray diffraction (XRD) equipped with a Cu anode (λ: 1.54056 Å) in 2θ range from 10 to 80° and step size of 0.026 °/s. A TOC analyzer (TOC/TN analyzers, Skalar Analytical B.V., Netherlands) equipped with a nondispersive infrared (NDIR) detector was used for the determination of TOC concentration. A DR-5000 UV-VIS spectrophotometer (HACH, Germany) was employed for the measurement of ultraviolet absorbance at 254 nm (UV254). The pH value of aquatic solution was measured using a digital pH meter (Jenway, UK). Moreover, the removal efficiency of humic substances was calculated using the following equation:

$$\text{Humic substances removal (\%)} = \frac{C_0 - C_f}{C_0} \times 100 \quad (1)$$

where C_0 and C_f are the initial and final concentrations of humic substances.

Results and Discussion

3.1 Characterization of ZnO nanoparticles

The SEM images and XRD pattern of ZnO nanostructures are illustrated in figure 1. Accordingly, the SEM image confirmed the ordered arrangement of pores on the surface of the ZnO nanostructures. The XRD spectra indicated sharp peaks of ZnO nanocrystal structure according to the standard references organization (Joint Committee; Standard card number 36–1451). The peaks are quite ordered and well-defined indicating the crystalline nature of the particles. Thus, these results demonstrate that high-purity ZnO nanostructures have been produced. Similar results have been reported by Masoumbaigi et al.[25]

Table 1. The experimental central composite design (CCD) matrix and results

Run	Initial concentration	pH	Degradation time	Degradation percentage	Color removal percentage
1	0	1.682	0	11.76	14.41
2	1	-1	-1	55.50	36.80
3	0	0	-1.682	30.00	38.99
4	-1	1	-1	61.40	64.45
5	-1	-1	-1	76.50	73.45
6	-1	-1	1	95.50	87.80
7	0	0	0	59.00	40.00
8	0	0	0	58.50	39.00
9	0	-1.682	0	86.00	39.00
10	1	1	1	34.50	28.80
11	-1.682	0	0	100.00	93.50
12	0	0	0	57.70	39.00
13	-1	1	1	73.60	75.40
14	1.682	0	0	20.10	12.40
15	0	0	0	57.40	40.00
16	0	0	0	59.10	38.00
17	0	0	0	57.40	39.00
18	0	0	1.682	60.66	41.20
19	1	1	-1	28.70	25.90
20	1	-1	1	41.30	38.80

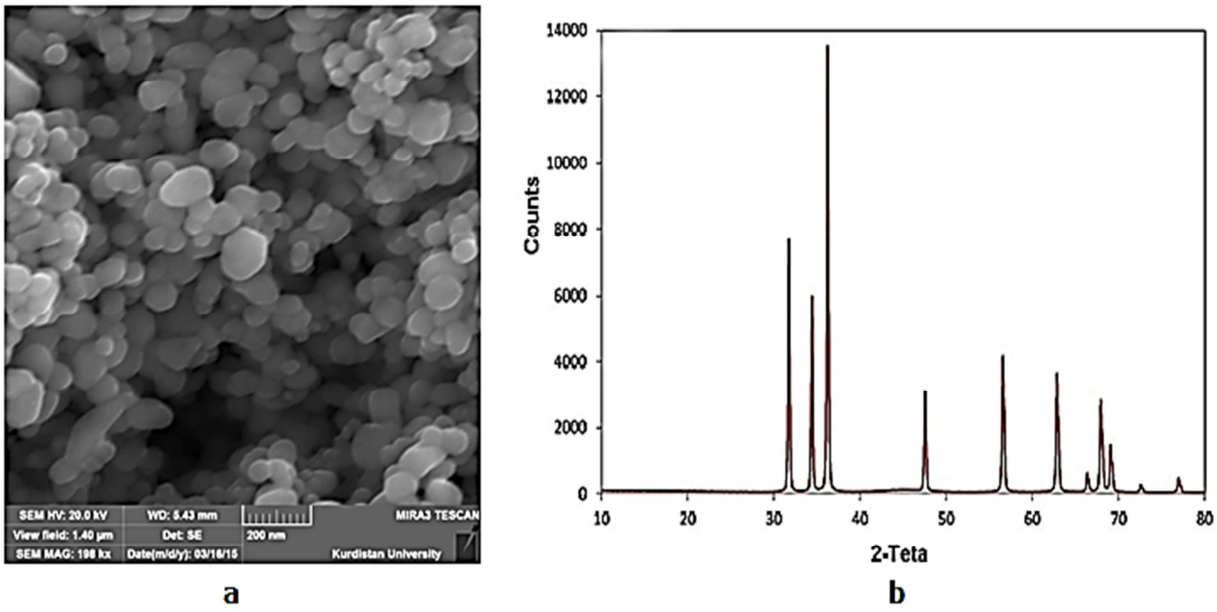

Figure 1. Scanning electron microscopy (SEM) images with 198 k × MAG (a) and X-ray diffraction (XRD) pattern of ZnO nanostructures (b)

3.2 ANOVA

According to the defined runs, a total of 20 runs of the CCD experimental design and response are shown in table 1. The ANOVA for the predicted 2FI model are presented in table 2. Accordingly, the model's *F*-value (14.96) and low probability value ($P < 0.0001$) indicate that the model is significant with regard to 95% confidence interval. The lack of fit is statistically significant ($P > 0.05$). A significant lack of fit suggests that there may be some systematic variation unaccounted for in the hypothesized model.[26]The predicted R2 of 0.81 is in reasonable agreement with the adjusted R2 of 0.5. The response surface model for predicting humic substances degradation efficiency was considered reasonable. The results of the quadratic model for predicting color removal efficiency as second response of the humic substances degradation are presented in table 3. Furthermore, the p-value for this response is significant.

Table 2. ANOVA for humic substances degradation response surface

Source	Sum of squares	df	Mean square	F value	P
Model	9218.77	6	1536.46	14.96	< 0.0001
x_1-Initial concentration	5797.24	1	5797.24	56.46	< 0.0001
x_2-pH	2797.36	1	2797.36	27.24	0.0002
x_3-Time	404.92	1	404.92	3.94	0.0686
x_1 x_2	1.44	1	1.44	0.014	0.9074
x_1 x_3	196.02	1	196.02	1.91	0.1904
x_2 x_3	21.78	1	21.78	0.21	0.6527
Residual	1334.84	13	102.68		
Lack of fit	1331.77	8	166.47	271.27	< 0.0001
Pure error	3.07	5	0.61		
Correct total	10553.61	19			
Standard deviation(SD)	10.13		R-Squared		0.87
Mean	56.23		Adjusted R-Squared		0.81
C.V. %	18.02		Predicted R-Squared		0.50

Table 3. ANOVA for color removal response surface

Source	Sum of squares	df	Mean square	F value	P
Model	8620.37	9	957.82	13.71	0.0002
x_1-Initial concentration	6909.92	1	6909.92	98.88	< 0.0001
x_2-pH	512.43	1	512.43	7.33	0.0220
x_3-Time	84.23	1	84.23	1.21	0.2980
x_1 x_2	0.03	1	0.031	4.47E-04	0.9835
x_1 x_3	52.02	1	52.02	0.74	0.4085
x_2 x_3	0.78	1	0.78	0.011	0.9179
x_1^2	881.20	1	881.20	12.61	0.0053
x_2^2	30.69	1	30.69	0.44	0.5225
x_3^2	154.54	1	154.54	2.21	0.1678
Residual	698.84	10	69.88		
Lack of fit	696.01	5	139.20	245.65	< 0.0001
Pure error	2.83	5	0.57		
Correct total	9319.21	19			
Standard deviation(SD)		8.35		R-Squared	0.92
Mean		45.29		Adjusted R-Squared	0.85
C.V. %		18.45		Predicted R-Squared	0.435

The final 2FI and quadratic models regressions in terms of coded factors are represented as follows:

HS degradation efficiency (%) = +56.23 - 20.6x_1 - 14.31x_2 + 5.54x_3 + 0. 43x_1x_2 - 4.95x_1x_3 + 1.65x_2 x_3 (2)

Color removal (%) = +38.72 - 22.49x_1 - 6.13x_2 + 2.48x_3 + 0.063x_1x_2 - 2.55x_1x_3 - 0.31x_2x_3 + 7.82$x_1$2 - 1.46$x_2$2 + 3.27$x_3$2 (3)

Usually, the adequacy of the model can be evaluated by diagnostic plots, such as a normal probability plot of the studentised residuals and a plot of predicted versus actual values. The normal probability plots of the studentised residuals for humic substances degradation and color removal are presented in figure 2.

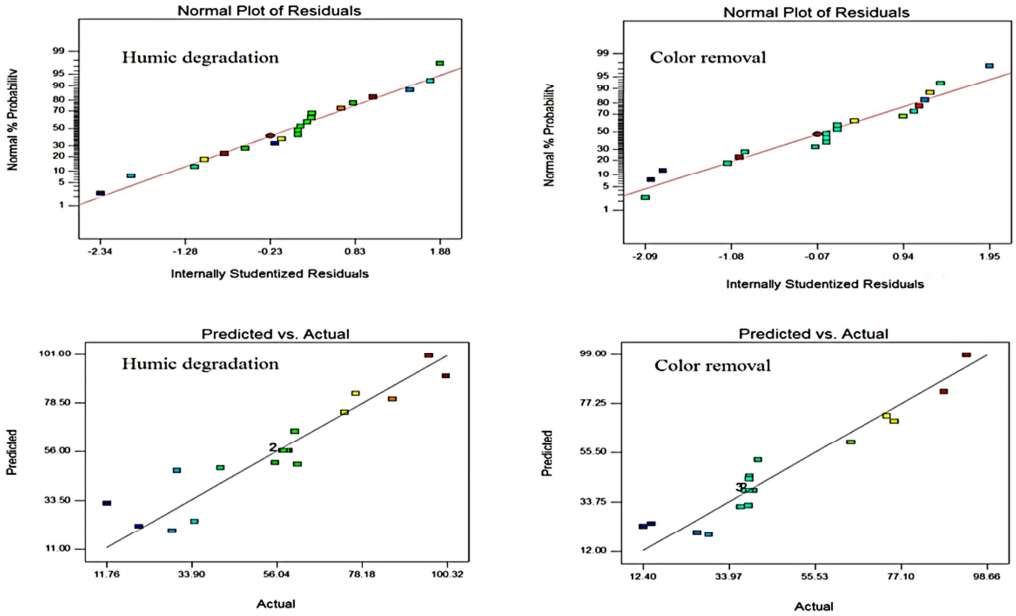

Figure 2. Normal probability and predicted vs. actual values plots for photocatalytic humic substances degradation

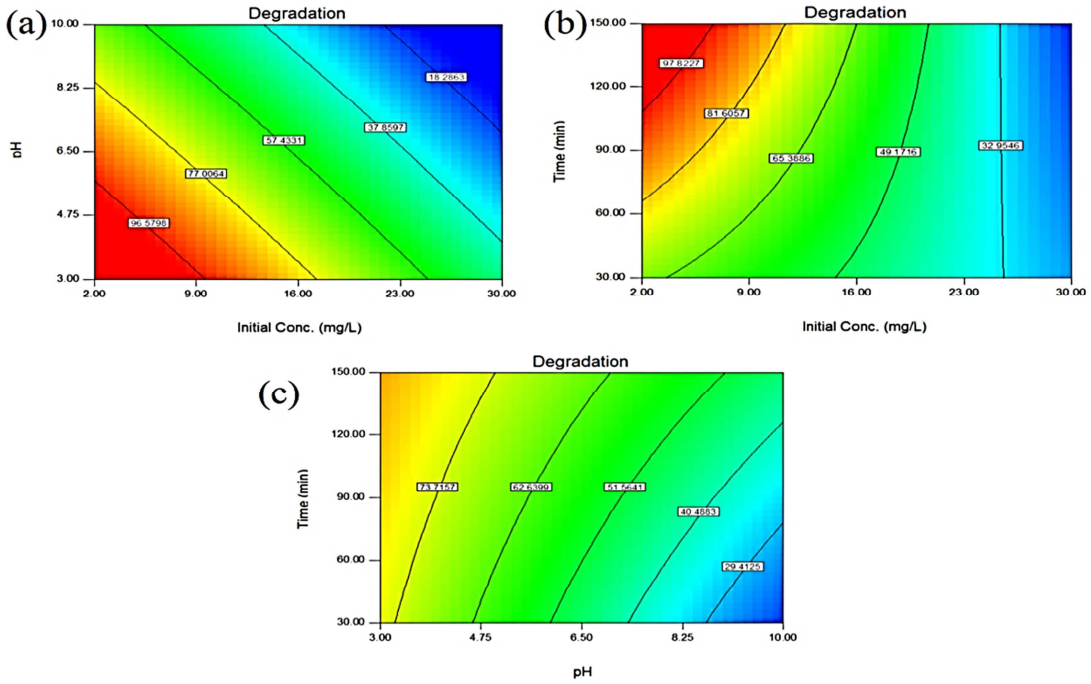

Figure 3. Two-dimensional plots for photocatalytic humic substances degradation

Figure 2 represents the predicted versus actual efficiency data.

3.3 Effects of independent variables

3.3.1 Catalytic degradation of humic substances

The three-dimensional graphics of response surface for catalytic degradation of humic substances are illustrated in figure 3. Accordingly, the interaction between independent variables is observed. It can be seen that the degradation rate increased to a maximum value when initial humic substances and pH were decreased. On the other hand, catalytic degradation improved with longer contact time. However, it can be concluded that optimal conditions were obtained through providing the desirable time, acidic pH, and low amount of humic substances. Humic substances are soluble at high pH values, but not in weak acidic environments. Furthermore, with regard to the zero-point charge of pure ZnO nanoparticles (about 9), the degradation efficiency increased with the decrease in pH value. This may be due to a positive charge on ZnO nanoparticles surface, which favors adsorption of MO anions onto ZnO surface.[16,27]

In addition, at high pH values, humic acid could not be adsorbed onto the negatively charged ZnO nanostructure surface. Hoseinzadeh et al. reported a pH_{PZC} of ZnO nanoparticles of about 7.51.[28] This result demonstrates that at pH values of higher than 7.51, ZnO characteristics improved. Xue et al. reported that when initial concentrations of humic acid were decreased, the kinetic constants of humic acid degradation significantly improved.[29]

3.3.2 Catalytic color removal

The pattern in color removal was similar to that of humic substances degradation results (Figure 4). Significant color removal efficiency was obtained with increased time duration and lower amounts of initial concentration and pH values. Soltani et al. have reported that when the initial dye concentration decreases, more hydroxyl radicals (OH) are available to decompose the dye structure, and consequently, removal efficiency increases.[16].

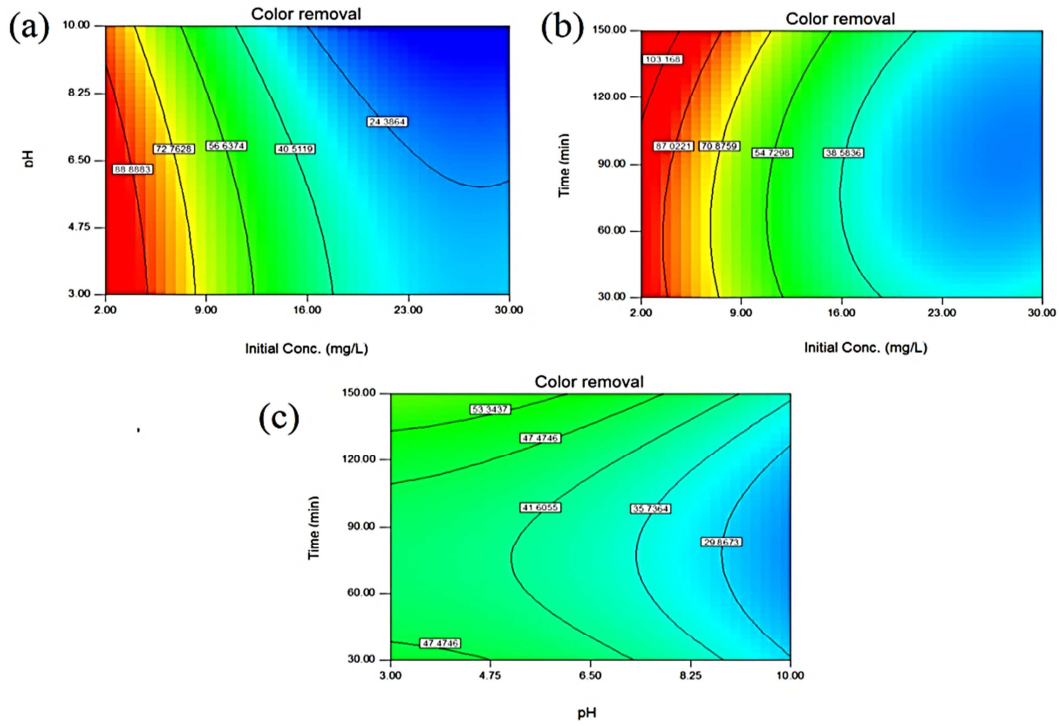

Figure 4. Two-dimensional plots for photocatalytic color removal

Based on literature review, ZnO nanostructures have many applications in catalyst configuration. ZnO nanostructures are used for color and dye degradation (Table 4). Accordingly, relatively complete removal efficiency is provided for ZnO nanomaterial.

3.4 Optimization

To achieve maximized performance, the desired goal for operational parameters was the "within the range" status, while "maximum removal" was selected as the humic substances degradation and color removal efficiency. Therefore, the optimal points of working conditions and predicated removal efficiencies of ammonia were established. Table 5 illustrates the optimal processing conditions

Table 4. Literature review

Catalyst type of ZnO	Target	Removal efficiency	References
ZnO	Photocatalytic degradation of model textile dyes	-	Chakrabarti[30]
UV/ZnO and photo-Fenton	organic reactive dye	74.2% TOC removal, 100% color removal	Peternel[31]
nano-sized ZnO and composite TiO2/ZnO powders under ultrasonic irradiation	degradation of some dyestuffs	-	Wang [32]
hydrothermally synthesized ZnO	rhodamine B dye	~ 100% color removal	Byrappa[33]
Macroporous ZnO/MoO3/SiO2	Removal of organic dye (Safranin T)	95.4%,TOC removal 95.3%, Decolorization 93.2%COD removal	Yuan [34]
ZnO@graphene composite	removal of dye from water	~ 100% color removal	Li[35]

Table 5. Optimal processing conditions from numerical optimization

Initial concentration	pH	Time	Degradation (%)	Color removal (%)
7.68	4.42	125.68	100	82.37

Conclusion

The effects of the main independent parameters such as initial humic substance concentration, initial pH, and contact time on the photocatalytic degradation of humic substances as expressed by the humic substances degradation and color removal percentages were presented based on the application of RSM. A similar pattern was observed in humic substances degradation and color removal. Higher removal efficiency was obtained with lower amounts of initial concentration and pH values and increasing pH. The optimum conditions were initial concentration of 7.68 mg/l, pH of 4.42, and contact time of about 125.6 minutes. The results showed that the immobilized form of ZnO can be used as an efficient nanocatalyst for effective degradation of humic substances in water.

Conflict of Interests

Authors have no conflict of interests.

Acknowledgements

The authors would like to thank the Deputy of Research of Kurdistan University of Medical Sciences (Iran) for their financial supports.

References

1. Valencia S, Marin J, Velasquez J, Restrepo G, Frimmel FH. Study of pH effects on the evolution of properties of brown-water natural organic matter as revealed by size-exclusion chromatography during photocatalytic degradation. Water Research 2012; 46(4): 1198-206.
2. Maleki A, Safari M, Shahmoradi B, Zandsalimi Y, Daraei H, Gharibi F. Photocatalytic degradation of humic substances in aqueous solution using Cu-doped ZnO nanoparticles under natural sunlight irradiation. Environ Sci Pollut Res Int 2015; 22(21): 16875-80.
3. Yuan R, Zhou B, Hua D, Shi C. Enhanced photocatalytic degradation of humic acids using Al and Fe co-doped TiO2 nanotubes under UV/ozonation for drinking water purification. J Hazard Mater 2013; 262: 527-38.
4. Remoundaki E, Vidali R, Kousi P, Hatzikioseyian A, Tsezos M. Photolytic and photocatalytic alterations of humic substances in UV (254 nm) and Solar Cocentric Parabolic Concentrator (CPC) reactors. Desalination 2009; 248(1-3): 843-51.
5. Wang X, Wu Z, Wang Y, Wang W, Wang X, Bu Y, et al. Adsorption-photodegradation of humic acid in water by using ZnO coupled TiO2/bamboo charcoal under visible light irradiation. J Hazard Mater 2013; 262: 16-24.
6. Parilti NB, Demirel CSU, Bekbolet M. Response surface methodological approach for the assessment of the photocatalytic degradation of NOM. J Photoch Photobio A 2011; 225(1): 26-35.
7. Valencia S, Marin JM, Restrepo G, Frimmel FH. Application of excitation-emission fluorescence matrices and UV/Vis absorption to monitoring the photocatalytic degradation of commercial humic acid. Sci Total Environ 2013; 442: 207-14.
8. Selcuk H, Bekbolet M. Photocatalytic and photoelectrocatalytic humic acid removal and selectivity of TiO(2) coated photoanode. Chemosphere 2008; 73(5): 854-8.
9. Songlin W, Ning Z, Si W, Qi Z, Zhi Y. Modeling the oxidation kinetics of sono-activated persulfate's process on the degradation of humic acid. Ultrason Sonochem 2015; 23: 128-34.
10. Amin MM, Safari M, Maleki A, Ghasemian M, Rezaee R, Hashemi H. Feasibility of humic substances removal by enhanced coagulation process in surface water. Int J Env Health Eng 2012; 1: 29.
11. Jafari A, Mahvi AH, Nasseri S, Rashidi A, Nabizadeh R, Rezaee R. Ultrafiltration of natural organic matter from water by vertically

aligned carbon nanotube membrane. J Environ Health Sci Eng 2015; 13: 51.
12. Ulu F, Barsci S, Kobya M, Sarkka H, Sillanpaa M. Removal of humic substances by electrocoagulation (EC) process and characterization of floc size growth mechanism under optimum conditions. Sep Purif Technol 2014; 133: 246-53.
13. Li C, Dong Y, Wu D, Peng L, Kong H. Surfactant modified zeolite as adsorbent for removal of humic acid from water. Appl Clay Sci 2011; 52(4): 353-7.
14. Mahvi A, Maleki A, Rezaee R, Safari M. Reduction of humic substances in water by application of ultrasound waves and ultraviolet irradiation. Journal of Environmental Health Science & Engineering 2009; 6(4): 233-40.
15. Yuan R, Zhou B, Zhang X, Guan H. Photocatalytic degradation of humic acids using substrate-supported Fe(3+)-doped TiO2 nanotubes under UV/O3 for water purification. Environ Sci Pollut Res Int 2015; 22(22): 17955-64.
16. Soltani RDC, Rezaee A, Khataee AR, Safari M. Photocatalytic process by immobilized carbon black/ZnO nanocomposite for dye removal from aqueous medium: Optimization by response surface methodology. J Ind Eng Chem 2014; 20(4): 1861-8.
17. Zandsalimi Y, Teymouri P, Darvishi Cheshmeh Soltani R, Rezaee R, Abdullahi N, Safari M. Photocatalytic removal of Acid Red 88 dye using zinc oxide nanoparticles fixed on glass plates. J AdvEnviron Health Res 2015; 3(2): 102-10.
18. Khataee AR, Pons MN, Zahraa O. Photocatalytic degradation of three azo dyes using immobilized TiO2 nanoparticles on glass plates activated by UV light irradiation: influence of dye molecular structure. J Hazard Mater 2009; 168(1): 451-7.
19. Sen Kavurmaci S, Bekbolet M. Photocatalytic degradation of humic acid in the presence of montmorillonite. Appl Clay Sci 2013; 75–76: 60-6.
20. Darvishi Cheshmeh Soltani R, Rezaee A, Rezaee R, Safari M, Hashemi H. Photocatalytic degradation of methylene blue dye over immobilized ZnO nanoparticles: Optimization of calcination conditions. J Adv Environ Health Res 2015; 3(1): 8-14.
21. Darvishi Cheshmeh Soltani R, Khataee AR, Godini H, Safari M, Ghanadzadeh MJ, Rajaei MS. Response surface methodological evaluation of the adsorption of textile dye onto biosilica/alginate nanobiocomposite: Thermodynamic, kinetic, and isotherm studies. Desalination and Water Treatment 2015; 56(5): 1389-402.
22. Vepsalainen M, Ghiasvand M, Selin J, Pienimaa J, Repo E, Pulliainen M, et al. Investigations of the effects of temperature and initial sample pH on natural organic matter (NOM) removal with electrocoagulation using response surface method (RSM). Sep Purif Technol 2009; 69(3): 255-61.
23. Darvishi Cheshmeh Soltani R, Rezaee A, Safari M, Khataee AR, Karimi B. Photocatalytic degradation of formaldehyde in aqueous solution using ZnO nanoparticles immobilized on glass plates. Desalination and Water Treatment 2015; 53(6): 1613-20.
24. Hossini H, Rezaee A, Ayati B, Mahvi AA. Optimizing ammonia volatilization by air stripping from aquatic solutions using response surface methodology (RSM). Desalination and Water Treatment 2015.
25. Masoumbaigi H, Rezaee A, Hosseini H, Hashemi SA. Water disinfection by zinc oxide nanoparticle prepared with solution combustion method. Desalination and Water Treatment 2015; 56(9): 2376-81.
26. Bashir MJK, Aziz HA, Yusoff MS, Adlan M. Application of response surface methodology (RSM) for optimization of ammoniacal nitrogen removal from semi-aerobic landfill leachate using ion exchange resin. Desalination 2010; 254(1–3): 154-61.
27. Akyol A, Bayramoglu M. Photocatalytic degradation of Remazol Red F3B using ZnO catalyst. J Hazard Mater 2005; 124(1-3): 241-6.
28. Hoseinzadeh E, Alikhani MY, Samarghandi MR, Shirzad-Siboni M. Antimicrobial potential of synthesized zinc oxide nanoparticles against gram positive and gram negative bacteria. Desalination and Water Treatment 2014; 52(25-27): 4969-76.
29. Xue G, Liu H, Chen Q, Hills C, Tyrer M, Innocent F. Synergy between surface adsorption

and photocatalysis during degradation of humic acid on TiO2/activated carbon composites. J Hazard Mater 2011; 186(1): 765-72.
30. Chakrabarti S, Dutta BK. Photocatalytic degradation of model textile dyes in wastewater using ZnO as semiconductor catalyst. J Hazard Mater 2004; 112(3): 269-78.
31. Peternel IT, Koprivanac N, Bozic AM, Kusic HM. Comparative study of UV/TiO2, UV/ZnO and photo-Fenton processes for the organic reactive dye degradation in aqueous solution. J Hazard Mater 2007; 148(1-2): 477-84.
32. Wang J, Jiang Z, Zhang L, Kang P, Xie Y, Lv Y, et al. Sonocatalytic degradation of some dyestuffs and comparison of catalytic activities of nano-sized TiO2, nano-sized ZnO and composite TiO2/ZnO powders under ultrasonic irradiation. Ultrason Sonochem 2009; 16(2): 225-31.
33. Byrappa K, Subramani AK, Ananda S, Lokanatha Rai KM, Dinesh R, Yoshimura M. Photocatalytic degradation of rhodamine B dye using hydrothermally synthesized ZnO. B Mater Sci 2006; 29(5): 433-8.
34. Yuan M, Wang S, Wang X, Zhao L, Hao T. Removal of organic dye by air and macroporous ZnO/MoO3/SiO2 hybrid under room conditions. Appl Surf Sci 2011; 257(18): 7913-9.
35. Li B, Cao H. ZnO@graphene composite with enhanced performance for the removal of dye from water. J Mater Chem. J Mater Chem 2011; 21(10): 3346-9.

JAEHR Journal of Advances in Environmental Health Research

Reproductive health indicators of immature common carp exposed to municipal wastewater of Behbahan, Iran

Mahdi Banaee[1], Somayeh Tahery[1], Maryam Vaziriyan[1], Shima Shahafve[1], Behzad Nemadoost-Haghi[1]

1 Department of Aquaculture, School of Natural Resource and Environment, Behbahan Khatam Alanbia University of Technology, Behbahan, Iran

Original Article

Abstract

Exogenous estrogens or pollutants with estrogen-like activity can induce vitellogenin (VTG) synthesis in male and juvenile fish, making this protein a useful indicator of chemicals that mimic estrogenic activity. The purpose of this study was to investigate the impact of municipal wastewater on blood biochemical parameters of common carp (Cyprinus carpio). Under experimental conditions, biomarkers such as sex steroid levels, alkali-labile phosphate levels, cholesterol and triglycerides, high-density lipoprotein (HDL), and low-density lipoprotein (LDL) were assessed in immature fish exposed to municipal wastewaters collected from a sewage canal in Behbahan, Khuzestan Province, Iran. No significant changes were found in testosterone levels on day 21; however, estradiol, alkali-labile phosphate, triglycerides, cholesterol, and LDL-cholesterol significantly increased in the fish exposed to municipal wastewater compared with the control group. A significant decrease in HDL-cholesterol levels was observed in the fish exposed to municipal wastewater at the end of the experiment. In conclusion, the results of the present study indicated that sewage effluent of Behbahan may contain endocrine disrupters and exposure to sublethal concentrations of municipal wastewater may cause dysfunction in reproductive health indicators of common carp.

KEYWORDS: Alkali-Labile Phosphate, Carp, Endocrine Disrupting Chemicals, Municipal Wastewater

Date of submission: 15 Apr 2015, ***Date of acceptance:*** 15 Jun 2015

Citation: Banaee M, Tahery S, Vaziriyan M, Shahafve Sh, Nemadoost-Haghi B. **Reproductive health indicators of immature common carp exposed to municipal wastewater of Behbahan, Iran.** J Adv Environ Health Res 2015; 3(3): 164-71.

Introduction

While 300 cities and towns in Iran are thinking of new ways to use wastewater, most cities leave their wastewater untreated to find its way to ground basins. Moreover, 75 cities use traditional systems of wastewater collection and the raw wastewater is used for irrigation or is directly discharged into channels.[1] The total wastewater generated annually in this country is increasing faster than the development of wastewater treatment plants. In 2004–2005, 4% of the wastewater produced in Iran was from households and other municipal sources, while about 96% of it was generated by industrial and commercial sectors. However, there is no exact figure for the amount of wastewater generated in the agricultural section and only 10 to 30% of it is treated in wastewater treatment plants. In fact, a significant portion of municipal and industrial sewage is discharged into underground and surface water or used in farmlands without any treatment.[1]

The millions of cubic meters of untreated sewage discharged into surface water reservoirs can have a significant effect on the

Corresponding Author:
Mahdi Banaee
Email: mahdibanaee2@gmail.com

health of aquatic organisms.[2-4] Literature reviews show that sewage effluents contain a complex mixture of substances including endocrine disrupting chemicals (EDCs) and pharmaceuticals.[5] These chemicals are poorly removed in the sewage system,[5,6] thus increasing their presence in the aquatic environment. This results in substantial effects of EDCs on aquatic organisms; effects which are amplified by almost continual exposure to manufactured compounds designed to persist in the environment.

Changes in the levels of sex hormones and gonad size, increased or decreased vitellogenin (VTG)[7,8] and delayed sexual maturation, decreased fecundity, testicular and ovarian damage[9], and steroidogenesis disruption[10], alterations in reproductive and parental behavior[11,12], impaired olfactory function and reproductive migration disorder[13,14], and courtship behavior deficits of male and female fish, and delay time of spawning[10,15] are the most important physiological changes observed in fish exposed to municipal wastewater.

Many rivers have been contaminated with effluents in recent decades; therefore, their fish populations have experienced a degree of chemical exposure throughout their lifetime. Lack of urban wastewater treatment plants and a considerable volume of surface runoff are among the most important environmental issues in Khuzestan Province, Iran. These issues have adverse effects on the health of the area's wildlife and residents.

The hypothesis for this study is that a high percentage of EDCs and pharmaceuticals are found in sewage canals in Behbahan, Khuzestan Province. It is therefore hypothesized that fish directly exposed to sewage effluents will exhibit signs of changes in blood biochemical parameters. Therefore, the main purpose of this study was to investigate estrogenic and androgenic effects of EDCs in municipal wastewater on blood biochemical parameters of common carp (Cyprinus carpio). Common carp were chosen as the studied species because they are more resistant to temperature fluctuations and laboratory conditions compared to other fish species, and have been shown to respond to sewage effluent exposure in a way similar to fish species native[16,17] to Maroon River (Behbahan).

Materials and Methods

In the present study, 144 immature common carp (mean weight: 42.75 ± 5.45 g) were obtained from a private farm (Behbahan, Iran). The fish were maintained in 80-l tanks filled with 70 l of aerated water at the animal holding facilities of the Department of Fisheries and Aquaculture, Behbahan Khatam Alanbia University, Iran. Water quality was monitored daily for deionized ammonia (< 0.05 mg/l), dissolved oxygen (6.5 ± 0.5 mg/l), temperature (24 ± 2 °C), and pH (7.4 ± 0.2). The experiment was performed after a 2-week acclimation period. During the experiment, the fish were fed a formulated diet obtained from Beyza Feed Mill (Shiraz, Iran).

Sewage samples were collected from 6 different stations of the sewage canal in Behbahan on 26 April 2015. During the 7 days prior to sampling, there was no rain in the sampling area and the minimum and maximum air temperature was 17–32 °C. Duplicates of each sample were collected in brown glass bottles with Teflon stoppers. In order to disinfect and remove pathogens from wastewater, it was filtered and autoclaved at 121 °C for 15 minutes before use.

The fish were placed into anesthetic solution (200 mg/l clove powder) for 3-5 minutes before being weighed individually. The fish were randomly assigned to 4 groups and were placed in 12 80-l plastic tanks which were filled with 70 l of water. Group I fish were maintained in tap water as the control group. Group II was considered as a positive control in this experiment. Anesthetized common carp were intramuscularly injected with an estradiol

valerate (50 mg/Kg body weight/week) in 2 stages with an interval of 1 week.[18,19] Injections were carried out using sterile 1 ml syringes and 26-gauge needles. Group III and IV fish were maintained for 21 days[19] in water, respectively, polluted with 0.1 and 0.2 ml per liter of municipal wastewater collected from a sewage canal in Behbahan (equivalent of 7 ml and 14 ml per 70 l). Tanks were cleaned via siphoning and 40% of the water was changed daily to reduce the production of metabolic wastes and municipal wastewater was added to maintain municipal wastewater concentration constant (equivalent of 0.1 and 0.2 ml per l).

At the end of the experiment, each group of fish was harvested using a scoop net and immersed in anesthetic solution (200 mg/l clove powder). Using heparinized syringes, blood samples were collected from the caudal vein, centrifuged immediately at 6000 × g for 10 minutes, and stored at -25 °C.

Plasma samples were extracted twice with diethyl ether, and concentrations of testosterone and 17ß-estradiol were measured using competitive enzyme-linked immunosorbent assay (ELISA) as described by Hecker et al.[20]

Levels of VTG-like proteins in the plasma were immediately determined using an alkali-labile phosphate method and the quantity of alkali-labile phosphate in the plasma was obtained in a way similar to that used by Gange and Blaise.[21] Briefly, 500 µl of plasma was mixed with 500 µl of t-butyl methyl ether and incubated at room temperature for 30 minutes. The emulsion was centrifuged at 10000 × g for 10 minutes at 4 °C. The supernatant was mixed with 100 µl of 2 M NaOH for 60-90 minutes at 37 °C. Levels of free phosphates were determined according to the phosphomolybdenum method, and the optical absorbance was read at 660 nm.

The plasma biochemical parameters were assayed by enzymatic procedures using a UV/VIS spectrophotometer (UNICO 2100, USA). Plasma biochemical parameters including cholesterol, high density lipoprotein cholesterol (HDL-C), low density lipoprotein cholesterol (LDL-C), and triglycerides were tested using assay kits obtained from Pars Azmoon Co., Iran.

Difference in the biochemical characteristics of fish exposed to different concentrations of municipal wastewater was examined using one-way ANOVA. Data were examined for normality (Kolmogorov-Smirnov test). Significant means were compared using Duncan's test and P-values of less than 0.05 were considered statistically significant. Statistical analyses were performed using SPSS software (version 19, IBM Corp., Chicago, IL, USA). Data are presented as mean ± SD.

Results and Discussion

In this study, the effects of exposure to municipal effluent on the health and physiological response of fish were examined. Toxicants and xenobiotics which are found in sewage effluents have multiple effects on the health and biodiversity of aquatic organisms.[2-4] Many xenobiotics show endocrine disrupting properties and are mainly the result of human activities. Three main categories of estrogenic EDCs including steroidal estrogens, phenolic compounds, and phthalate esters are found in sewage effluents in low concentrations.[22-24] The main source of these chemicals in domestic sewage is human waste.[25] No mortality was observed during the experiment.

Figure 1 shows the effects of intramuscular administration of estradiol valerate, and exposure to municipal wastewater on estradiol in immature fish. Plasma levels of 17β-estradiol (E2) significantly increased in experimental fish when compared to the control group ($P < 0.05$). However, E2 levels in the fish treated with estradiol valerate was significantly higher than those in fish exposed to municipal wastewater (Figure 1). The present study indicates that municipal wastewater shows some estrogenic activity, as

suggested by the increased E2 levels in exposed immature common carp. E2 seems to be affected by exposure to municipal sewage effluent, as shown by E2 increase both in fish exposed to 0.1 and 0.2 ml of municipal wastewater. Therefore, municipal wastewater may have a specific effect on estradiol levels in the plasma of immature fish. Alterations in sex hormone were reported in crucian carp, Carassius carassius, exposed to treated sewage effluent.[26]

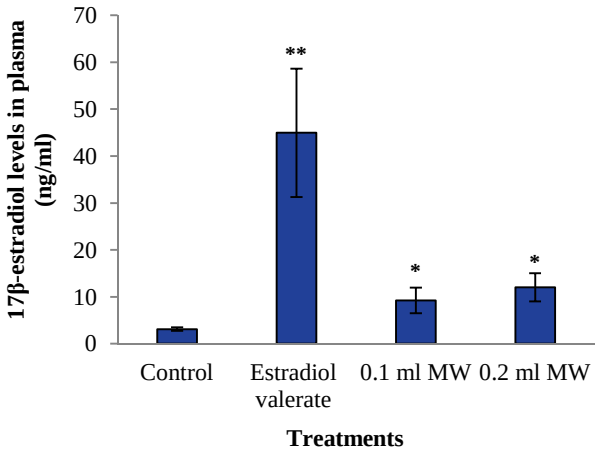

Figure 1. Plasma 17β-estradiol levels in immature common carp treated with estradiol valerate and different concentrations of municipal wastewater for 21 days (mean ± SD) (n = 9)

Asterisk (*) indicates that the difference between the experimental and control groups was significant at P < 0.05

Xenobiotics with estrogenic properties can bind to nuclear estrogen receptors in fish. This in turn may affect testicular androgen production.[27] Nevertheless, in the present study, no statistical differences were detected in testosterone levels (Figure 2). Loomis and Thomas found that xenoestrogens have a negative effect on androgen production in fish.[27] Decreased plasma levels of 11-ketotestosterone, and VTG induction were observed in wild male chub living in water contaminated with sewage effluent.[28]

Figure 3 shows that the alkali-labile phosphate levels in the plasma of fish treated with estradiol valerate were much higher than those in other groups. Our results show that the alkali-labile phosphorus levels increased in fish exposed to sewage effluents, which may suggest induction of VTG synthesis caused by endocrine disruptor compounds present in sewage effluents (Figure 3). VTG is a blood protein normally synthesized by females during oocyte maturation, but VTG in male fish living downstream of wastewater outfalls can serve as a biomarker of exposure to environmental estrogens.[29]

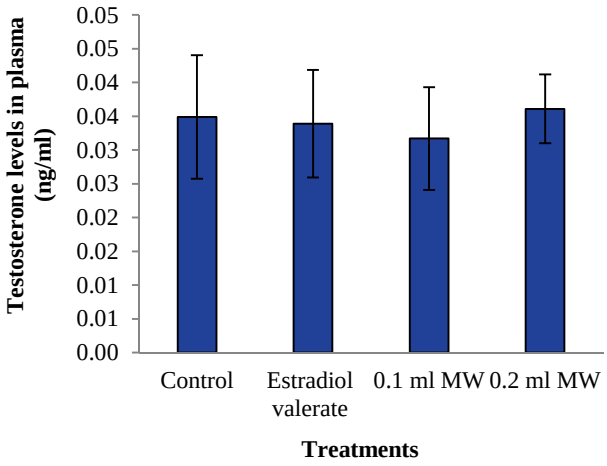

Figure 2. Plasma testosterone levels in immature common carp treated with estradiol valerate and different concentrations of municipal wastewater for 21 days (mean ± SD) (n = 9)

Asterisk (*) indicates that the difference between the experimental and control groups was significant at P < 0.05

Males and juveniles are also capable of VTG gene expression, but typically do not have sufficient circulating estrogens to stimulate a significant production of the protein.[29] Common carp VTG is a lipophosphoprotein (79% protein, 19% lipid, 0.6-0.8% alkali-labile phosphorus) that contains carbohydrate and binds calcium (0.3%).[30] The 19% lipid contains 13% phospholipids, 4% triglycerides, and 2% cholesterol. The presence of alkali-labile protein phosphorus in fish plasma is specifically associated with the lipophosphoprotein VTG. Increases in VTG induction in adult male fathead minnows,

Pimephales promelas,[31] and mirror carp, Cyprinus carpio,[32] exposed to treated municipal sewage effluent confirms the results of the present study. Elevated serum VTG levels were reported in C. carassius exposed to treated sewage effluent in laboratory conditions.[26]

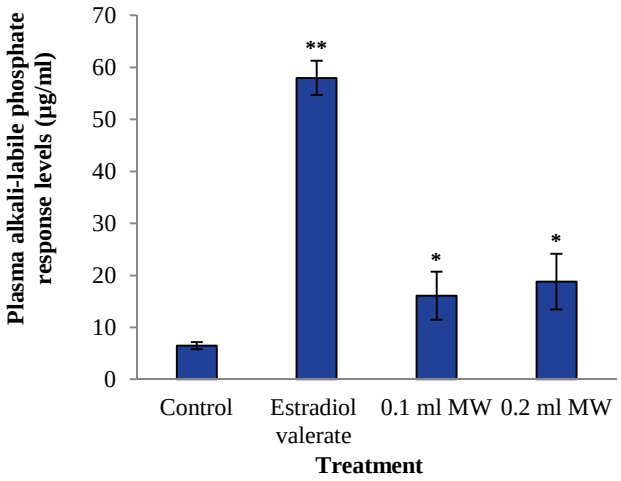

Figure 3. Plasma alkali-labile phosphate levels in immature common carp treated with estradiol valerate and different concentrations of municipal wastewater for 21 days (mean ± SD) (n = 9)
Asterisk (*) indicates that the difference between the experimental and control groups was significant at P < 0.05

Cholesterol serves as the substrate for all steroid hormones.[33] Results show that exposure to municipal wastewater significantly (P < 0.05) increased plasma cholesterol levels in fish (Figure 4). This effect appears to be due to an increase in the detoxification rate of environmental estrogens in liver tissue. Increase in stress hormones such as cortisol in blood of fish exposed to municipal wastewater, which stimulates lipid breakdown in adipose tissue, has been reported by Ikonomou et al.[34] and Quinn et al.[35] Moreover, destruction of cell membranes can also lead to increased levels of cholesterol in plasma. Significant changes in cholesterol, HDL-C, and LDL-C levels in plasma of fish exposed to treated sewage effluents were reported by Samuelsson et al.[36]

Triglyceride levels significantly (P < 0.05) increased in both fish treated with estradiol valerate and municipal wastewater compared with the control group (Figure 5). The higher triglyceride levels may be associated with both a reduction in the uptake of triglycerides in adipose tissue and liver dysfunction.

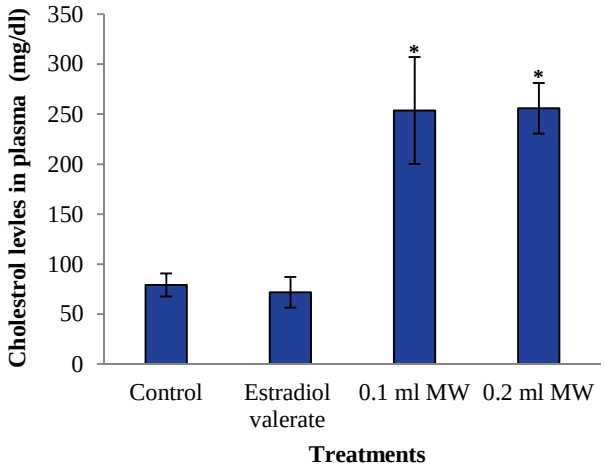

Figure 4. Plasma cholesterol levels in immature common carp treated with estradiol valerate and different concentrations of municipal wastewater for 21 days (mean ± SD) (n = 9)
Asterisk (*) indicates that the difference between the experimental and control groups was significant at P < 0.05

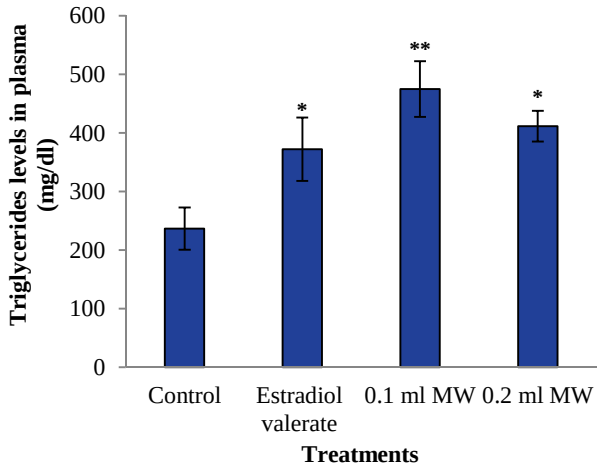

Figure 5. Plasma triglyceride levels in immature common carp treated with estradiol valerate and different concentrations of municipal wastewater for 21 days (mean ± SD) (n = 9)
Asterisk (*) indicates that the difference between the experimental and control groups was significant at P < 0.05

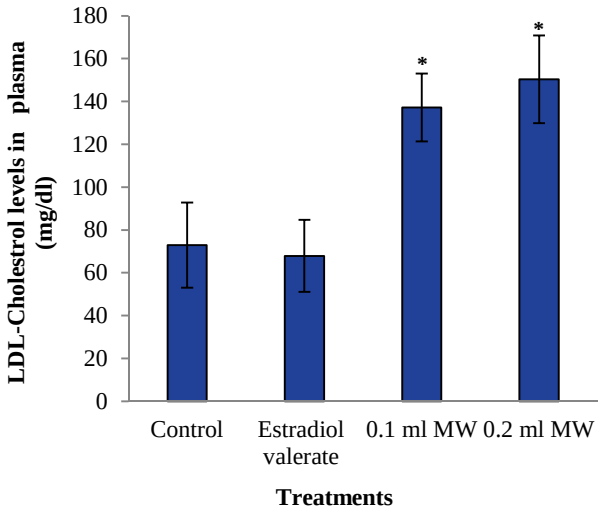

Figure 6. Plasma low-density lipoprotein cholesterol levels in immature common carp treated with estradiol valerate and different concentrations of municipal wastewater for 21 days (mean ± SD) (n = 9)

Asterisk (*) indicates that the difference between the experimental and control groups was significant at P < 0.05

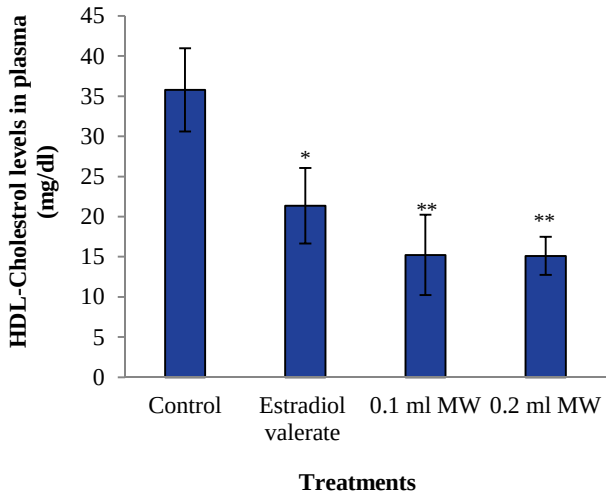

Figure 7. Plasma high-density lipoprotein cholesterol levels in immature common carp treated with estradiol valerate and different concentrations of municipal wastewater for 21 days (mean ± SD) (n = 9)

Asterisk (*) indicates that the difference between the experimental and control groups was significant at P < 0.05

Although a significant increase was observed in plasma LDL-C levels of fish exposed to municipal wastewater (Figure 6), no significant difference was observed in LDL-C levels between fish treated with estradiol valerate and the control group. The significant increase in plasma LDL-C levels in fish exposed to municipal sewage effluent may be correlated with the role of LDL in delivering cholesterol to cells for the synthesis of steroid and corticosteroid hormones in the adrenal glands.

Plasma HDL-C levels were significantly ($P < 0.05$) lower in immature common carp exposed to municipal wastewater than in the control group (Figure 7). Available evidence indicates that estrogens can have significant effects on the rate of syntheses and secretion of HDL in the liver and intestines.[37] The decreased HDL in the fish exposed to sewage effluent might affect the excretion of excess cholesterol from the body via the liver, which secretes cholesterol in bile or converts it to bile salts. Studies have shown that administration of estrogen can decrease HDL-C.[37]

Conclusion

This study shows that municipal wastewater effluents collected from a sewage canal in Behbahan possess estrogenic activity. This is clearly shown by increased alkali-labile phosphate and estradiol levels, which provide evidence of the presence chemical compounds capable of affecting the endocrine system of fish in municipal sewage effluents in Behbahan.

Conflict of Interests

Authors have no conflict of interests.

Acknowledgements

This study was supported by a grant from Behbahan Khatam Alanbia University of Technology. Moreover, the authors are grateful to Ms. Maryam Banaee for proofreading the manuscript.

References

1. Shaigan JA, Afshari A. The treatment situation of municipal and industrial wastewater in Iran. Water and Wastewater 2004; 15(1): 58-69. [In Persian].

2. Jobling S, Tyler CR. Introduction: The ecological relevance of chemically induced endocrine disruption in wildlife. Environ Health Perspect 2006; 114(Suppl 1): 7-8.
3. Jobling S, Burn RW, Thorpe K, Williams R, Tyler C. Statistical modeling suggests that antiandrogens in effluents from wastewater treatment works contribute to widespread sexual disruption in fish living in English rivers. Environ Health Perspect 2009; 117(5): 797-802.
4. Gilbert N. Water under pressure. Nature 2012; 483(7389): 256-7.
5. Kanda R, Churchley J. Removal of endocrine disrupting compounds during conventional wastewater treatment. Environ Technol 2008; 29(3): 315-23.
6. Johnson AC, Sumpter JP. Removal of endocrine-disrupting chemicals in activated sludge treatment works. Environ Sci Technol 2001; 35(24): 4697-703.
7. Orn S, Svenson A, Viktor T, Holbech H, Norrgren L. Male-biased sex ratios and vitellogenin induction in zebrafish exposed to effluent water from a Swedish pulp mill. Arch Environ Contam Toxicol 2006; 51(3): 445-51.
8. Miller DH, Jensen KM, Villeneuve DL, Kahl MD, Makynen EA, Durhan EJ, et al. Linkage of biochemical responses to population-level effects: a case study with vitellogenin in the fathead minnow (Pimephales promelas). Environ Toxicol Chem 2007; 26(3): 521-7.
9. Woodling JD, Lopez EM, Maldonado TA, Norris DO, Vajda AM. Intersex and other reproductive disruption of fish in wastewater effluent dominated Colorado streams. Comp Biochem Physiol C Toxicol Pharmacol 2006; 144(1): 10-5.
10. Al-Salhi R, Abdul-Sada A, Lange A, Tyler CR, Hill EM. The xenometabolome and novel contaminant markers in fish exposed to a wastewater treatment works effluent. Environ Sci Technol 2012; 46(16): 9080-8.
11. Coe TS, Soffker MK, Filby AL, Hodgson D, Tyler CR. Impacts of early life exposure to estrogen on subsequent breeding behavior and reproductive success in zebrafish. Environ Sci Technol 2010; 44(16): 6481-7.
12. Harris CA, Hamilton PB, Runnalls TJ, Vinciotti V, Henshaw A, Hodgson D, et al. The consequences of feminization in breeding groups of wild fish. Environ Health Perspect 2011; 119(3): 306-11.
13. Kolodziej EP, Gray JL, Sedlak DL. Quantification of steroid hormones with pheromonal properties in municipal wastewater effluent. Environ Toxicol Chem 2003; 22(11): 2622-9.
14. Geem ZW, Kim JH. Wastewater treatment optimization for fish migration using harmony search. MATH PROBL ENG 2014; 2014: 5.
15. Coe TS, Hamilton PB, Hodgson D, Paull GC, Tyler CR. Parentage outcomes in response to estrogen exposure are modified by social grouping in zebrafish. Environ Sci Technol 2009; 43(21): 8400-5.
16. Barber LB, Loyo-Rosales JE, Rice CP, Minarik TA, Oskouie AK. Endocrine disrupting alkylphenolic chemicals and other contaminants in wastewater treatment plant effluents, urban streams, and fish in the Great Lakes and Upper Mississippi River Regions. Sci Total Environ 2015; 517: 195-206.
17. Gilannejad N, Dorafshan S, Heyrati FP, Soofiani NM, Asadollah S, Martos-Sitcha JA, et al. Vitellogenin expression in wild cyprinid Petroleuciscus esfahani as a biomarker of endocrine disruption along the Zayandeh Roud River, Iran. Chemosphere 2016; 144: 1342-50.
18. Wang J, Bing X, Yu K, Tian H, Wang W, Ru S. Preparation of a polyclonal antibody against goldfish (Carassius auratus) vitellogenin and its application to detect the estrogenic effects of monocrotophos pesticide. Ecotoxicol Environ Saf 2015; 111: 109-16.
19. Wang J, Wang W, Zhang X, Tian H, Ru S. Development of a lipovitellin-based goldfish (Carassius auratus) vitellogenin ELISA for detection of environmental estrogens. Chemosphere 2015; 132: 166-71.
20. Hecker M, Kim WJ, Park JW, Murphy MB, Villeneuve D, Coady KK, et al. Plasma concentrations of estradiol and testosterone, gonadal aromatase activity and ultrastructure of the testis in Xenopus laevis exposed to estradiol or atrazine. Aquat Toxicol 2005; 72(4): 383-96.
21. Gagne F, Blaise C. Organic alkali-labile phosphates in biological materials: A generic assay to detect vitellogenin in biological tissues. Environmental Toxicology 2000; 15(3): 243-7.
22. Snyder SA, Villeneuve DL, Snyder EM, Giesy JP. Identification and quantification of estrogen receptor agonists in wastewater effluents. Environ Sci Technol 2001; 35(18): 3620-5.
23. Folmar LC, Hemmer M, Denslow ND, Kroll K, Chen J, Cheek A, et al. A comparison of the estrogenic potencies of estradiol, ethynylestradiol, diethylstilbestrol, nonylphenol and methoxychlor in vivo and in vitro. Aquat Toxicol 2002; 60(1-2): 101-10.
24. Rutishauser BV, Pesonen M, Escher BI, Ackermann GE, Aerni HR, Suter MJ, et al. Comparative analysis of estrogenic activity in sewage treatment plant effluents involving three in vitro assays and chemical analysis of steroids. Environ Toxicol Chem 2004; 23(4): 857-64.
25. Shore LS, Shemesh M. Naturally produced steroid

hormones and their release into the environment. Pure Appl Chem 2003; 75(11-12): 1859-71.
26. Diniz MS, Peres I, Magalhaes-Antoine I, Falla J, Pihan JC. Estrogenic effects in crucian carp (Carassius carassius) exposed to treated sewage effluent. Ecotoxicol Environ Saf 2005; 62(3): 427-35.
27. Loomis AK, Thomas P. Effects of estrogens and xenoestrogens on androgen production by Atlantic croaker testes in vitro: evidence for a nongenomic action mediated by an estrogen membrane receptor. Biol Reprod 2000; 62(4): 995-1004.
28. Randak T, Zlabek V, Pulkrabova J, Kolarova J, Kroupova H, Siroka Z, et al. Effects of pollution on chub in the River Elbe, Czech Republic. Ecotoxicol Environ Saf 2009; 72(3): 737-46.
29. Palumbo AJ. Vitellogenin, a marker of estrogen mimicking contaminants in fishes: Characterization, quantification and interference by anti-estrogens [PhD Thesis]. Berkeley, CA: University of California; 2008. p. 121.
30. Lv XF, Zhao YB, Zhou QF, Jiang GB, Song MY. Determination of alkali-labile phosphoprotein phosphorus from fish plasma using the Tb(3+)-tiron complex as a fluorescence probe. J Environ Sci (China) 2007; 19(5): 616-21.
31. Hemming JM, Allen HJ, Thuesen KA, Turner PK, Waller WT, Lazorchak JM, et al. Temporal and spatial variability in the estrogenicity of a municipal wastewater effluent. Ecotoxicol Environ Saf 2004; 57(3): 303-10.
32. Diniz MS, Peres I, Pihan JC. Comparative study of the estrogenic responses of mirror carp (Cyprinus carpio) exposed to treated municipal sewage effluent (Lisbon) during two periods in different seasons. Sci Total Environ 2005; 349(1-3): 129-39.
33. Murray RK, Bender DA, Botham KM, Kennelly PJ, Rodwell VW, Weil PA. Harpers illustrated biochemistry. 26th ed. New York, NY: McGraw-Hill Medical; 2003. p. 702.
34. Ikonomou MG, Cai SS, Fernandez MP, Blair JD, Fischer M. Ultra-trace analysis of multiple endocrine-disrupting chemicals in municipal and bleached kraft mill effluents using gas chromatography-high-resolution mass spectrometry. Environ Toxicol Chem 2008; 27(2): 243-51.
35. Quinn B, Gagne F, Costello M, McKenzie C, Wilson J, Mothersill C. The endocrine disrupting effect of municipal effluent on the zebra mussel (Dreissena polymorpha). Aquat Toxicol 2004; 66(3): 279-92.
36. Samuelsson LM, Bjorlenius B, Forlin L, Larsson DG. Reproducible (1)H NMR-based metabolomic responses in fish exposed to different sewage effluents in two separate studies. Environ Sci Technol 2011; 45(4): 1703-10.
37. Mardones P, Quinones V, Amigo L, Moreno M, Miquel JF, Schwarz M, et al. Hepatic cholesterol and bile acid metabolism and intestinal cholesterol absorption in scavenger receptor class B type I-deficient mice. J Lipid Res 2001; 42(2): 170-80.

JAEHR Journal of Advances in Environmental Health Research

Evaluation of corrosion and scaling potential of drinking water supply sources of Marivan villages, Iran

Shouresh Amini[1], Reza Rezaee[1], Ali Jafari[2], Afshin Maleki[1]

1 Environmental Health Research Center, Kurdistan University of Medical Sciences, Sanandaj, Iran
2 Department of Environmental Health Engineering, School of Health and Nutrition, Lorestan University of Medical Sciences, Khorramabad, Iran

Original Article

Abstract

Corrosion and scaling in drinking water sources can lead to economic and health damages. These processes produce by-products in distribution systems, reduce chemical water quality, and are the cause of health issues among consumers. The aim of this study was to evaluate the corrosion and scaling potential of water supply sources of Marivan villages, Iran. In total, 106 water samples were collected through grab sampling from 64 wells and 42 springs in Marivan villages. The values of the Langelier saturation index (LSI), Ryznar stability index (RSI), Aggressive index (AI), and Puckorius index (PI) were calculated using parameters such as temperature, calcium hardness, total alkalinity (TA), total dissolved solids (TDS), and pH according to the last edition of the standard methods. Based on the RSI, 3% of the springs and 9% of the wells were in stable condition, 97% of the springs were corrosive and 90% of the wells had scale forming potential. The LSI was positive for 57% of the springs and 78% of the wells. The AI value of 40% of the springs and 64% of the wells was higher than 12 and the PI value was lower than 6 for all the springs and wells. The results of this study indicated that most of the springs were corrosive and a few of them had scale-forming potential. It was also found that the wells had scaling tendency. Thus, routine monitoring of the sources is necessary to control corrosion and scaling and maintain water quality.

KEYWORDS: Water Quality, Corrosion, Scaling, Natural Springs, Water Wells

Date of submission: 18 Apr 2015, ***Date of acceptance:*** 12 Jun 2015

Citation: Amini Sh, Rezaee R, Jafari A, Maleki A. **Evaluation of corrosion and scaling potential of drinking water supply sources of Marivan villages, Iran.** J Adv Environ Health Res 2015; 3(3): 172-8.

Introduction

The provision of safe drinking water is an essential factor in maintaining and improving the health of a community. To achieve this target, the chemical quality of water is very important. Corrosion and scaling potentials are among the main indicators for water quality assessment. However, these phenomena are essential in the water industry and impact the economic, technical, engineering, and aesthetic dimensions, and consequently, have adverse effects on public health.[1] Scaling results in the formation of a hard deposition on surfaces due to saturation of water with dissolved solids. In this process, divalent metal ions combine with calcium and magnesium deposits and produce calcium carbonate, magnesium carbonate, calcium sulfate, and magnesium chloride.[2] Scaling can clog the pips, reduce the flow and performance of valves, and increase water pressure, energy efficiency, and the pumpage cost.[3] Corrosion is the decaying of a matter resulting from reaction with a media that can occur in the presence of physical, chemical, biological, or electrochemical activities.[1,4] Corrosion is influenced by multiple factors including physical (cavitations, erosion, and

Corresponding Author:
Afshin Maleki
Email: maleki43@yahoo.com

abrasion by sand), chemical (pH, CO_2, hardness, alkalinity, temperature, dissolved solids, oxygen concentration, residual chlorine, sulfate, and other chemical compounds), and biological agents (sulfate reducing bacteria, and iron bacteria).[5] Corrosive water in the presence of iron, zinc, copper, and manganese in solution can cause secondary pollution and produce odor, taste, and staining in water systems.[6] In addition, the products of corrosion and scaling can settle or accumulate in water sources and distribution networks and protect microbial agents from disinfection.[7] Annually, a significant amount of money is spent on corrosion and scaling problems. In addition to the costs for the repair and replacement of damaged pipes, more than 30% of water volume is lost due to the deterioration of transportation line and water systems.[8] Due to the importance of these processes in chemical water quality, and the health and economic damages caused by these factors, several measures have been proposed to predict the corrosion and scaling potential in water sources. These include the Langelier saturation index (LSI), Ryznar stability index (RSI), Aggressive index (AI), and Puckorius index (PI). Due to the limited application of other indices, they were not used in this research. The evaluation of the indices is based on their ability to determine the undersaturated, unsaturated, and saturated conditions in terms of calcium carbonate and predict the capacity of water for calcium carbonate scaling or dissolution.[9] Due to the importance of this issue, the aim of the present study was to investigate the corrosion and scale forming potential of water in Marivan villages, Iran.

Materials and Methods

Marivan is located in Kurdistan Province, Western Iran (35 º 48' to 2° 35' N and 46º 45' 45º to 58' W). The average annual temperature of Marivan is 21 ºC and average annual precipitation is about 1050 mm. The current population of Marivan is 178,000, 47,000 of whom are residents of rural areas and living in 145 villages. In general, 106 of the villages (study points of this study) are under the coverage of the Water And Wastewater Management Company of Marivan.

This cross-sectional study was conducted on samples from 64 wells and 42 springs in 2015. Temperature, conductivity, turbidity, and pH were measured on site. Sample volumes of 3 l were collected in prewashed polyethylene (PE) containers and immediately transferred to the laboratory for total dissolved solids (TDS), total hardness (TH), calcium hardness, and alkalinity measurements. All used chemicals and reagents were of analytical grade (Merck, Germany). The collection, preservation, and analysis of samples were performed according to standard methods.[10] Corrosion and scaling potential were calculated using the LSI, RSI, AI, and PI. The results of all the sampling locations and water supplies were recorded separately for each of the 4 corrosion indices. To increase the accuracy of the experiments and control experimental errors, all four indices were used in this study.

Water quality parameters were analyzed for each of the 106 water sources, and then, accordingly corrosion indices were calculated. First, the saturation pH (pHs) was calculated using the values of alkalinity, temperature, and pH according to equation (1).[11]

$$pH_s = (9.3 + A + B) - (C + D) \quad (1)$$

In this equation the values of A, B, C, and D were calculated using equations (2), (3), (4), and (5), respectively.[11]

$$A = (\mathrm{Log}[TDS] - 1)/10 \quad (2)$$
$$B = -3.12 \times \mathrm{Log}\,(°C + 273) + 34.55 \quad (3)$$
$$C = \mathrm{Log}^{10} - 0.4 \quad (4)$$
$$D = \mathrm{Log}^{10} \quad (5)$$

In the above equations, A was TDS (mg/l), B temperature (°C), C TH (mg/l of calcium carbonate), and D was total alkalinity (TA)

(mg/l of calcium carbonate). After calculating pHs, corrosion and scaling potential were calculated using the following formula:

$$LSI = pH - pH_s \quad (6)$$

The interpretation of LSI equation (6) is presented in table 1.[11]

The RSI equation (7) is presented below and its interpretation is presented in table 2.[12]

$$RI = 2\,(pH_s) - pH \quad (7)$$

Table 1. Langelier saturation index range

LSI value	State
LSI < 0	Corrosive
LSI = 0	Noncorrosive and no scaling
LSI > 0	Scaling

LSI: Langelier saturation index

Table 2. Ryznar saturation index range

RSI value	State
RSI < 5.5	Highly scaling
5.5 < RSI < 6.2	Scaling and slightly corrosive
6.2 < RSI < 6.8	Noncorrosive and no scaling
6.8 < RSI < 8.5	Corrosive and slightly scaling
RSI > 8.5	Highly corrosive

RSI: Ryznar stability index

The AI and its interpretation are presented in equation (8) and table 3, respectively.[13,14]

$$AI = pH - Log\,(A.H) \quad (8)$$

The PI equation (9) is presented below:

$$PI = 2\,pH_s - pH_{eq} \quad (9)$$

Where pH_{eq} is the pH of water calculated using equation (10).[15]

$$pH_{eq} = 1.465\,Log\,(T - AIK) + 4.54 \quad (10)$$

The interpretation of PI is presented in table 4.[15]

Table 3. Aggressive index values range

AI value	State
AI < 10	Highly corrosive
10 < AI < 12	Moderately corrosive
AI > 12	Slightly corrosive

AI: Aggressive index

Table 4. Interpretation of Puckorius index values

PI value	State
PI < 6	Scaling
PI > 6	Corrosive

PI: Puckorius index

The indices were calculated using Excel software and the results were analyzed using SPSS software (version 16, SPSS Inc., Chicago, IL, USA). Finally, the scaling and corrosion status of water sources was evaluated.

Results and Discussion

In order to assess the corrosion and scaling potential of drinking water supplies of Marivan rural areas, temperature, pH, TDS, calcium hardness, and TA were measured. Physical and chemical factors were examined for each of the sources and are presented in table 5 as the minimum, average, maximum, and standard deviation (SD).

Table 5. Minimum, average, maximum, and mean and standard deviation of the sources

Source	Parameter	Unit	Minimum	Average	Maximum	SD	National standard	
							Desirable	Permissible
Spring	T	°C	16.60	24.49	31.40	4.03	15	23
	pH	-	6.93	7.76	8.77	0.35	7-8.5	6.5-9
	TDS	mg/l	83.00	267.90	484.00	86.36	500	1500
	Ca	mg/l	18.30	67.88	94.45	18.68	25	200
	TA	mg/l as $Caco_3$	81.15	231.30	402.00	70.18	-	500
Well	T	°C	16.50	24.13	31.60	4.11	15	23
	pH	-	7.19	7.79	8.86	0.37	7-8.5	6.5-9
	TDS	mg/l	162.30	269.40	389.40	51.20	500	1500
	Ca	mg/l	44.50	85.34	138.10	18.67	25	200
	TA	mg/l as $Caco_3$	182.40	270.70	389.40	49.90	-	500

T: temperature; TDS: total dissolved solids; TA: total alkalinity

Among the 106 villages, the water supply sources of 64 rural areas (60.37%) were wells and 42 villages (39.63%) were springs. Based on the measured parameters (Table 5), the minimum, average, and maximum values of temperature in the two water supply sources (spring and wells) were almost equal. Moreover, pH values of the two supply sources were almost equal. The higher solubility of solids in the wells can be explained by the higher TDS of wells than springs. The average calcium in wells (67.88 mg/l) was higher than that of spring (85.34 mg/l). The average of TA (carbonate, bicarbonate, and hydroxides) in the well water supplies (270.7 mg/l $CaCO_3$) was also higher than that of springs (231.3 mg/l $CaCO_3$). The minimum, maximum, and average values of measured parameters in Marivan drinking water sources are presented in table 5. The result of analysis for each of the sources of drinking water was calculated according to the formulas listed for corrosion and scaling indices (LSI, RSI, AI, and PI) calculations. For each village, water supplies were coded according to their type, wells or springs. The calculated indices for each location code are presented in table 6. The minimum, average, maximum and standard deviation values for each index for both sources (well and spring) are presented in table 7.

Distributions of the indices were assessed according to the type of water supply. The results are presented in table 8. LSI of springs with corrosion value of 40.47% and scaling value of 57.14% revealed that some sources are corrosive and others are scale forming. However, a balanced state was only observed in location code S10. It is clear that the scaling location codes of wells (78.13%) are much more than corrosive codes (21.78%). RSI highlights that many springs (96.62%) were corrosive and none of the springs were scale forming. In sources provided by wells, RSI were different, scaling was 0, and sources were mostly corrosive (90.62%). Gupta et al. evaluated the groundwater of Kota city in Rajasthan, India, and assessed RSI and LSI.[15] They showed scale forming property to be the dominant characteristic of the groundwater resources.[15] Rabbani et al. studied the scaling and corrosion potential of rural water sources of Kashan, Iran, and showed that of the 39 sources, the sources in 18 villages were corrosive and in 21 villages were scaling.[16]

PI in both sources showed that 100% of all the sources were corrosive and none of the sources were scale forming. The PI of water samples with a pH of greater than 8 was more suitable; in this case, the results based on this index will be more accurate than other indices. Malakootian et al. examined scaling and corrosion potential of drinking water in Kerman, Iran, and reported that 40% of water supplies had PI values of greater than 6 and had corrosive potential.[17]

AI values, as a measure of the tendency of water to deteriorate the asbestos-cement pipes, revealed no corrosion potential in either source, while 40.48% and 59.52% of spring sources were scale forming and stable, respectively. However, 64.04% and 35.96% of well sources were scale forming and stable, respectively, and their scaling state was lower than springs. Shams et al. studied corrosion potential using AI.[18] They showed that AI with an average value of 12.1 indicated the low tendency of water supplies to corrosion state.[18]

Results of LSI, PI, and AI in the two types of water sources confirmed that there was almost no significant difference between the two sources. However, RSI revealed significant differences between corrosion and scaling potential of the sources; 97.62% of the springs tended to be corrosive, and scaling was 0, while well sources' tendency toward corrosion was 0 and their tendency toward scale forming was 90.62%.

Table 6. Corrosion and scaling potential values of rural drinking water sources

Code	LSI	RSI	PI	AI	code	LSI	RSI	PI	AI
W1	0.27	7.44	7.46	12.23	W54	-0.13	7.88	7.35	11.94
W2	0.22	7.46	7.33	12.18	W55	-0.03	7.84	7.59	12.02
W3	0.25	7.34	7.08	12.22	W56	-0.09	7.97	7.76	11.95
W4	0.08	7.49	7.08	12.07	W57	-0.07	7.85	7.56	11.97
W5	0.28	7.26	6.99	12.25	W58	-0.52	8.34	7.60	11.55
W6	0.15	7.39	6.99	12.13	W59	0.21	7.11	6.32	12.26
W7	0.80	6.69	6.93	12.79	W60	0.19	7.16	6.38	12.26
W8	0.38	7.26	7.32	12.35	W61	0.23	7.26	6.77	12.27
W9	0.62	6.96	7.12	12.59	W62	-0.02	7.49	6.78	11.97
W10	0.40	7.24	7.19	12.34	W63	0.02	7.45	6.82	12.01
W11	0.34	7.13	6.73	12.28	W64	0.11	7.25	6.45	12.13
W12	0.29	7.18	6.70	12.25	S1	0.11	7.54	7.33	12.07
W13	1.05	6.68	7.46	12.97	S2	0.12	7.46	7.03	12.10
W14	1.17	6.48	7.32	13.09	S3	0.34	7.31	7.25	12.31
W15	0.36	7.12	6.91	12.23	S4	0.33	7.51	7.84	12.28
W16	1.07	6.67	7.46	13.00	S5	-0.08	8.19	8.44	11.88
W17	-0.01	7.61	7.20	11.87	S6	-0.80	9.49	10.04	11.10
W18	-0.06	7.70	7.30	11.82	S7	-0.45	8.69	8.90	11.48
W19	0.02	7.53	7.04	11.93	S8	0.28	7.41	7.41	12.18
W20	0.14	7.30	6.74	12.01	S9	-0.68	8.94	8.45	11.23
W21	0.01	7.43	6.67	11.88	S10	0.00	7.42	6.49	11.95
W22	0.42	7.17	7.13	12.27	S11	0.09	7.57	7.36	12.00
W23	0.31	7.16	6.84	12.19	S12	0.06	7.65	7.46	11.96
W24	0.33	7.17	6.89	12.20	S13	0.27	7.15	6.52	12.24
W25	0.28	7.21	6.92	12.15	S14	0.42	7.10	6.83	12.37
W26	0.35	7.08	6.70	12.23	S15	1.07	6.63	7.38	12.99
W27	0.37	7.06	6.67	12.24	S16	0.84	6.87	7.42	12.76
W28	1.20	6.45	7.33	13.13	S17	0.09	7.49	7.24	11.95
W29	0.10	7.28	6.48	12.01	S18	0.16	7.34	6.92	12.01
W30	0.02	7.39	6.55	11.94	S19	-0.24	8.50	9.11	11.54
W31	-0.25	7.93	7.34	11.55	S20	-0.03	7.71	7.39	11.80
W32	0.09	7.70	7.72	11.97	S21	-0.21	8.03	7.81	11.62
W33	0.04	7.51	7.13	11.80	S22	0.07	7.67	7.64	11.88
W34	0.09	7.43	7.05	11.86	S23	-0.10	7.71	7.29	11.68
W35	0.14	7.26	6.79	11.91	S24	-0.18	7.77	7.21	11.62
W36	1.18	6.31	6.90	12.95	S25	-0.95	8.84	8.07	10.76
W37	0.69	7.05	7.53	12.41	S26	-0.90	8.80	8.08	10.81
W38	0.27	7.15	6.68	12.11	S27	0.83	6.83	7.28	12.59
W39	0.20	7.15	6.47	12.05	S28	0.34	7.26	7.13	12.10
W40	0.11	7.42	6.96	11.92	S29	0.17	7.29	6.71	11.97
W41	-0.33	7.86	6.74	11.48	S30	0.14	7.35	6.80	11.96
W42	-0.19	7.66	6.69	11.63	S31	0.04	7.39	6.61	11.87
W43	-0.13	7.59	6.66	11.69	S32	-0.12	7.55	6.63	11.70
W44	0.31	7.43	7.56	12.17	S33	-0.02	7.56	6.99	11.84
W45	0.26	7.44	7.48	12.12	S34	0.33	7.28	7.25	12.18
W46	0.05	7.65	7.40	11.92	S35	0.40	7.24	7.34	12.25
W47	0.04	7.37	6.53	11.95	S36	0.03	7.86	7.97	11.94
W48	-0.04	7.53	6.80	11.86	S37	0.18	7.61	7.72	12.09
W49	0.28	7.21	6.89	12.16	S38	-0.74	8.72	8.20	11.17
W50	-0.13	7.85	7.56	11.74	S39	0.25	7.28	6.95	12.19
W51	0.19	7.42	7.15	12.08	S40	-0.11	7.85	7.33	11.97
W52	0.24	7.37	7.15	12.13	S41	-0.13	8.06	7.85	11.91
W53	0.18	7.43	7.13	12.12	S42	-0.11	7.74	7.14	11.91

LSI: Langelier saturation index; RSI: Ryznar stability index, PI: Puckorius index; AI: Aggressive index

Table 7. Minimum, maximum, and average values of calculated indices in drink water sources of Marivan

Source	Index	Minimum	Average	Maximum	SD
Spring	LSI	-0.95	0.03	1.07	0.42
	RSI	6.63	7.71	9.49	0.61
	PI	6.49	7.50	10.04	0.71
	AI	10.76	11.91	12.99	0.44
Well	LSI	-0.52	0.23	1.20	0.34
	RSI	6.31	7.37	8.34	0.37
	PI	6.32	7.03	7.76	0.36
	AI	11.48	12.14	13.13	0.35

LSI: Langelier saturation index; RSI: Ryznar stability index, PI: Puckorius index; AI: Aggressive index; SD: Standard deviation

Table 8. Frequency distribution of scaling and corrosion indices in rural drinking water sources of Marivan

Source	Number	State	Index Number (%)			
			LSI	RSI	PI	AI
Spring	42	Corrosive	17 (40.47)	41 (97.62)	42 (100)	-
		Stable	1 (2.38)	1 (2.38)	-	25 (59.52)
		Scale forming	24 (57.14)	-	-	17 (40.48)
Well	64	Corrosive	14 (21.87)	-	64 (100)	-
		Stable	-	6 (9.38)	-	23 (35.94)
		Scale forming	50 (78.13)	58 (90.62)	-	41 (64.04)

LSI: Langelier saturation index; RSI: Ryznar stability index, PI: Puckorius index; AI: Aggressive index

Conclusion

The comparison of the measured parameters indicated that pH values in both springs and wells (24.49 and 7.76, respectively) were within the national standard range. Average TDS, TA, and total calcium in springs and wells were approximately equal, but the standard deviation of spring water was higher, indicating a significant difference in minimum and maximum values and wider distribution of the data. Comparison of the corrosion and scaling indices showed that, based on LSI, both sources tend to be corrosive. RSI indicated that the spring sources were more inclined toward the corrosion state, but the scaling state was dominant in well sources. PI illustrated that both sources were strongly corrosive, while AI showed that both sources were slightly corrosive. The overall results of this study indicated that spring sources tend to be corrosive and well sources tend to be scale forming. The findings of this study were in accordance with the actual reports of the Office of Operation and Maintenance Division for the Marivan Rural Water and Wastewater Affairs regarding broken cases of pipes, leakage, and constriction of transport lines and distribution networks.

Conflict of Interests

Authors have no conflict of interests.

Acknowledgements

The authors appreciate the assistance and cooperation of the Rural Water and Wastewater Affairs of Kurdistan Province especially the division of quality control and the laboratory staff.

References

1. Dietrich AM, Glindemann D, Pizarro F, Gidi V, Olivares M, Araya M, et al. Health and aesthetic impacts of copper corrosion on drinking water. Water Sci Technol 2004; 49(2): 55-62.
2. Ryznar JW. A new index for determining amount of calcium carbonate scale formed by water. Journal of American Water Works Association 1944; 36(4).
3. Farley M, Trow S. Losses in water distribution networks: A practitioner's guide to assessment, monitoring and control. London, UK: IWA Publishing; 2016.

4. Angell P. Understanding microbially influenced corrosion as biofilm-mediated changes in surface chemistry. Curr Opin Biotechnol 1999; 10(3): 269-72.
5. Edwards M. Controlling corrosion in drinking water distribution systems: a grand challenge for the 21st century. Water Sci Technol 2004; 49(2): 1-8.
6. Kessel SL, Rogers CE, Bennett JG. Corrosivity test methods for polymeric materials. part 5- a comparison of four test methods. J Fire Sci 1994; 12(2): 196-233.
7. American Water Works Association, Letterman RD. Water quality and treatment: A handbook of community water supplies. New York, NY: McGraw-Hill; 1999.
8. Pontius FW. Water quality and treatment. New York, NY: McGraw-Hill, 1990.
9. Chien CC, Kao CM, Chen CW, Dong CD, Chien HY. Evaluation of biological stability and corrosion potential in drinking water distribution systems: a case study. Environ Monit Assess 2009; 153(1-4): 127-38.
10. Eaton AD, Franson MA. Standard methods for the examination of water & wastewater. Washington, DC: American Public Health Association; 2005.
11. Imran SA, Dietz JD, Mutoti G, Ginasiyo T, Taylor JS, Randall AA, et al. Red water release in drinking water distribution systems. J Am Water Works Ass 2005; 97(9): 93-100.
12. Benson AS, Dietrich AM, Gallagher DL. Evaluation of iron release models for water distribution systems. Critical Reviews in Environmental Science and Technology 2012; 42(1): 44-97.
13. Abyaneh HZ, Varkeshi MB, Mohammadi K, Howard K, Marofi S. Assessment of groundwater corrosivity in Hamedan Province, Iran using an adaptive neuro-fuzzy inference system (ANFIS). Geosci J 2011; 15(4): 433-9.
14. Ghanizadeh GH, Ghaneeian MT. Corrosion and precipitation potential of drinking-water distribution systems in military centers. J Mil Med 2009; 11(3): 155-60. [In Persian].
15. Gupta N, Nafees SM, Jain MK, Kalpana S. Assessment of groundwater quality of outer skirts of Kota city with reference to its potential of scale formation and corrosivity. J Chem 2011; 8(3): 1330-8.
16. Rabbani D, Miranzadeh M B, Paravar A. Evaluating the corrosive and scale-forming indices of water in the villages under the coverage of Kashan rural water and Wastewater company during 2007-9. Feyz 2011; 15(4): 382-8. [In Persian].
17. Malakootian M, Fatehizadeh A, Meydani E. Investigation of corrosion potential and precipitation tendency of drinking water in the Kerman distribution system. Toloo e Behdasht 2012; 11(3): 1-10. [In Persian].
18. Shams M, Mohamadi A, Sajadi SA. Evaluation of corrosion and scaling potential of water in rural water supply distribution networks of Tabas, Iran. World Appl Sci J 2012; 17(11): 1484-89.

JAEHR Journal of Advances in Environmental Health Research

Adsorption of Co(II) ions from aqueous solutions using $NiFe_2O_4$ nanoparticles

Soheil Sobhanardakani[1], Raziyeh Zandipak[2]

1 Department of Environment, Hamadan Branch, Islamic Azad University, Hamadan, Iran
2 Young Researchers and Elite Club, Hamadan Branch, Islamic Azad University, Hamadan, Iran

Original Article

Abstract

In this study, $NiFe_2O_4$ nanoparticles ($NiFe_2O_4$ NPs) were prepared through co-precipitation method and subsequently used for the removal of Co(II) ions from aqueous solutions. The $NiFe_2O_4$ NPs were characterized by transmission electron microscopy (TEM), X-ray diffraction spectrometry (XRD), and Brunauer-Emmett-Teller (BET) surface area analysis. In batch tests, the effects of variables such as pH (2-10), adsorbent dose (0.006-0.08 g), contact time (0-90 minutes), and temperature (25-55 °C) on Co(II) ions removal were examined and optimized values were found to be 7, 0.02 g, 70 minutes, and 25 °C, respectively. In addition, the experimental data were fitted well to the Langmuir isotherm model and the maximum adsorption capacity was found to be 322.5 mg/g. Kinetic experiments were also conducted to determine the rate at which Co(II) ions are adsorbed onto the $NiFe_2O_4$ NPs.

KEYWORDS: Cobalt, Removal, Nanoparticles, Kinetics

Date of submission: 17 Apr 2015, ***Date of acceptance:*** 22 Jun 2015

Citation: Sobhanardakani S, Zandipak R. **Adsorption of Co(II) ions from aqueous solutions using $NiFe_2O_4$ nanoparticles.** J Adv Environ Health Res 2015; 3(3): 179-87.

Introduction

Cobalt contamination in natural waters is the cause of worldwide environmental concern since cobalt-polluted water can pose a great risk to human health due to its high toxicity.[1,2] The main anthropogenic pathway through which Co(II) enters water is via wastewaters from various industrial processes such as nuclear power plants, and metallurgical, mining, and electronic industries and pigments and paints.[3,4] Everyone is exposed to low levels of Co(II) present in air, water, and food. The permissible limits of Co in irrigation water and live-stock watering are 0.05 and 1.0 mg/l, respectively.[2] Small amounts of Co(II) is essential for human health, because it is known to be an essential element at trace levels in human beings, animals, and plants for metabolic processes.[4] Although Co(II) is essential for humans, large amounts of it can cause paralysis, diarrhea, asthma, pneumonia, lung irritations, weight loss, vomiting, nausea, and damage to the thyroid and liver.[5] Various treatment technologies for the removal of Co(II), such as precipitation, coagulation, ion exchange, biological treatment, and chemical reduction, have limited applications because of their relatively high cost and the production of secondary pollution.[6-9] Adsorption is an effective and economic method for the removal of heavy metals from wastewaters.[10-12] Activated carbon, zeolites, natural clays, chitosan, and by-products have been used as adsorbents for removal of metals from wastewaters.[13-15]

Corresponding Author:
Raziyeh Zandipak
Email: raziyeh.zandi@yahoo.com

Recently, magnetic nanomaterials have attracted much interest, because they not only have a large removal capacity, fast kinetics, and reactivity for contaminant removal, but also have high separation efficiency and reusability. In recent years, magnetic nanoparticles (NPs) with the general formula of MFe_2O_4 (M = Fe, Co, Cu, Mn, Ni, and etc.) have been among the most popular materials in analytical biochemistry, medicine, removal of heavy metals, and biotechnology.[16] Moreover, they have been increasingly applied to immobilize proteins, enzymes, and other bioactive agents due to their unique advantages.[16]

$NiFe_2O_4$ nanoparticles ($NiFe_2O_4$ NPs) are recognized as an adsorbent because of their good biocompatibility, strong super paramagnetic property, low toxicity, easy preparation, and high adsorption capacity.[17] $NiFe_2O_4$ NPs with an inverse spinel structure show ferrimagnetism that originates from the magnetic moment of antiparallel spins between Fe^{3+} ions at tetrahedral sites and Ni^{2+} ions at octahedral sites. $NiFe_2O_4$ NPs exhibit high surface area and low mass transfer resistance. Moreover, the magnetic behavior of these nanoparticles depends mostly on their size.[18]

In this study, the removal of Co(II) ions from aqueous solutions using $NiFe_2O_4$ NPs has been described. Effects of various parameters such as pH of the solutions, amount of adsorbent, contact time, and temperature were investigated. In addition, isotherm and kinetic studies of Co(II) ions removal in batch system were carried out.

Materials and Methods

All chemicals and reagents used in this work were of analytical grade and purchased from Merck Company (Merck, Darmstadt, Germany). A stock solution of Co(II) (1000 mg/l) was prepared by dissolving $Co(NO_3)_2 \cdot 6H_2O$ in double-distilled water.

The concentration of Co(II) ions in the solution was measured using an inductively coupled plasma optical emission spectrometer (ICP-OES) (JY138 Ultrace, France). All pH measurements were conducted with a 780 pH meter (780, Metrohm, Switzerland) combined with a glace-calomel electrode.

The crystal structure of synthesized materials was determined through X-ray powder diffraction (XRD) (38066 Riva, d/G.Via M. Misone, 11/D (TN), Italy) at ambient temperature. The structure of the $NiFe_2O_4$ NPs was characterized using a transmission electronic microscope (TEM) (CM10, 100 KV, Philips, Eindhoven, Netherlands). Specific surface area and porosity were defined through N_2 adsorption-desorption porosimetry (77 K) using a porosimeter (Bel Japan, Inc.). The elemental analysis was conducted using a scanning electron microscope energy dispersive X-ray spectroscope (SEM-EDX, XL 30, Philips, Netherland).

The $NiFe_2O_4$ samples were prepared through co-precipitation method. In a typical synthesis, 0.2 M (20 ml) solution of iron nitrate [$(Fe(NO_3)_3.9H_2O)$] and 0.1 M (20 ml) solution of nickel nitrate [$(Ni(NO_3)_2.6H_2O)$] were prepared and vigorously mixed through stirring for 1 hour at 80 ^oC. Then, 0.2 g of polyethylene oxide (PEO) was added to the solution as a capping agent. Subsequently, 5 ml of hydrazine hydrate ($NH_2.NH_2.H_2O$) was added drop by drop to the solutions and brown-colored precipitates were formed. Finally, the precipitates were separated through centrifugation and dried in a hot air oven for 4 hours at 100 ^oC. The acquired substance was annealed for 10 hours at 300 ^oC.[19]

The point of zero charge pH (pH_{pzc}) for the adsorbents was determined by introducing 0.02 g of $NiFe_2O_4$ NPs into 8 Erlenmeyer flasks (100 ml) containing 0.1 M $NaNO_3$ solution. The pH values of the solutions were adjusted to 2, 3, 4, 5, 6, 7, 8, and 9 using solutions of 0.01 mol/l HNO_3 and NaOH. The solution mixtures were allowed to equilibrate in an isothermal shaker (25 °C) for 24 hours. The final pH was measured after 24 hours. The pH_{pzc} is the point at which the $pH_{initial}$ is equal to pH_{final}. [19]

To perform an adsorption isotherm analysis, adsorption experiments were carried out by adding 0.02 g of $NiFe_2O_4$ NPs to a 25 ml conical flask containing 20 ml of Co(II) solution at room temperature. The initial Co(II) concentrations varied from 60 mg/l to 540 mg/l. The pH of the solution was adjusted to 2-10 using 0.1 mol/l HCl and/or 0.1 mol/l NaOH solutions. After adding $NiFe_2O_4$ NPs, the flasks were transferred to a temperature controlled shaking water bath and shaken at 180 rpm for 24 hours. Then, the $NiFe_2O_4$ NPs was separated using an external magnet and the concentration of the remaining Co(II) ions in the solution was determined through ICP-OES. The concentration of the remaining Co(II) ions in the adsorbent phase (q_e, mg/g) was calculated using equation (1):

$$q_e = \frac{(C_0 - C_e)V}{W} \quad (1)$$

where C_0 and C_e (mg/l) are initial and equilibrium concentrations, respectively, V (l) is the volume of solution, and W (g) is the mass of the adsorbent.[20]

Finally, Co(II) ions removal efficiency was calculated using equation (2):

$$R\ (\%) = \frac{C_0 - C_e}{C_0} \times 100 \quad (2).$$

Results and Discussion

Characterization of $NiFe_2O_4$

The XRD pattern (Figure 1) shows that the peaks at the 2 values of 30.1, 35.3, 43.0, 53.7, 56.5, and 62.4 can be assigned as (220), (311), (400), (422), (511), and (440) crystal planes of spinel $NiFe_2O_4$, respectively. The average crystallite size of the $NiFe_2O_4$ NPs was estimated at 15 nm from the XRD data according to the Scherer equation. The TEM micrograph and calculated histogram of the $NiFe_2O_4$, as shown in figure 2, revealed that the diameter of the synthesized $NiFe_2O_4$ NPs was around 12 nm.

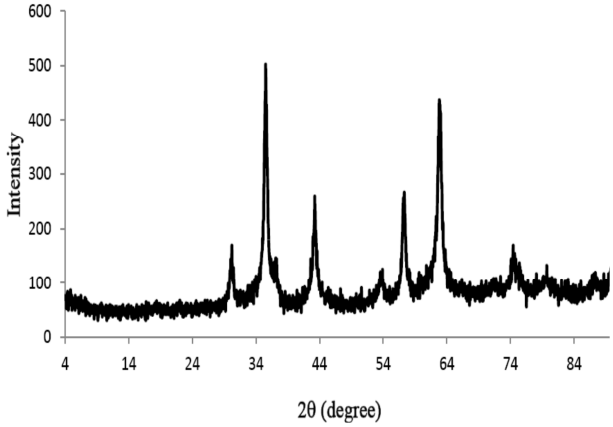

Figure 1. The X-ray diffraction pattern of $NiFe_2O_4$ nanoparticles.

a b

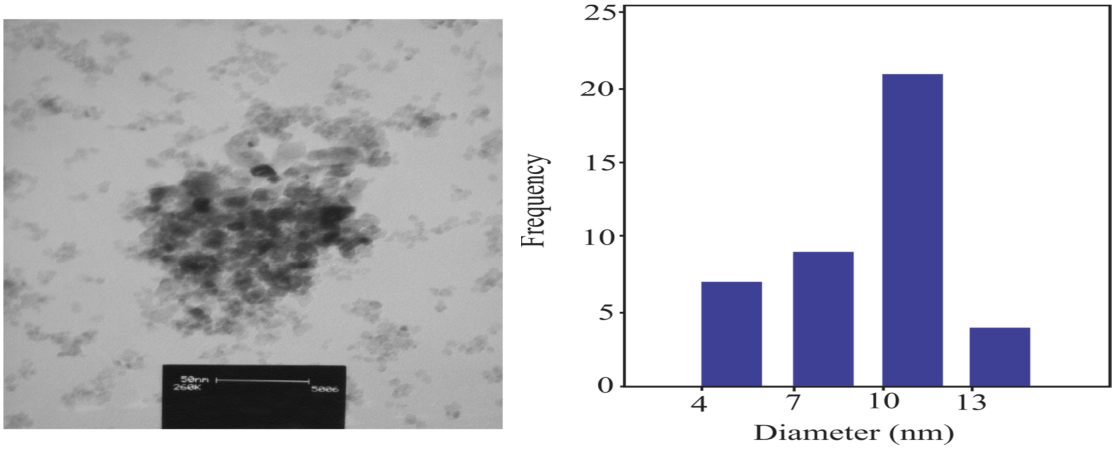

Figure 2. (a) Transmission electron micrograph and (b) calculated histogram of NiFe2O4 nanoparticles

The particle size measured directly on the TEM micrograph is in accordance with that determined by the XRD results. Figure 3 shows a typical SEM-EDX elemental analysis of $NiFe_2O_4$ NPs. The results demonstrate that only Ni, Fe, and O appear in $NiFe_2O_4$ NPs samples. Moreover, the results have a good agreement with previous studies.Specific surface areas are commonly reported as Brunauer-Emmett-Teller (BET) surface areas obtained through applying the BET theory to nitrogen adsorption/desorption isotherms measured at 77 K. This is a standard procedure for the determination of the specific surface area of a sample. The specific surface area of the sample is determined by physical adsorption of a gas on the surface of the solid and by measuring the amount of adsorbed gas corresponding to a monomolecular layer on the surface. The data are treated according to the BET theory.[21] The results of the BET method showed that the average specific surface area of $NiFe_2O_4$ NPs was 63.7 m^2/g. It can be concluded from these values that the synthesized nanoparticles have relatively large specific surface areas and may be better for adsorption.

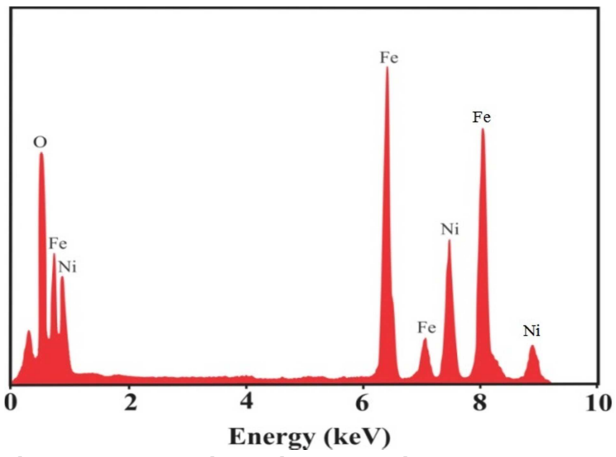

Figure 3. Scanning electron microscope energy dispersive X-ray spectrum of $NiFe_2O_4$ nanoparticles

Effect of solution pH

The solution pH has an important impact on the active sites of adsorbent as well as the metal speciation during the adsorption process. To evaluate the effect of pH on the adsorption percentage of the Co(II) ions, experiments were performed at initial concentration of 60 mg/l and pH range 2-10 (Figure 4b).

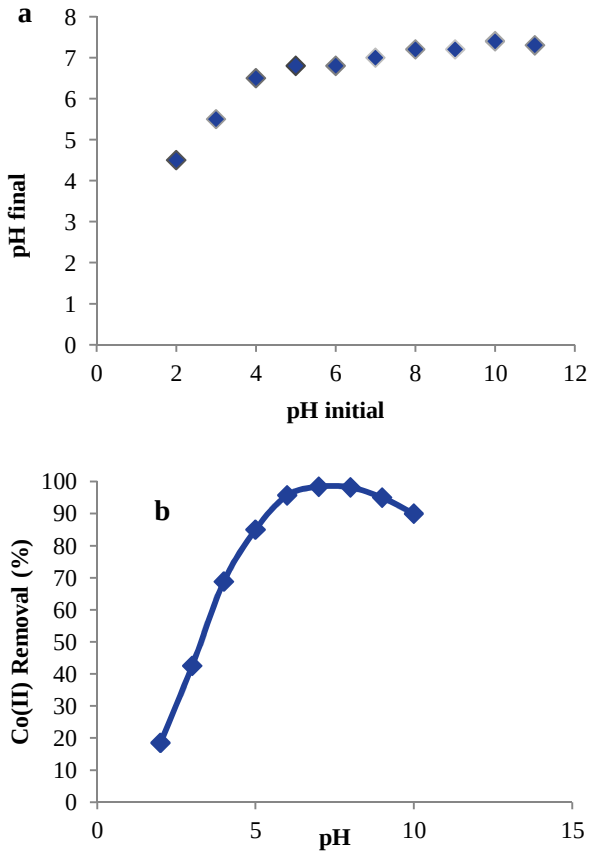

Figure 4. (a) The determination of the point of zero charge of the $NiFe_2O_4$ nanoparticles (b) Effect of solution pH on the removal efficiency of Co(II) by $NiFe_2O_4$ nanoparticles (C_0 = 60 mg/l, contact time = 70 minutes, dose of adsorbent = 0.02 g, and temperature = 25 ºC)

The Co(II) ions removal was found to increase significantly with increase in solution pH from pH of 2 to 7. The highest Co(II) ions removal (98.4%) was achieved at pH 7. This could be attributed to the surface properties of the adsorbent and ionization/dissociation of the adsorbate molecules. As observed in figure 4a, the pH_{pzc} for $NiFe_2O_4$ NPs is 7.0. The concentration of H^+ ion increased gradually in

the system with the decrease of pH value and the $NiFe_2O_4$ NPs surface became more positively charged because of the protonation of molecules on the $NiFe_2O_4$ NPs surface. The increase in Co(II) ions removal with the increases in pH (> pH_{pzc}) can be explained on the basis of a decrease in competition between protons and Co(II) cations for the same functional groups and by the decrease in positive surface charge, which results in a lower electrostatic repulsion between the surface of $NiFe_2O_4$ NPs and Co(II) ions before adsorption.

Generally, various Co species in aqueous solution are present in the form of Co^{2+}, $Co(OH)^+$, $Co(OH)_2$, and $Co(OH)_3^-$ at a function of pH values. At a pH of less than 9, the predominant cobalt species is Co^{2+} and the removal of Co(II) is accomplished through the adsorption process. A similar phenomenon has also been shown in the adsorption of Co(II) ion from water by carboxylated sugarcane bagasse.[1]

Effect of adsorbent dose

Dose of adsorbent is an important parameter in the determination of adsorption capacity and adsorption efficiency. The effect of adsorbent amount on removal of Co(II) ions was investigated by adding various amounts of adsorbent in the range of 0.006-0.08 g and pH of 7 with initial metal concentration of 60 mg/l. The results are illustrated in figure 5. As can be seen, removal of Co(II) increases from 68% to 99.3% for 0.006-0.02 g. This could be attributed to the fact that by increasing the $NiFe_2O_4$ NPs amount for the same concentration of Co(II) solution, the number of sites available for adsorption continue increasing. However, in the next stage, removal attained its maximum limit and further increase had no effect. Similar results were observed by Deravanesiyan et al. who investigated the effect of adsorbent dose on removal of Co(II) ions from aqueous solution by alumina nanoparticles immobilized zeolite and indicated that adsorption increases with increase in adsorbent dose.[22]

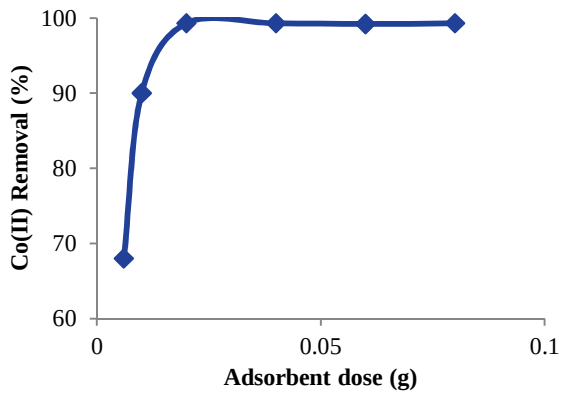

Figure 5. Effect of adsorbent dose on the removal efficiency of Co(II) by $NiFe_2O_4$ nanoparticles (C_0 = 60 mg/l, solution pH = 7, contact time = 70 minutes, and temperature = 25 ºC)

Effect of temperature

In order to study the effect of temperature, experiments were carried out at 25, 35, 45, and 55 ºC and the results are presented in figure 6. The increase in the temperature of Co(II) solution from 25 to 55 ºC resulted in a decrease in the adsorption efficiency of the $NiFe_2O_4$ NPs. This indicates that the adsorption of Co(II) ions on $NiFe_2O_4$ NPs is exothermic in nature. The decrease in adsorption with the increase in temperature may be attributed to the weakening of adsorptive forces between the active sites of the $NiFe_2O_4$ NPs and Co(II) ions. Similar results have been found by Zandipak et al. [19]

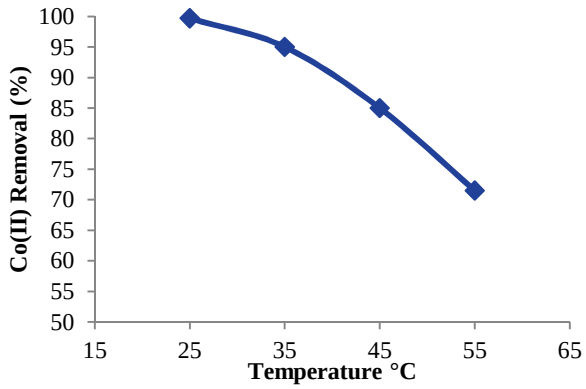

Figure 6. Effect of temperature on the removal efficiency of Co(II) by $NiFe_2O_4$ nanoparticles (C_0 = 60 mg/l, solution pH = 7, dose of adsorbent = 0.02 g, contact time = 70 minutes, and temperature = 25 ºC)

Adsorption isotherms

Isotherms are the equilibrium relations between the adsorbate concentration in the solid phase and the liquid phase. The equilibrium isotherms for adsorption of Co(II) by $NiFe_2O_4$ NPs were investigated with varying initial concentrations of Co(II) (from 60 to 540 mg/l) at 7.0 pH and 25 °C. The results indicate that adsorption is high at lower metal concentrations and decreases gradually with increase in metal concentration. In this study, the Langmuir [Equation (3)] and Freundlich [Equation (4)] isotherms were used to fit the adsorption data of Co(II) ions onto $NiFe_2O_4$ NPs. The linear equations are as follows: [23,24]

$$\frac{C_e}{q_e} = \frac{C_e}{q_m} + \frac{1}{q_m b_l} \quad (3)$$

$$\ln q_e = \frac{1}{n}\ln C_e + \ln k_f \quad (4)$$

where c_e (mg/l) is the equilibrium concentration of Co(II) ions in solution, q_e (mg/g) is the equilibrium adsorption capacity of $NiFe_2O_4$ NPs, q_m (mg/g) is the maximum adsorption capacity of $NiFe_2O_4$ NPs for monolayer coverage, b (l/mg) is a constant related to the adsorption free energy, K_f (mg1/(1/n)L1/n/g) is a constant related to adsorption capacity, and n is an empirical parameter related to adsorption. The parameters of the isotherm equations for Co(II) ions on the $NiFe_2O_4$ NPs are presented in table 1. As seen in table 1, the R^2 values obtained from the Langmuir model are much closer to one than those from the Freundlich model, suggesting that the Langmuir model is better than the other isotherms (Figure 7). Thus, the adsorption can be described by the Langmuir isotherm and the Co(II) ions adsorption occurs on a homogeneous surface through monolayer adsorption without interaction between the adsorbed ions. Through the comparison of q_{max} values of Co(II) adsorption capacity of other adsorbents to NiFe2O4 NPs (Table 2), it is evident that $NiFe_2O_4$ NPs presented the highest adsorption capacity of the reported adsorbents.

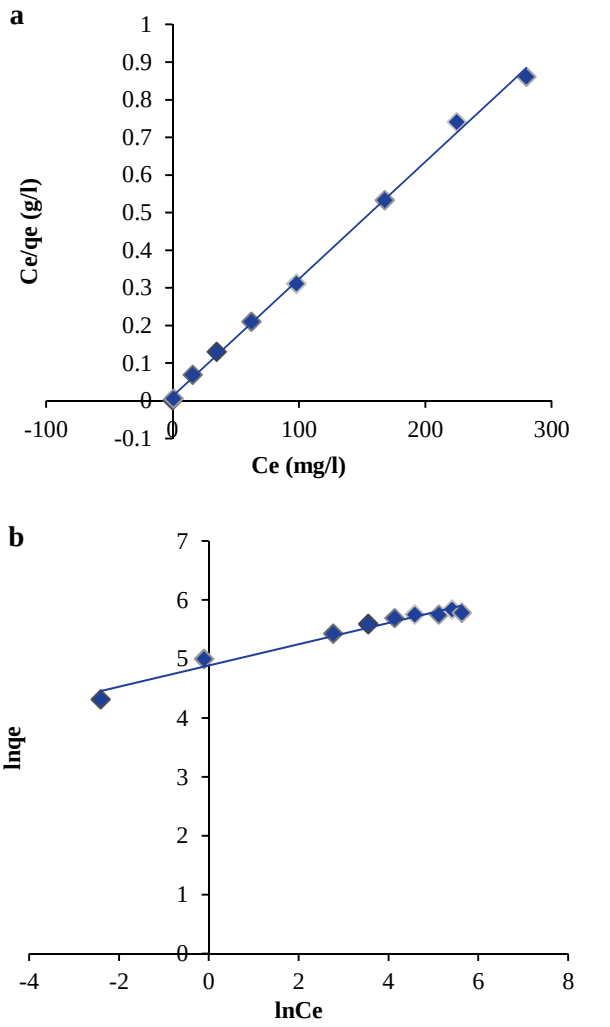

Figure 7. (a) Langmuir and (b) Freundlich isotherms for Co(II) ions adsorption onto $NiFe_2O_4$ nanoparticles

Table 1. Isotherm parameters of adsorption of Co(II) ions onto $NiFe_2O_4$ nanoparticles at 25 °C

Langmuir			Freundlich		
b (l mg^{-1})	q_m (mg g^{-1})	R^2	K_f ($mg^{1-(1/n)}$ $l^{1/n}$ g^{-1})	n	R^2
0.265	322.5	0.997	132.55	5.54	0.967

q_m: Maximum adsorption capacity; R^2: Pearson correlation coefficient; K_f: Freundlich constant related to adsorption capacity; n: Empirical parameter related to adsorption

Table 2. Comparison of maximum adsorption capacity (q_m) of different adsorbents for Co(II)

Adsorbent	Maximum adsorption capacity (mg/g)	Reference
Amination graphene oxide	116.30	2
Alumina nanoparticles immobilized zeolite	5.05	22
Nano-magnesso ferrite	62.68	5
Chrysanthemum indicum	14.84	25
Granular activated carbon	1.19	26
Chelating resin	71.29	6
$NiFe_2O_4$ nanoparticles	322.50	This work

Adsorption kinetics

The adsorption of Co(II) ions by $NiFe_2O_4$ NPs as a function of time at three different initial Co(II) concentrations (60, 80, and 120 mg/l) is displayed in figure 8. As can be observed, the adsorption efficiency of Co(II) ions increased with increasing contact time, and finally, reached equilibrium after approximately 70 minutes. A rapid adsorption was observed within 50 minutes which showed the availability of a large number of vacant sites. Subsequently, the diminishing availability of the remaining active sites and the decrease in the driving force led to the slowing of the adsorptive process.

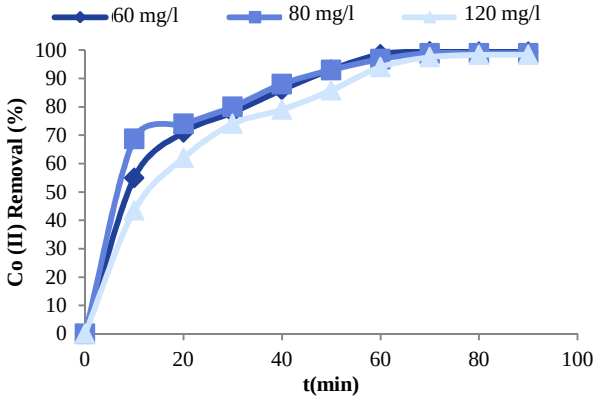

Figure 8. Effect of contact time on the removal efficiency of Co(II) by $NiFe_2O_4$ nanoparticles (C_0 = 60, 80 and 120 mg/l, solution pH = 7, dose of adsorbent = 0.02 g, and temperature = 25 ºC)

To evaluate the kinetics of the adsorption process, the experimental data were compared to those predicted by two kinetic models, the pseudo-first order and pseudo-second order. The pseudo-first order and pseudo-second order kinetic models can, respectively, be expressed by equation (5) and (6):[27]

$$\ln(q_e - q_t) = \ln(q_e) - \frac{k_1 t}{2.303} \quad (5)$$

$$\frac{t}{q_t} = \frac{1}{k_2 q_e^2} + \frac{t}{q_e} \quad (6)$$

where q_e and q_t are the amount of Co(II) ions adsorbed (mg/g) at equilibrium and time t (minute), k_1 is the rate constant of pseudo-first order ($minute^{-1}$), k_2 is the rate constant of pseudo-second order (g/mg/ minute) for adsorption. The pseudo-first order and pseudo-second order kinetics plots are presented in figure 9. The kinetic constants and correlation coefficients of these two models are calculated and given in table 3. The results show that the correlation coefficients (R^2) (0.998, 0.998, and 0.997) for the pseudo-second order models are higher than the pseudo-first order models (0.923, 0.851, and 0.838). This indicates that the adsorption of Co(II) ions on $NiFe_2O_4$ NPs follows a pseudo-second order kinetic model. The results indicate that chemical adsorption might be the rate-limiting step.

Conclusion

In this work, $NiFe_2O_4$ NPs were successfully synthesized and used as a novel adsorbent for the rapid individual adsorption of Co(II) ions. The size of the nanostructures, according to TEM, was around 12 nm. The $NiFe_2O_4$ NPs can be easily separated from the aqueous solution by the external magnetic field before and after the adsorption process. The results indicate

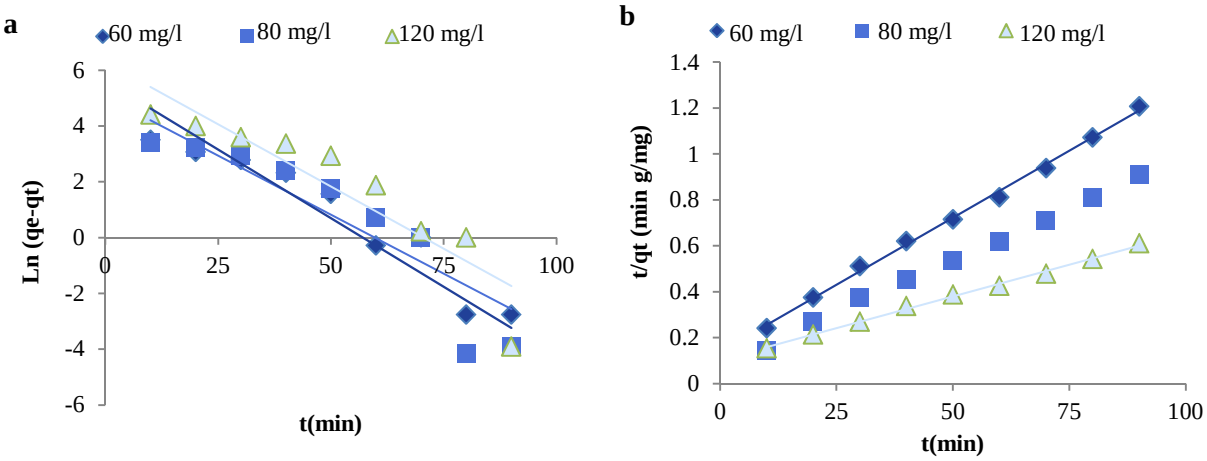

Figure 9. (a) Pseudo-first order and (b) pseudo-second order kinetics plots of Co(II) ions adsorption onto $NiFe_2O_4$ nanoparticles

Table 3. Pseudo-first order and pseudo-second order kinetic model parameters for the adsorption of Co(II) ions onto $NiFe_2O_4$ nanoparticles at 25 ºC

C_0 (mg/l)	Pseudo-first order kinetic model				Pseudo-second order kinetic model		
	q_e exp (mg/g)	q_{e1} (mg/g)	k_1 (minute^{-1})	R^2	q_{e2} (mg/g)	k_2 (g/mg/minute)	R^2
60	56.0	21.40	0.09	0.923	54.21	0.020	0.998
80	73.4	67.25	0.08	0.851	72.95	0.010	0.998
120	107.8	84.65	0.03	0.838	105.7	0.005	0.997

q_e: Amount of Co(II) ions adsorbed at equilibrium; k_1: Rate constant of pseudo-first order; R^2: Pearson correlation coefficient; k_2: Rate constant of pseudo-second order for adsorption

that the adsorption was dependent on the pH of solution and temperature. The adsorption kinetics and adsorption isotherms showed that the adsorption kinetic could be modeled by the pseudo-second order rate equation, and the isotherm equilibrium data were well fitted with the Langmuir model. The adsorption capacity of Co(II) onto $NiFe_2O_4$ NPs was determined as 322.5 mg/g. Thus, $NiFe_2O_4$ NPs can potentially be used to treat Co(II)-contaminated wastewater.

Conflict of Interests

Authors have no conflict of interests.

Acknowledgements

The authors are very grateful to the Young Researchers and Elite Club, Hamedan Branch, Islamic Azad University for providing us with facilities to conduct and complete this study.

References

1. Carmo Ramos S, Pedrosa Xavier A, Teodoro F, Cota Elias M, Jorge Goncalves F, Frederic Gil L, et al. Modeling mono- and multi-component adsorption of cobalt(II), copper(II), and nickel(II) metal ions from aqueous solution onto a new carboxylated sugarcane bagasse. Part I: Batch adsorption study. Industrial Crops and Products 2015; 74: 357-71.
2. Fang F, Kong L, Huang J, Wu S, Zhang K, Wang X, et al. Removal of cobalt ions from aqueous solution by an amination graphene oxide nanocomposite. J Hazard Mater 2014; 270: 1-10.
3. Nazari AM, Cox PW, Waters KE. Biosorption of copper, nickel and cobalt ions from dilute solutions using BSA-coated air bubbles. Journal of Water Process Engineering 2014; 3: 10-7.
4. Negm NA, El Sheikh R, El-Farargy AF, Hefni Hassan H, Bekhit M. Treatment of industrial wastewater containing copper and cobalt ions using modified chitosan. Journal of Industrial and Engineering Chemistry 2015; 21: 526-34.
5. Srivastava V, Sharma YC, Sillanpaa M. Application of nano-magnesso ferrite (n-MgFe2O4) for the removal of Co^{2+} ions from synthetic wastewater: Kinetic, equilibrium and thermodynamic studies.

Applied Surface cience 2015; 338: 42-54.
6. Ceglowski M, Schroeder G. Preparation of porous resin with Schiff base chelating groups for removal of heavy metal ions from aqueous solutions. Chemical Engineering Journal 2015; 263: 402-11.
7. Zhu J, Baig SA, Sheng T, Lou Z, Wang Z, Xu X. Fe_3O_4 and MnO_2 assembled on honeycomb briquette cinders (HBC) for arsenic removal from aqueous solutions. J Hazard Mater 2015; 286: 220-8.
8. Jian M, Liu B, Zhang G, Liu R, Zhang X. Adsorptive removal of arsenic from aqueous solution by zeolitic imidazolate framework-8 (ZIF-8) nanoparticles. Colloids and Surfaces A: Physicochem Eng Aspects 2015; 465: 67-76.
9. Arshadi M, Faraji AR, Amiri MJ. Modification of aluminum□silicate nanoparticles by melamine-based dendrimer l-cysteine methyl esters for adsorptive characteristic of Hg(II) ions from the synthetic and Persian Gulf water. Chemical Engineering Journal 2015; 266: 345-55.
10. Sobhanardakani S, Zandipak R, Sahraei R. Removal of Janus Green dye from aqueous solutions using oxidized multi-walled carbon nanotubes. Toxicol Environ Chem 2013; 95(6): 909-18.
11. Ahmad MA, Alrozi R. Removal of malachite green dye from aqueous solution using rambutan peel-based activated carbon: Equilibrium, kinetic and thermodynamic studies. Chemical Engineering Journal 2011; 171(2): 510-6.
12. Ghaedi M, Mosallanejad N. Study of competitive adsorption of malachite green and sunset yellow dyes on cadmium hydroxide nanowires loaded on activated carbon. Journal of Industrial and Engineering Chemistry 2014; 20(3): 1085-96.
13. Sun Q, Hu X, Zheng S, Sun Z, Liu S, Li H. Influence of calcination temperature on the structural, adsorption and photocatalytic properties of TiO_2 nanoparticles supported on natural zeolite. Powder Technology 2015; 274: 88-97.
14. Wan Ngah WS, Teong LC, Hanafiah MA. Adsorption of dyes and heavy metal ions by chitosan composites: A review. Carbohydrate Polymers 2011; 83(4): 1446-56.
15. Yu L, Luo YM. The adsorption mechanism of anionic and cationic dyes by Jerusalem artichoke stalk-based mesoporous activated carbon. Journal of Environmental Chemical Engineering 2014; 2(1): 220-9.
16. Teymourian H, Salimi A, Khezrian S. Fe3O4 magnetic nanoparticles/reduced graphene oxide nanosheets as a novel electrochemical and bioeletrochemical sensing platform. Biosensors and Bioelectronics 2013; 49: 1-8.
17. Khosravi I, Eftekhar M. Characterization and evaluation catalytic efficiency of NiFe2O4 nano spinel in removal of reactive dye from aqueous solution. Powder Technology 2013; 250: 147-53.
18. Patil JY, Nadargi DY, Gurav JL, Mulla IS, Suryavanshi SS. Synthesis of glycine combusted NiFe2O4 spinel ferrite: A highly versatile gas sensor. Materials Letters 2014; 124: 144-7.
19. Zandipak R, Sobhanardakani S. Synthesis of NiFe2O4 nanoparticles for removal of anionic dyes from aqueous solution. Desalination and Water Treatment 2016; 57: 24-11348.
20. Wang XS, Zhu L, Lu HJ. Surface chemical properties and adsorption of Cu (II) on nanoscale magnetite in aqueous solutions. Desalination 2011; 276(1-3): 154-60.
21. Brunauer S, Emmett PH, Teller E. Adsorption of Gases in Multimolecular Layers. J Am Chem Soc 1938; 60(2): 309-19.
22. Deravanesiyan M, Beheshti M, Malekpour A. Alumina nanoparticles immobilization onto the NaX zeolite and the removal of Cr (III) and Co (II) ions from aqueous solutions. Journal of Industrial and Engineering Chemistry 2015; 21: 580-6.
23. Langmuir L. The adsorption of gases on plane surfaces of glass, mica and platinum. J Am Chem Soc 1918; 40(9): 1361-403.
24. Freundlich H, Heller W. The Adsorption of cis- and trans-Azobenzene. J Am Chem Soc 1939; 61(8): 2228-30.
25. Vilvanathan S, Shanthakumar S. Biosorption of Co(II) ions from aqueous solution using Chrysanthemum indicum: Kinetics, equilibrium and thermodynamics. Process Safety and Environmental Protection 2015; 96: 98-110.
26. Sulaymon AH, Abid BA, Al-Najar JA. Removal of lead copper chromium and cobalt ions onto granular activated carbon in batch and fixed-bed adsorbers. Chemical Engineering Journal 2009; 155(3): 647-53.
27. Azizian S. Kinetic models of sorption: a theoretical analysis. J Colloid Interface Sci 2004; 276(1): 47-52.

JAEHR Journal of Advances in Environmental Health Research

Effect of temperature on pH, turbidity, and residual free chlorine in Sanandaj Water Distribution Network, Iran

Asad Nouri[1], Behzad Shahmoradi[1], Saeed Dehestani-Athar[1], Afshin Maleki[1]

1 Environmental Health Research Center, Kurdistan University of Medical Sciences, Sanandaj, Iran

Original Article

Abstract

One of the parameters responsible for decreased water quality in a distribution system is temperature changes. This study was conducted to examine the effect of temperature on pH, turbidity, and residual chlorine in Sanandaj, Iran, Water Distribution System. The required water samples were taken from 85 stations during April to October 2014. Sampling was carried out over 6 months and twice per month. The average amount of residual chlorine measured at these stations was 0.58 and 0.52 mg/l, and turbidity was 0.86 and 0.98 nephelometric turbidity unit (NTU) in winter and spring, respectively. The temperature did not have any effect on pH, the amount of pH in winter and spring were 7.56 and 7.57, respectively. The results showed significant differences in the concentration of residual chlorine and turbidity of Sanandaj Water Distribution Network between winter and spring ($P \leq 0.01$). Thus, the concentration of residual chlorine and turbidity varies in warm and cold seasons. However, no significant difference was observed in pH ($P \geq 0.01$). The research results indicated that temperature does not have any effect on the qualitative parameters measured in the study area.

KEYWORDS: Chlorine, Temperature, Water Quality, Iran

Date of submission: 12 Apr 2015, ***Date of acceptance:*** 10 Jun 2015

Citation: Nouri A, Shahmoradi B, Dehestani-Athar S, Maleki A. **Effect of temperature on pH, turbidity, and residual free chlorine in Sanandaj Water Distribution Network, Iran.** J Adv Environ Health Res 2015; 3(3): 188-95.

Introduction

Water distribution networks are considered vital arteries of rural and urban communities.[1] The purpose of any water distribution system is not only to provide water pressure, but also to provide high quality water in terms of taste, smell, appearance, and health.[2] The least treatment performed on water resources is disinfection. Chlorine and its derivatives are used as disinfectants due to their low relative cost, ease of use, and appropriate functionality to eliminate pathogenic microorganisms in drinking water distribution networks.[3]

Corresponding Author:
Behzad Shahmoradi
Email: bshahmorady@gmail.com

Before drinking water leaves the treatment plant, a final chlorination step is frequently carried out to maintain residual chlorine in the distribution system, and thus, to prevent microbiological regrowth.[4] When chlorine reacts with water, it is hydrolyzed and produces hypochlorous acid (HClO) and hypochlorite ion (ClO^-). It is well known that HClO is more efficient than ClO^- as disinfectant.[5] The relative concentrations of HClO depend on pH and somewhat on temperature.[6] At pH of 7.6 and 6.6, the ratio of $HClO/ClO^-$ roughly equals 50% and 90%, respectively. The disinfecting power of chlorine increases with increasing pH and reduces with increasing temperature.[5] Raising the temperature increases the amount of

chlorine in the distribution network and the amount of residual chlorine is variable in winter and summer.[3] In water supplemented with biodegradable organic matter (BOM), a strong linear correlation was found between temperature and free residual chlorine required to control biofilm.[7] According to the Iranian Drinking Water Standards (Code 1053), the optimum amount of free residual chlorine at any point of the distribution network should be 0.2-0.8 mg/l under normal conditions. This value should be 1 mg/l in the case of natural disasters, emergencies, and epidemics, considering pH.[8]

Turbidity of water is a physical parameter that is determined through measuring the absorption or scattering of light by suspended solids.[9] The Safe Drinking Water Act (SDWA) has recommended the turbidity value of 1 nephelometric turbidity unit (NTU) and a maximum limit of 5 NTU.[10] Turbidity in water distribution systems may result from incomplete removal of particles during treatment, from the pipe material itself, and from line repair within a system. All of these cases can present a potential health threat through decreasing disinfection effectiveness.[11] Water quality degradation could occur in municipal drinking water systems because of intermittent short duration events resulting in high turbidity, particle counts, and heterotrophic plate counts.[12]

The pH of a solution is a numeric scale used to specify the acidity or alkalinity of that solution. It is usually expressed as the negative of the logarithm to base 10 of the activity of the hydrogen ion. The solution is referred to as acidic if pH is less than 7 and it is considered as alkaline or basic if pH is higher than 7.[13]

Pure water is neutral.[14] Water pH is a crucial parameter in water treatment, disinfection, and corrosion control. Water corrosion rate depends largely on water pH.[15] One of the most important physical factors in the occurrence of corrosion and deposition is temperature changes, which have destructive impact on water pH.[16] The Iranian National Standard for pH is 7-8.5 and the maximum allowable range is 6.5-9.[8]

Therefore, the aim of this study was to assess the effect of temperature on residual chlorine, pH, and turbidity in Sanandaj, Iran, Water Distribution Network, in two different seasons.

Materials and Methods

Sanandaj City is located at 14° 35´ north latitude and 46° east longitude (Figure 1) from the meridian of Greenwich and it is between 1450 and 1538 meters above sea level, varying in different parts of the city, and has an area of 2906 km^2.[17]

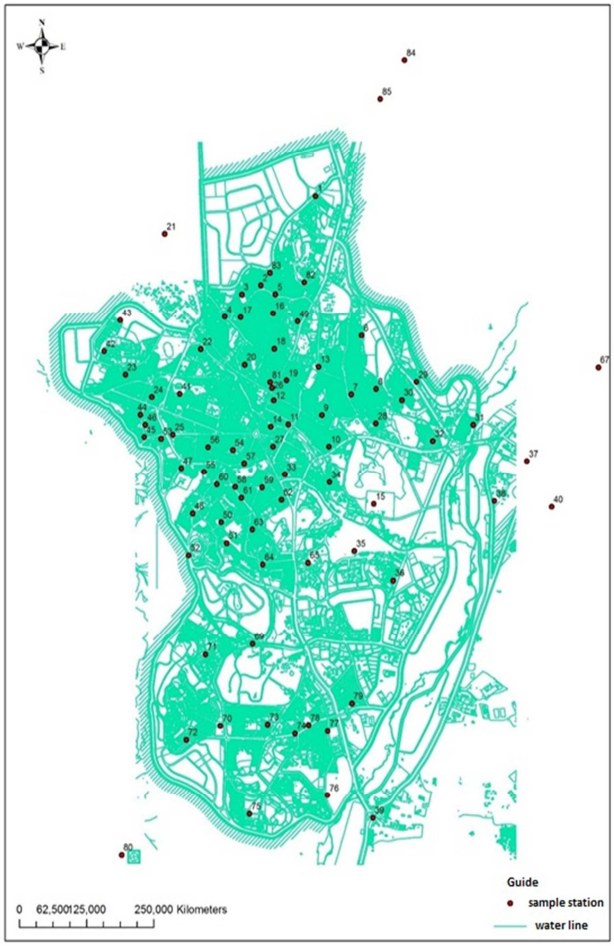

Figure 1. The location of sampling stations in Sanandaj

The main water supply for Sanandaj is Vahdat Dam. Because of the special topography of the city, 14 active tanks provide the required pressure for 1397 km long distribution network and serve 373,987 people. These tanks are fed by the main tank, Faizabad, which takes its water directly from the water treatment plant.

This study was conducted during 6 months from April to October 2014. First, the map of water distribution network and the layout of tanks were obtained from the Urban Water and Wastewater Company, Kurdistan Province, Sanandaj. In order to determine sampling stations, various factors were considered including topographic conditions, texture of the city, the population under coverage of the distribution network, area of the distribution network, type of network, number of tanks, chlorination system, and financial constraints.

The total length of the main lines, substations, and water network connections in Sanandaj is 1397 km. Therefore, the total length of the network was assumed as the sample size; a sample station was considered at every 16.5 km of pipeline. On the other hand, considering the abovementioned parameters, 85 sample stations were selected randomly from the areas which had the inclusion criteria.

The amount of residual chlorine and temperature were measured using portable digital devices (DKK-TOA model RC-31PT, UK). Turbidity and pH were measured using turbidity and pH meters (Wagtech, UK), respectively. Before the measurements, the digital devices were calibrated according to the manufacturers' instructions using standard solutions.

Results and Discussion

The normality of data was assessed using Kolmogorov-Smirnov test, then, the data obtained were analyzed using paired t-test and the Pearson correlation matrix in SPSS software (version 16, SPSS Inc., Chicago, IL, USA). Results of analyses of independent t-test and Pearson correlation are presented in tables 1 and 2, respectively.

The results of independent t-test indicated that the seasonal (spring and winter) difference was statistically significant ($P \leq 0.01$) in the case of residual chlorine (Table 1). Moreover, a significant correlation was found between residual chlorine and temperature ($P \leq 0.01$) (Table 2).

In addition, in the case of turbidity, the results of independent t-test (Table 1) indicated that the seasonal (spring and winter) difference was statistically significant ($P \leq 0.01$); however, no significant correlation existed between turbidity and temperature ($P \geq 0.01$) (Table 2).

As presented in table 1, the results of t-test showed that the seasonal (spring and winter) differences in pH were not statistically significant ($P \geq 0.01$). The Pearson correlation coefficient test (Table 2) showed no significant relationship ($P \geq 0.01$) between temperature and pH.

Table 1. The results of the Pearson correlation

		Paired Differences				t	df	P (2-tailed)
		Mean ± SD	SD Error Mean	95% Confidence Interval of the Difference				
				Lower	Upper			
Pair 1	Cl Winter-Cl Spring	0.056 ± 0.156	0.017	0.022	0.089	3.31	84	0.001
Pair 2	pH Winter-pH Spring	-0.003 ± 0.426	0.462	-0.095	0.088	-0.77	84	0.939
Pair 3	Turbidity Winter-Turbidity Spring	-0.126 ± 0.371	0.040	-0.206	-0.046	-3.14	84	0.002
Pair 4	T Winter-T Spring	-5.960 ± 1.830	0.198	-6.354	-5.565	-30.02	84	< 0.001

SD: Standard deviation; df: Degree of freedom

Table 2. The results of paired samples statistics for winter and spring

Correlations		Cl	pH	Turbidity	Temperature
Cl	Pearson Correlation	1	-0.370*	0.610*	-0.230*
	P (2-tailed)		< 0.001	< 0.001	0.002
	N	170.000	170.000	170.000	170.000
pH	Pearson Correlation	-0.370*	1.000	-0.035	0.078
	P (2-tailed)	< 0.001		0.652	0.312
	N	170.000	170.000	170.000	170.000
Turbidity	Pearson Correlation	0.610*	-0.030	1.000	-0.075
	P (2-tailed)	< 0.001	0.650		0.330
	N	170.000	170.000	170.000	170.000
Temperature	Pearson Correlation	-0.230*	0.078	-0.075	1.000
	P (2-tailed)	0.002	0.312	0.332	
	N	170.000	170.000	170.000	170.000

* Correlation is significant at the 0.01 level (2-tailed)

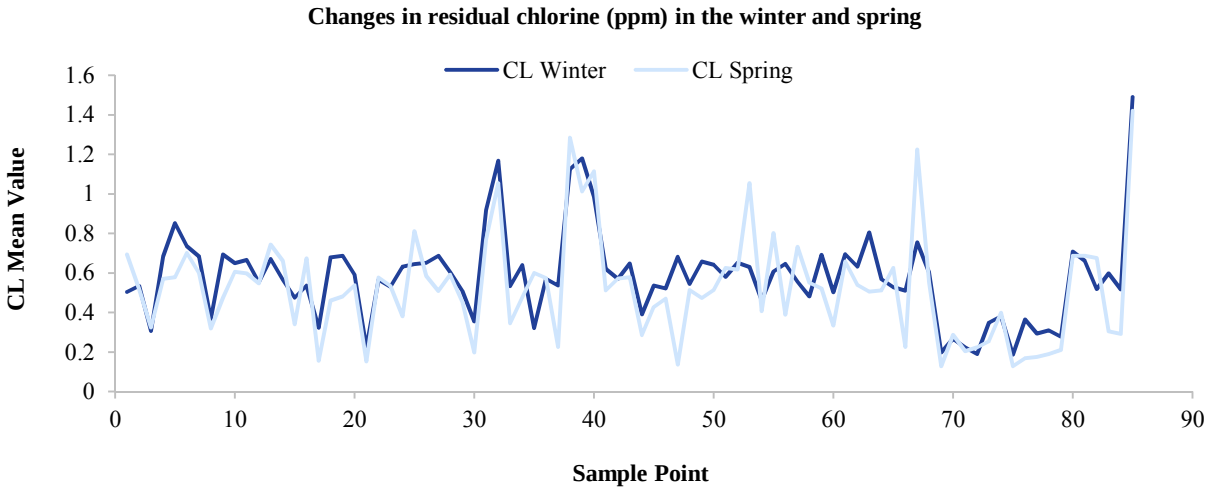

Figure 2. Average residual chlorine in winter and spring

The results of independent t-test, in the case of temperature indicated that the seasonal (spring and winter) difference was statistically significant ($P \leq 0.01$) and the amount of temperature differs in winter and spring (Table 1).

The results of statistical tests showed that the average concentration of residual chlorine varies during winter and spring (Tables 1 and 2). The average amount of residual chlorine measured at 85 stations in winter and spring was 0.58 ± 0.22091 and 1.45 ± 0.26401 mg/l, respectively. The range of the residual chlorine measured in winter and spring was 0.186-1.49 and 0.128-1.42 mg/l, respectively. Temperature has a crucial impact on chlorine decay; this effect should be considered in chlorine decay modeling because of the large seasonal variability, common in many distribution systems.[18,19] Temperature and pH are important factors and have inverse relationships with the reduction of residual chlorine in water distribution networks.[20,21]

As shown in figure 2, residual chlorine changed over winter and spring at different stations; the difference between the amount of residual chlorine in stations 37, 47, 53, and 67 was much higher than elsewhere. Based on the line slope of the liner equation (Figures 3 and 4), variation coefficient of the amount of residual chlorine with the temperature in both winter and spring is 0.05585, indicating the negligible

effect of temperature on residual chlorine. Such results could be attributed to the special weather conditions during the study time. Although Sanandaj was once famous for its very cold winter, the temperature fluctuation has not been tangible during recent years.

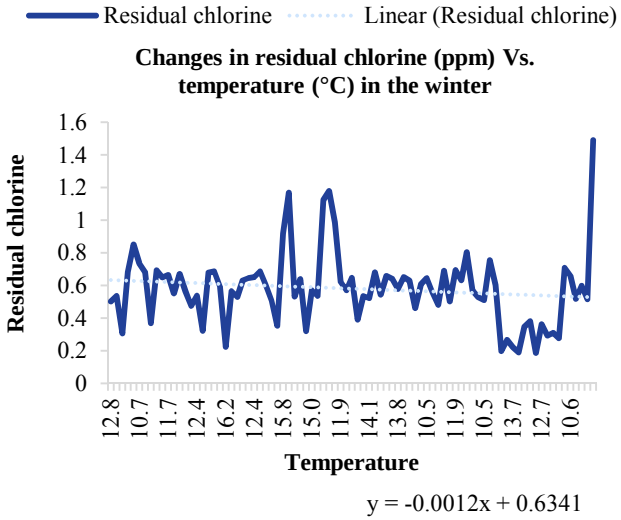

Figure 3. Residual chlorine fluctuation in winter

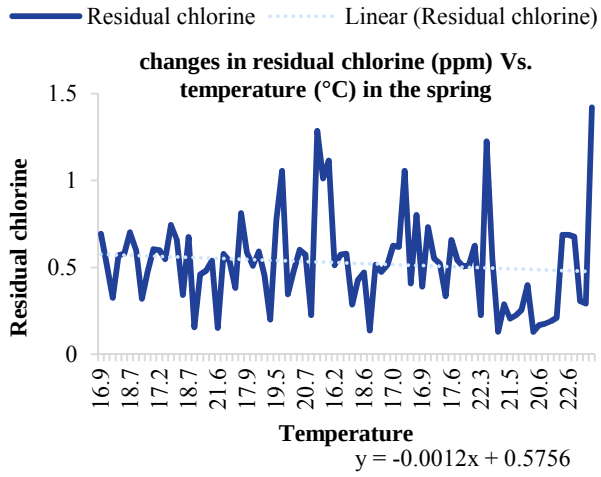

Figure 4. Residual chlorine fluctuation in spring

The average amount of turbidity measured was 0.859 ± 0.3156 NTU and 0.985 ± 0.3420 NTU in winter and spring, respectively. This research found that the range of turbidity fluctuation was 0.05-2.015 and 0.07-2.16 NTU in winter and spring, respectively (Figures 5, 6, and 7). This finding is in contradiction with the reports of Case; they reported a direct relationship between temperature and turbidity.[22] Moreover, Ghorbani et al. found a significant difference in heterotrophic plate count (HPC), free residual chlorine, temperature, and turbidity between different months and seasons of the year.[23]

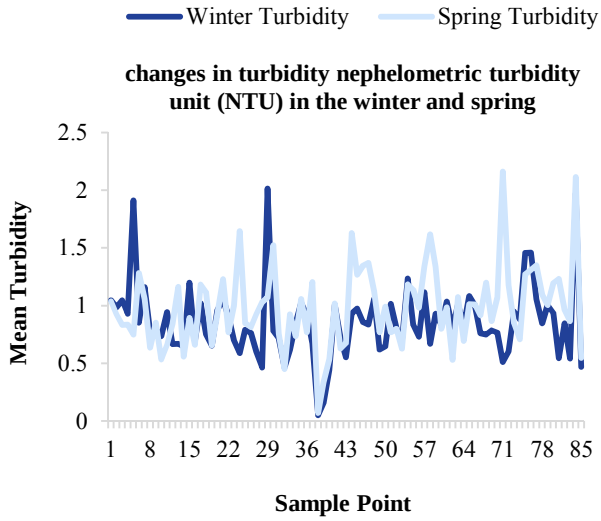

Figure 5. Average turbidity in the winter and spring

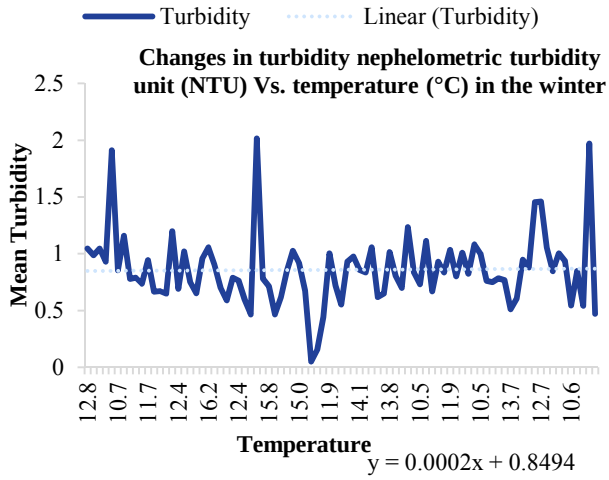

Figure 6. Turbidity fluctuation in winter

These changes could be attributed to the fact that Sanandaj Water Distribution Network is very old and, in some areas, the pipeline has not been replaced for more than 30 years. Moreover, the long retention time in end points may result in decreased residual chlorine and increased turbidity.[24,25]

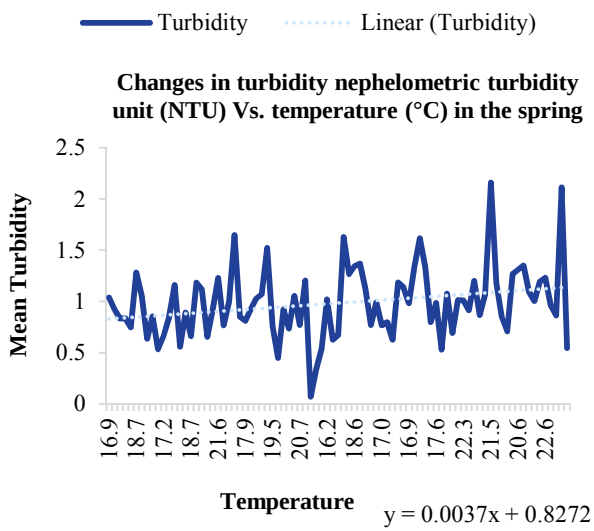

Figure 7. Turbidity fluctuation in spring

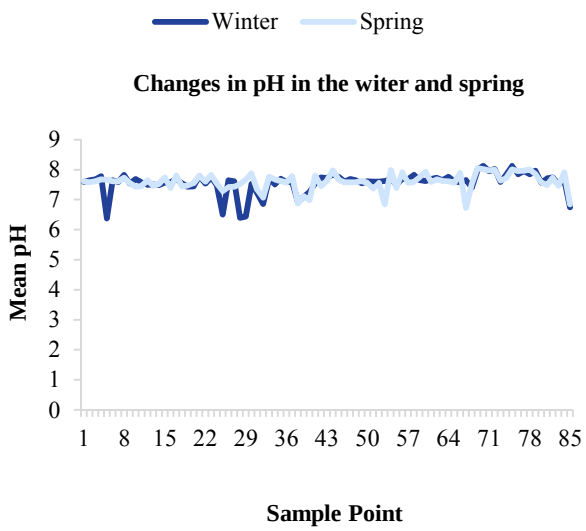

Figure 8. Average pH in the winter and spring

Paired t-test results showed that pH changes in winter and spring were not statistically significant (P ≥ 0.01), which means pH was not affected by temperature. Molar relationship between residual chlorine and pH is presented in equation 1.[26] Moreover, the relationship between pKa and temperature is presented in equation 2, which yields a range of 7.82-7.39 over a temperature range of 0-50 °C. The temperature impact on pK_α could be neglected as the impact of temperature on the species-specific rate constants which is more significant in the typical pH range of distribution systems than the impact of temperature on the extent of dissociation of HOCl.[27] On the other hand, the changes in pH are independent of temperature, as confirmed in this research (Figures 8 and 9).

$$\frac{[HOCl]}{OCl^-} = 10^{apK_a - pH} \qquad \text{(Eq. 1)}$$

$$pK_a = \frac{3000}{T} - 10.0686 + 0.0253T \qquad \text{(Eq. 2)}$$

Conclusion

This research assessed the effect of temperature fluctuation in winter and spring on 3 physicochemical parameters (free residual chlorine, turbidity, and pH) in Sanandaj Water Distribution Network.

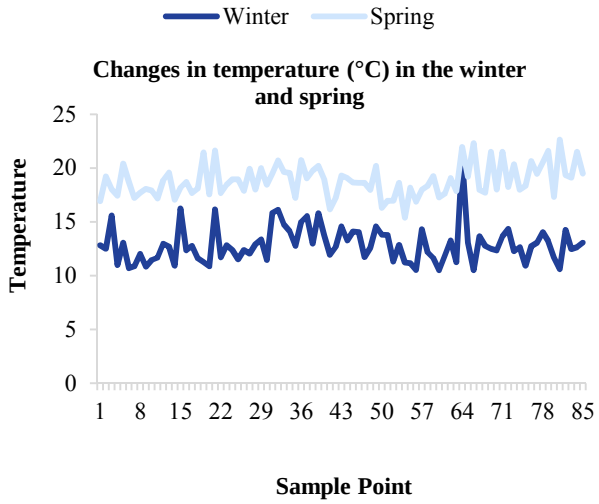

Figure 9. Average temperature in the winter and spring

The research showed that temperature did not cause significant changes in pH; however, turbidity and free residual chlorine were influenced by temperature changes, as data from 85 sampling stations revealed. Although Sanandaj Water Distribution Network has a loop form, the water quality was not uniform with respect to the parameters studied; thus, this factor requires further examination.

Conflict of Interests

Authors have no conflict of interests.

Acknowledgements

This paper is a part of the first author's MSc. dissertation and the authors are thankful to the Kurdistan University of Medical Sciences, Sanandaj, for the financial support.

References

1. Bostani A, Golmaie SH, Ansari H. Pipe water distribution network modeling platform and by finite element method with Ansys and Plaxis. Proceedings of the 2nd National Conference on Water; 2010 Mar 19-20; Mashhad, Iran. [In Persian].
2. Stavros G, Vantas K, Tzimopoulos C, Christos E. Modeling distribution system water quality with hydrosim model. Proceedings of the 7th International Conference European Water Resources Association (EWRA); 2009 Jun 25-27; Limassol, Cyprus.
3. Tabesh M, Azadi B, Rouzbahani A. Optimization of chlorine injection dosage in water distribution networks using a genetic algorithm. Water and Wastewater 2011; 22(1): 2-11. [In Persian].
4. Hassani AH, Jafari MA, Torabifar B. Trihalomethanes concentration in different components of watertreatment plant and water distribution system in the north of Iran. In ternational Journal of Enviromental Research 2010; 34(4): 887-92.
5. Lu W, Kiene L, Levi Y. Chlorine demand of biofilms in water distribution systems. Water Research 1999; 33(3): 827-35.
6. Qasim SR, Motley EM, Zhu G. Water Works Engineering: Planning, Design, and Operation. New York, NY: Prentice Hall PTR; 2000.
7. Ndiongue S, Huck PM, Slawson RM. Effects of temperature and biodegradable organic matter on control of biofilms by free chlorine in a model drinking water distribution system. Water Res 2005; 39(6): 953-64.
8. Institute of Standards and Industrial Research of Iran. Drinking water -Physical and chemical specifications. No. 1053. 5th ed. Tehran, Iran: Institute of Standards and Industrial Research of Iran; 2006. [In Persian].
9. Crittenden JC, Hand DW, Howe KJ. MWH's Water Treatment: Principles and Design. New Jersey, NJ: John Wiley & Sons; 2012.
10. Power KN, Nagy LA. Relationship between bacterial regrowth and some physical and chemical parameters within Sydney's drinking water distribution system. Water Research 1999; 33(3): 741-50.
11. Obi CL, Igumbor JO, Momba MN, Samie A. Interplay of factors involving chlorine dose, turbidity flow capacity and pH on microbial quality of drinking water in small water treatment plants. Water SA 2008; 34(5): 565-72.
12. McCoy WF, Olson BH. Relationship among turbidity, particle counts and bacteriological quality within water distribution lines. Water Research 1986; 20(8): 1023-9.
13. Lewis MJ, Bamforth CW. Essays in Brewing Science. Berlin, Germany: Springer Science & Business Media; 2007.
14. American Water Works Association. Water Quality and Treatment: A Handbook of Community Water Supplies. 4th ed. New York, NY: McGraw-Hill; 1990.
15. Ghanizadeh G, Ghanian MT. Evaluation of corrosion and scaling potential sources of drinking water in Noor city by using of corrosion indices. J Military of Medicine 2009; 11(3): 155-60. [In Persian].
16. Nemerow NL, Agardy FJ, Salvato JA. Environmental Engineering: Water, Wastewater, Soil and Groundwater Treatment and Remediation. 6th ed. New Jersey, NJ: Wiley; 2009.
17. Governor Sanandaj. Detailed results of the general census of population and housing in 2011 [Online]. [cited 2011]; Available from: URL: http://ostan-kd.ir/Default.aspx?TabID=51 [In Persian].
18. Andalib A, Ganjidoust H, Ayati B, Khodadadi A. Investigation of Amount and Effective Factors on Trihalomethane Production in PotableWater of Yazd. Iran J Health Environ 2011; 4(2): 137-48.
19. Powell JC, Hallam NB, West JR, Forester CF, Simms J. Factors which control bulk chlorine decay rates. Water Res 2000; 34(1): 117-26.
20. Liu B, Reckhow DA, Li Y. A two-site chlorine decay model for the combined effects of pH, water distribution temperature and in-home heating profiles using differential evolution. Water Res 2014; 53: 47-57.
21. Li X, Gu DM, Qi JY, M U, Zhao HB. Modeling of residual chlorine in water distribution system. J Environ Sci (China) 2003; 15(1): 136-44.
22. Case ME. Determining the Relationship between a Water Sample's Temperature and Its Turbidity Level [Project]; California, CA: California State Science Fair; 2010.
23. Ghorbani J, Moradianfard Sh, Reisi P, Shehni Gheysari M. Survey of heterotrophic bacteria population changes in Kerman drinking water distribution system and GIS zoning. Eur J Exp Biol 2013; 3(2): 476-83.
24. Wang S, Qian X, Wang QH, Xiong W. Modeling Turbidity Intrusion Processes in Flooding Season of a Canyon-Shaped Reservoir, South China. Procedia Environmental Sciences 2012; 13: 1327-37.
25. Shamsaei H, Jaafar O, Basri N. Effects Residence

Time to Water Quality in Large Water Distribution Systems. J Sci Res Eng 2013; 5(4): 449-57.
26. Liu B, Reckhow DA. DBP formation in hot and cold water across a simulated distribution system: effect of incubation time, heating time, pH, chlorine dose, and incubation temperature. Environ Sci Technol 2013; 47(20): 11584-91.
27. Morris JC. The Acid Ionization Constant of HOCl from 5 to 35°. J Phys Chem 1966; 70(12): 3798-805.

JAEHR Journal of Advances in Environmental Health Research

Simultaneous degradation and adsorption of cyanide using modified fly Ash and TiO_2/UV

Shima Rezaei[1], Hadi Rezaei[2], Meghdad Pirsaheb[3], Saeb Ahmadi[4], Hooshyar Hossini[3]

1 Research Center for Environmental Health AND School of Public Health, Kurdistan University of Medical Sciences, Sanandaj, Iran
2 Sanandaj Health Center AND Department of Environmental Health Engineering, School of Public Health, Kurdistan University of Medical Sciences, Sanandaj, Iran
3 Department of Environmental Health Engineering, School of Health, Kermanshah University of Medical Sciences, Kermanshah, Iran
4 Department of Chemical Engineering, School of Chemical Engineering, Tarbiat Modares University, Tehran, Iran

Original Article

Abstract

Due to the present water shortage and environmental problems associated with industrial effluent, investigation of novel treatment technologies is an essential approach. Being a highly toxic chemical of asphyxiating characteristics, cyanide is seen as a major environmental pollutant in a wide range of industrial effluents. The present study aimed to address the adsorption and photocatalytic degradation of cyanide using activated fly ash and TiO_2/UV. To investigate the removal efficiency of cyanide, two sets of experiments were designed. First, cyanide was absorbed by activated fly ash and degraded via a photocatalytic process, individually. Second, simultaneous adsorption and degradation was examined. The removal efficiency of cyanide by modified fly ash (MFA), TiO_2/UV, and their combination (MFA-TiO_2/UV) was 76.1%, 81%, and 86.6%, respectively. Optimal conditions for the combination of activated fly ash AFA-TiO_2/UV were contact time of 6 hours, temperature of 100 °C, and AFA: TiO_2 ratio (w/w) of 1:1. Under these conditions, a maximum removal rate of 92.4% was obtained when 1.2 g of MFA/TiO_2 was used with a pH value of 3 in the presence of UV light. Based on the results of cyanide removal, it can be concluded that the combination of adsorption and photocatalytic degradation with MFA-TiO_2/UV can be utilized to improve the removal of cyanide from wastewater.

KEYWORDS: Adsorption, MFA-TiO_2/UV, Cyanide, Photocatalytic Degradation

Date of submission: 22 Apr 2015, ***Date of acceptance:*** 12 Jun 2015

Citation: Rezaei Sh, Rezaei H, Pirsaheb M, Ahmadi S, Hossini H. **Simultaneous degradation and adsorption of cyanide using modified fly Ash and TiO_2/UV.** J Adv Environ Health Res 2015; 3(3): 196-203.

Introduction

As a result of the increasingly growing rate of pollutant discharge by industries into the environment and ecosystem many problems are emerging such as health concerns and contamination of water resources. As a strong asphyxiating chemical group, cyanides are present in several industrial wastewaters including those of paint, oil refining, explosives, chemicals, plating, pesticides, synthetic fiber production, mining, electronics, and coking industries.[1-3] The health damages caused by high levels of cyanide exposure include headaches, dizziness, dermatitis, pruritus, weak and rapid pulse, nausea, and vomiting. Extreme levels of exposure may lead to brain damages, coma, and eventually death. A cyanide concentration of about 0.05 mg/dl

Corresponding Author:
Hooshyar Hossini
Email: h.hosseini@kums.ac.ir

can produce some toxins in the blood.[4,5] The lethal dose of cyanide for humans has been determined to be about 5 mg per kg of body weight.[6,7] Common processes of cyanide removal encompass physical, chemical, and biological techniques. Through physical techniques (such as membrane processes, ion exchange, and adsorption), the removal process is only completed by phase change. On the other hand, the toxicity of cyanide may limit the use of biological techniques to low concentrations, requiring a long duration of time to proceed. The most common chemical method for cyanide removal is alkaline chlorination, with its greatest limitation being the production of cyanogen chloride.[8-10] However, because of their incomplete cyanide removal and remarkably high cost, chemical methods are limited in application. Today, the use of the photocatalysis process as a strong and efficient yet green technology is growing in comparison to conventional methods.[11,1] Many researches have confirmed the efficiency of the photocatalysis process in cyanide removal.[12,13] Some researchers have suggested considerable improvements, provided the photocatalysis system is coupled with a primary adsorbent such as zeolite or activated carbon.[14] Absorption is an important part of photocatalytic removal;[16] thus, an increase in absorption capacity can improve photocatalytic characteristics.[15] Therefore, adding a high capacity adsorbent such as fly ash (FA) to a catalysis system such as TiO_2, in the presence of UV light, can improve the photocatalytic performance. The main decomposition mechanisms by combined modified fly ash (MFA)/TiO_2 are defined in the three steps of chemical species adsorption on the surface of MFA/TiO_2, optical dispersion over the surface, and desorption of final product from the surface of MFA/TiO_2. Hence, when TiO_2 is loaded on FA, the adsorbed analytes on FA move to the catalyst, via diffusion process, where they are decomposed.[17,18] The present study aimed not only to perform a simple modification process to enhance FA adsorption capacity, but also to mix MFA with TiO_2 nanoparticles in the presence of UV to achieve a higher removal efficiency for cyanide. To the best of our knowledge, no similar study has been reported.

Materials and Methods

All material and chemical regents were of analytical grade. The experimental study was conducted on both synthetic and real samples at the laboratory scale. Raw FA was collected from Zarand Thermal Power Plant (Kerman, Iran). Once prepared, FA was sieved to isolate particles of 100 to 200 mesh size. Then, FA was washed with distilled water at a liquid: solid ratio of about 10 for 48 hours, before being filtered and dried in an oven at 105 °C to obtain washed fly ash (WFA). The size and specific surface area of the used TiO_2 were 20 nm and 40 m^2/g, respectively.

In order to determine the optimum conditions for obtaining an optimal FA, 4 consecutive stages were evaluated following a single-factor optimization approach. In the FA modification process, effective parameters such as acid concentration, time modification, acid/WFA ratio, and temperature modification were set to their optimal values. At the end, MFA/TiO_2 ratio was evaluated. In order to determine acid concentration, raw fly ash (RFA) was modified at different concentrations of sulfuric acid, including 0.01, 0.1, 1, 1.8, and 2 M/l, at boiling point under reflux for 3 hours. After filtration using Whatman filter (pore size ~ 0.45 µm), FA was washed several times with distilled water, and then, rinsed using ethanol to bring its pH value to 0 (neutral pH). Then, FA was dried at 105 to 120 °C and stored in a desiccator for further analysis. In the next step, WFA was modified using different acid/WFA ratios of about 3, 7, 9, 10, 11, and 13. Subsequently, WFA was modified using different times (i.e., 1, 3, 6, and 9 hours) and temperatures (i.e., 29, 70, 85, 100, and 120 °C).

The effect of MFA:TiO_2 ratio was evaluated at the ratios (in w/w) of 0:4, 3:1, 1.5:2.5, 1:1, 2.5:1.5, 1:3, and 4:0.

At all steps, optimal values of effective parameters in cyanide removal by MFA-TiO_2/UV were selected as judging criteria.

In this section, other parameters effective on photocatalitic degradation [e.g., initial pH (2-11) and substrate dose (0.3-1.5 g)] were studied. Moreover, different concentrations of cyanide (2.5 to 75 mg/l) were brought into contact with the MFA-TiO_2/UV at optimum conditions. Degrees of oxidation reactions were also determined. To evaluate MFA-TiO_2/UV under actual conditions, real samples were prepared from the electroplating industry and treated under optimum conditions using MFA-TiO_2/UV.

All tests were analyzed at room temperature and conducted in duplicates to increase the accuracy of the results. Residual cyanide was determined using an atomic absorption spectrophotometer (Philips-PU 9100X) coupled with a mercury UV lamp (30 W, 338 mw/m^2) as light source with maximum wavelength of 360 nm. To avoid light reflection, the entire system was wrapped in aluminum foil.

Results and Discussion

Scanning Electron Microscopy-Energy-dispersive X-ray Spectroscopy (SEM-EDS)

Figure 1 shows the growth of porosity and active sites on FA surface after modification. These micropores can be occupied by TiO_2 nanoparticles on the surface of the adsorbent.

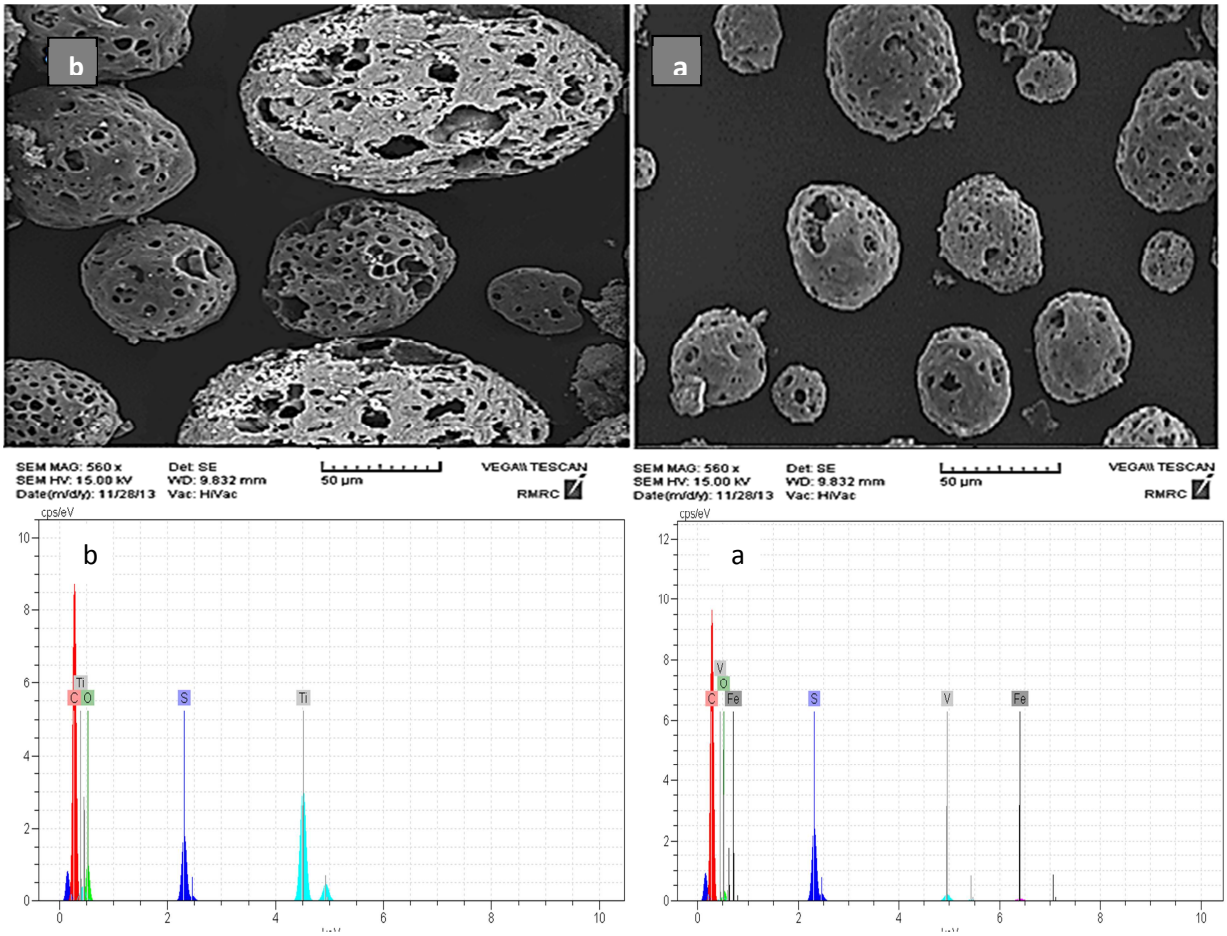

Figure 1. Scanning Electron Microscopy-Energy-dispersive X-ray Spectroscopy (SEM-EDS) images of raw fly ash (a) modified fly ash (MFA)-TiO_2 (b)

Simultaneous determination of electrical conductivity (EC) and total dissolved solids (TDS) after 48 hours of washing of FA indicated them to increase to about 2.3-4.07 mS/cm² and 80-1710 ppm, respectively. These results reveal that water-soluble compounds from FA had dissolved as a result of acidic treatment and the development of pores. EDS results demonstrate the weight percent (wt%) of different elements and metal oxides in FA, including carbon, sulfur, oxygen, CO_2, SO_3, iron, vanadium, V_2O_5, and Fe_2O_3. The weight percent of the abovementioned elements before FA modification were about 77.94, 7.73, 10.9, 91.97, 6.22, 1.32, 2.09, 1.2, and 0.61 wt%, respectively. After treatment, the values changed to 86.52, 6.8, 6.68, 92.94, 5.08, 0, 0, and 0% wt%, respectively, indicating an increase in carbon content after acidic treatment, which confirms the enhancement of adsorption capacity. The results were in agreement with those reported by Wang et al.[19]

Effect of acid concentration and activation time

Figure 2 illustrates the photocatalytic removal of cyanide by MFA-TiO_2 under different acidic conditions. Under these conditions, the removal rate increased with acid dose. The removal efficiency was 51.3% when WFA/TiO_2 was used alone. With the increasing of acid concentration from 0.01 to 2 M, the removal rate increased from 64 to 79.11%. Accordingly, 1 M was considered as the optimum acid concentration for the following experiments. Statistical analysis indicated that acid concentration was not significantly correlated with cyanide removal efficiency (P ~ 0.256). Figure 3 presents a demonstration of the effect of activation time. The results showed that the removal percentage was improved from 77.5 to 86.2% with the increasing of activation time from 2 to 10 hours. Through further evaluation of removal efficiency, the activation time of 6 hours was found to be the optimum value. In addition, a significant relationship was observed between activation time and removal efficiency (P ~ 0.026).

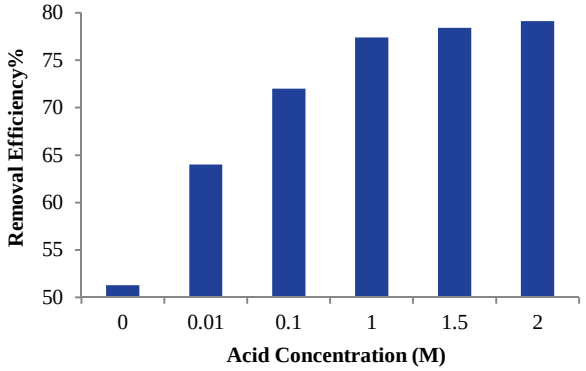

Figure 2. Effect of acid concentration on cyanide removal [cyanide: 30 mg/l, unadjusted pH]

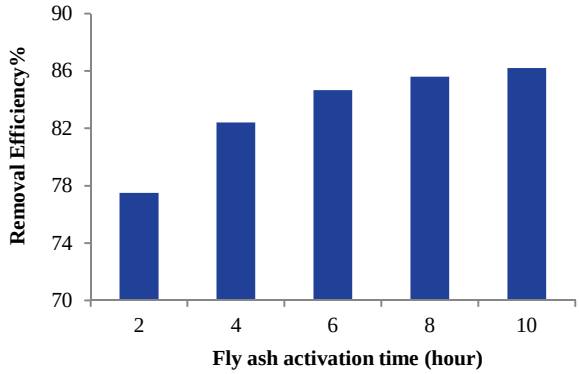

Figure 3. Effect of activation time on cyanide removal [cyanide: 30 mg/l, unadjusted pH]

Effect of temperature

Figure 4 shows cyanide removal efficiency when activation temperature changes from 26 (room temperature) to 120 °C. The figure indicates the significant effect of temperature on cyanide removal, where removal efficiency changes from 73.6 to 89.13% with the increasing of temperature. With regard to greater cyanide removal at 97 °C, boiling point of water was chosen as the optimum temperature for FA activation. Based on statistical analysis, there was a significant relationship between temperature and removal efficiency (P = 0.01). Panitchakarn et al. reported an initial increase in the purity of FA with increasing acid concentration, followed by

a relatively constant trend with further increase in the acid concentration.[21] The acid:FA ratio did not significantly contribute to the modification of fly ash. Porosity and surface area increased with the reduction in impurities due to longer activation time and higher treatment temperature.[20-22] According to the results, optimal acid/WFA ratio was found to be about 7 (data not reported). The removal of vanadium compounds by acid-treated adsorbent was confirmed in the studies by Kashiwakura et al.[23] and Kashiwakura et al.[24] in which dangerous substances such as arsenic and selenium were successfully removed.

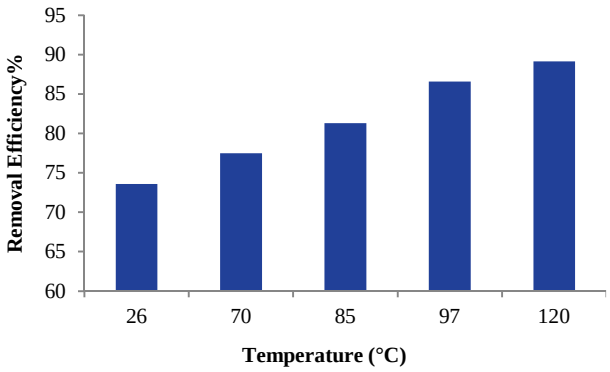

Figure 4. Effect of activation temperature on removal efficiency [cyanide: 30 mg/l, unadjusted pH]

Figure 5 shows changes in removal efficiency with MFA to nanoparticles ratio for different contact times. The cyanide removal efficiency for MFA, TiO_2/UV, and MFA-TiO_2/UV were found to be 76.1, 81, and 86.6%, respectively. Accordingly, the removal efficiency of MFA-TiO_2/UV was higher than that of either the absorbent or the catalyst alone. The appropriate ratio of TiO_2 to MFA was 1. No statistically significant relationship was found between MFA: TiO_2 ratio and removal efficiency ($P \sim 0.098$). By increasing the surface area, chemical species were provided with further area, which improved photocatalytic removal efficiency.[25] Optical dispersion rate of pollutants is affected by light absorption of the used catalyst and the active sites. Evidently, the photocatalytic process is likely to proceed more efficiently with appropriate adsorption. When TiO_2 is introduced into fly ash pore space, due to the proximity of contaminants and the catalyst, a better removal condition is provided. This can be associated with FA serving as an adsorbent. In other words, depending on the type of fly ash, the removal efficiency changed, leading to a reformed process.[26] In mixture substrate (MFA/TiO_2), a competition is established on active sites, with the located TiO_2 molecules on adsorbent surface behaving similar to its host. During this process, both substrates (MFA and TiO_2) are engaged with pollutants, and the absorption process takes place before the photocatalytic process. Chemical and structural changes in FA lead to changes in surface morphology, ultimately leading to important changes in the substrate affinity toward pollution before and after the modification. Such a sharp change confirmed the increase in EC and TDS by the deposition and dissolution processes.[27] Through studying the effect of radiation time, it was found that the longer the radiation time, the more free electrons were likely to be generated in the conductor band, which resulted in the enhancing of removal efficiency.

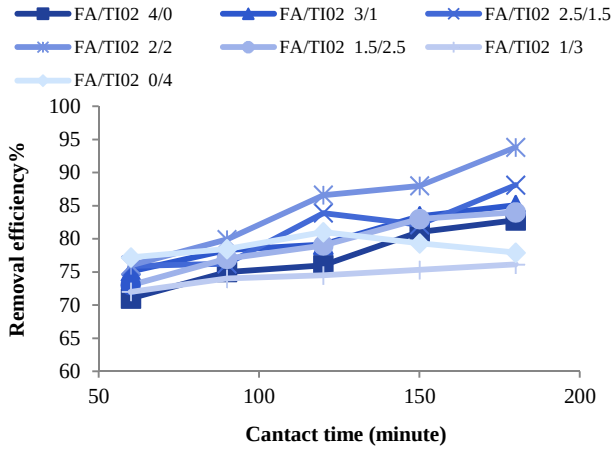

Figure 5. Effect of different FA:TiO_2 ratios on removal efficiency [cyanide: 30 mg/l, unadjusted pH]

Samarghandi et al. argued that increasing the radiation time from 15 minutes to 180 minutes may raise the efficiency of cyanide removal using UV/TiO_2 from 56.4% to 84.4%.[28] Moreover, the results of this research were consistent with those of the studies by Kim et al.[29] and Wahaab et al.[30]

Effect of MFA/TiO2 dosage and pH

Figure 6 shows cyanide removal efficiency for various pH values. Because the substrate surface contains more negative charges, the removal efficiency decreases with the increasing of pH,[28,31] so that higher cyanide removal efficiency was obtained for acidic pH values (herein ranging from 5 to 2). Accordingly, the acidic pH value of 3 was selected as the optimum pH value for further experiments. A statistically significant association was found between pH and removal efficiency (P = 0.001).

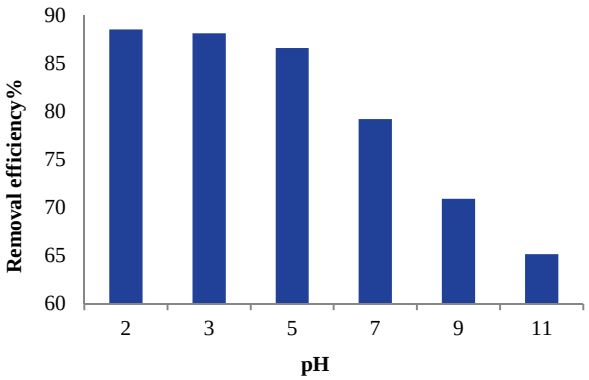

Figure 6. Effect of pH on the removal efficiency of cyanide [cyanide: 30 mg/l, pH: 2-11]

Figure 7 illustrates the effect of MFA/TiO_2 dosage. The presented results show that the removal rate increased with the increasing of composite dosage. However, further increasing of the MFA/TiO_2 ratio from 1.2 to 1.5 g showed a negative effect. Thus, 1.2 g was chosen as the optimum dose. The reduction of removal efficiency by increasing the substrate dose was possibly a result of increased solution turbidity which consequently disrupted the photons' traveling path. In addition, some responses can be effective in this regard, including reduced UV light penetration and total excitation surface.[32] Some authors reported that such an increase can lead to the adhesion of contaminants to the solid photocatalyst surface, and thus, prevent photons from being stimulated.[33] Similar results were reported by Shirzad Syboni et al., who obtained a higher removal effeciency of about 92.45%.[34] In addition, a significant relationship was obtained between the mixed substrate (MFA/TiO_2) dose and removal efficiency (P_v = 0.015).

Under optimal conditions, the influence of initial cyanide concentration was investigated by changing the concentration from 2.5 to 75 mg/l (data not reported), which caused the efficiency to decrease from 98.1 to 64.14%. It is clear that, when the concentration is increased, TiO_2 surface is quickly occupied by cyanide molecules, further inhibiting an effective photon-excitation of the catalyst surfaces.

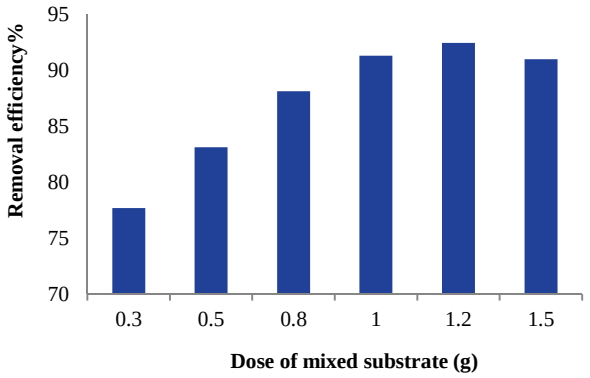

Figure 7. Effect of mixed substrate dose on removal efficiency [cyanide: 30 mg/l, pH: 3]

This may also be due to reduced light penetration due to increased pollutant concentration, as well as the reduced length of the incoming photons into the solution.[33]

High concentrations may degrade the pollutants and produce water-insoluble polymer compounds that attach to the catalyst surface and slow down the photocatalytic degradation.[35] The removal rate data was fitted to the second order kinetics equation and a high

correlation coefficient (R^2) of about 0.999 was determined. The removal efficiency in the real sample (74.4%) was lower than that in the synthetic sample because of the presence of intervening compounds.

Conclusion

In the present study, the adsorption and photocatalytic degradation of cyanide using activated fly ash (AFA) and TiO_2/UV was addressed. Based on the results, the removal efficiency of cyanide by MFA, TiO_2/UV, and their combination (MFA-TiO_2/UV) was about 76.1, 81, and 86.6%, respectively. Under optimum conditions, a maximum removal rate of about 92.4% was obtained. According to the results, it can be concluded that simultaneous adsorption and photocatalytic degradation using MFA-TiO_2/UV can successfully remove cyanide from wastewater.

Conflict of Interests

Authors have no conflict of interests.

Acknowledgements

We sincerely appreciate the financial and instrumental supports of Kurdistan University of Medical Sciences, Iran.

References

1. Dash RR, Gaur A, Balomajumder C. Cyanide in industrial wastewaters and its removal: a review on biotreatment. J Hazard Mater 2009; 163(1): 1-11.
2. Naveen G, Majumder CB, Mondal P, Shubha D. Biological treatment of cyanide containing wastewater. Res J Chem Sci 2011; 1(7): 15-21.
3. Dash RR, Balomajumder C, Kumar A. Removal of cyanide from water and wastewater using granular activated carbon. Chem Eng J 2009; 146(3): 408-13.
4. Shokuhi R, Mahvi A, Bonyadi Z. Efficiency compare of both sonochemical and photosonochemical technologies for cyanide removal from aqueous solutions. Iran J Health Environ 2010; 3(2): 177-84. [In Persian].
5. Baskin SI, Kelly JB, Maliner BI, Rockwood GA, Zoltani CK. Cyanide poisoning. In: Tuorinsky SD, Editor. Medical aspects of chemical warfare. Washington, DC: Walter Reed Army Medical Center; 2008. p. 371-410.
6. Nelson L. Acute cyanide toxicity: mechanisms and manifestations. J Emerg Nurs 2006; 32(4 Suppl): S8-11.
7. Malhotra S, Pandit M, Kapoor JC, Tyag DK. Photo-oxidation of cyanide in aqueous solution by the UV/H_2O_2 process. Journal of Chemical Technology and Biotechnology 2005; 80(1): 13-9.
8. Karunakaran C, Gomathisankar P, Manikandan G. Solar photocatalytic detoxification of cyanide by different forms of TiO_2. Korean J Chem Eng 2011; 28(5): 1214-20.
9. Kim JH, Lee HI. Effect of surface hydroxyl groups of pure TiO_2 and modified TiO_2 on the photocatalytic oxidation of aqueous cyanide. Korean J Chem Eng 2007; 21(1): 116-22.
10. Lu Z, Zhou W, Huo P, Luo Y, He M, Pan J, et al. Performance of a novel TiO_2 photocatalyst based on the magnetic floating fly-ash cenospheres for the purpose of treating waste by waste. Chemical Engineering Journal 2013; 225: 34-42.
11. Wang B, Li C, Pang J, Qing X, Zhai J, Li Q. Novel polypyrrole-sensitized hollow TiO_2/fly ash cenospheres: Synthesis, characterization, and photocatalytic ability under visible light. Appl Surf Sci 2012; 258(24): 9989-96.
12. Salinas-Guzmán R, Guzmán-Mar JL, Hinojosa-Reyes L, Peralta-Hernández JM, Ramírez H. Enhancement of cyanide photocatalytic degradation using sol–gel ZnO sensitized with cobalt phthalocyanine. J Solgel Sci Technol 2010; 54(1): 1-7.
13. Chiang K, Amal R, Tran T. Photocatalytic degradation of cyanide using titanium dioxide modified with copper oxide. Advances in Environmental Research 2002; 6(4): 471-85.
14. Rezaee A, Pourtaghi GH, Khavanin A, Saraf Mamoori R, Hajizadeh E, Valipour F. Elimination of toluene by application of ultraviolet irradiation on TiO_2 Nano particles photocatalyst. J Mil Med 2007; 9(3): 217-22. [In Persian].
15. Low W, Boonamnuayvitaya V. Enhancing the photocatalytic activity of TiO_2 co-doping of graphene–Fe^{3+} ions for formaldehyde removal. J. Environ. Manage 2013; 127: 142-9.
16. Visa M, Andronic L, Lucaci D, Duta A. Concurrent dyes adsorption and photo-degradation on fly ash based substrates. Adsorption 2011; 17(1): 101-8.
17. Shi Z, Yao S, Sui C. Application of fly ash supported

titanium dioxide for phenol photodegradation in aqueous solution. Catal Sci Technol 2011; 1(5): 817-22.
18. Zhang BH, Wu DY, Wang C, He SB, Zhang ZJ, Kong HN. Simultaneous removal of ammonium and phosphate by zeolite synthesized from coal fly ash as influenced by acid treatment. J Environ Sci (China) 2007; 19(5): 540-5.
19. Wang S, Boyjoo Y, Choueib A, Zhu ZH. Removal of dyes from aqueous solution using fly ash and red mud. Water Res 2005; 39(1): 129-38.
20. Li Y, Liu C, Luan Z, Peng X, Zhu C, Chen Z, et al. Phosphate removal from aqueous solutions using raw and activated red mud and fly ash. J Hazard Mater 2006; 137(1): 374-83.
21. Panitchakarn P, Klamrassamee T, Laosiripojana N, Viriya-empikul N, Pavasant P. Synthesis and testing of zeolite from industrial-waste coal fly ash as sorbent for water adsorption from ethanol solution. Engineering Journal 2014; 18(1): 1-12.
22. Wang S, Wu H. Environmental-benign utilisation of fly ash as low-cost adsorbents. J Hazard Mater 2006; 136(3): 482-501.
23. Kashiwakura S, Ohno H, Kumagai Y, Kubo H, Matsubae K, Nagasaka T. Dissolution behavior of selenium from coal fly ash particles for the development of an acid-washing process. Chemosphere 2011; 85(4): 598-602.
24. Kashiwakura S, Ohno H, Matsubae-Yokoyama K, Kumagai Y, Kubo H, Nagasaka T. Removal of arsenic in coal fly ash by acid washing process using dilute H_2SO_4 solvent. J Hazard Mater 2010; 181(1-3): 419-25.
25. Huo P, Yan Y, Li S, Li H, Huang W, Chen S, et al. H_2O_2 modified surface of TiO_2/fly-ash cenospheres and enhanced photocatalytic activity on methylene blue. Desalination 2010; 263(1-3): 258-63.
26. Visa M, Duta A. Methyl-orange and cadmium simultaneous removal using fly ash and photo-Fenton systems. J Hazard Mater 2013; 244-245: 773-9.
27. Visa M, Duta A. Adsorption behavior of cadmium and copper compounds on a mixture FA: TiO_2. Revue Roumaine de Chimie 2010; 55(3): 167-73.
28. Samarghandi M, Siboni M, Maleki A, Jafari S, Nazemi F. Kinetic determination and efficiency of titanium dioxide photocatalytic process in Removal of Reactive Black 5 (RB5) dye and cyanide from aquatic solution. J Mazandaran Univ Med Sci 2011; 21(81): 44-52. [In Persian].
29. Kim HJ, Lu L, Kim JH, Lee CH, Hyeon T, Choi W, et al. UV light induced photocatalytic degradation of cyanides in aqueous solution over modified TiO_2. Bull Korean Chem Soc 2001; 22(12): 1371-4.
30. Wahaab RA, Moawad AK, Taleb EA, Ibrahim H, El-Nazer HA. Combined photocatalytic oxidation and chemical coagulation for cyanide and heavy metals removal from electroplating wastewater. World Appl Sci J 2010; 8(4): 462-9.
31. Joshi K, Patil B, Shirsath D, Shrivastava V. Photocatalytic removal of Ni (II) and Cu (II) by using different Semiconducting materials. Advances in Applied Science Research 2011; 2(3): 445-54.
32. Tu Y, Xiong Y, Tian S, Kong L, Descorme C. Catalytic wet air oxidation of 2-chlorophenol over sewage sludge-derived carbon-based catalysts. J Hazard Mater 2014; 276: 88-96.
33. Ghaneian M, Ehrampoush M, Ghanizadeh G, Dehvary M, Abootoraby M, Jasemizad T. Application of solar irradiation/$K_2S_2O_8$ photochemical oxidation process for the removal of reactive blue 19 dye from aqueous solutions. Iran J Health Environ 2010; 3(2): 165-76. [In Persian].
34. Shirzad Siboni M, Samadi MT, Rahmani A, Khataee A, Bordbar M, Samarghandi M. Photocatalytic removal of hexavalet chromium and divalent nickel from aqueous solution by UV irradiation in the presence of titanium dioxide vanoparticles. Iran J Health Environ 2010; 3(3): 261-70. [In Persian].
35. Hemmati Borji S, Nasseri S, Nabizadeh Nodehi R, Mahvi A, Javadi A. Photocatalytic degradation of phenol in aqueous solutions by Fe (III)-doped TiO_2/UV process. Iran J Health Environ 2011; 3(4): 369-80. [In Persian].

JAEHR Journal of Advances in Environmental Health Research

Photocatalytic degradation of phenol in water solutions using ZnO nanoparticles immobilized on glass

Sedigheh Saeedi[1], Hatam Godini[2], Mohammad Almasian[3], Ghodratollah Shams-Khorramabadi[1], Bahram Kamarehie[1], Parvin Mostafaie[1], Fatemeh Taheri[1]

1 Department of Environmental Health Engineering, School of Health, Lorestan University of Medical Sciences, Khorramabad, Iran
2 Department of Environmental Health Engineering, School of Health, Alborz University of Medical Sciences, Karaj, Iran
3 Department of English Language, School of Medicine, Lorestan University of Medical Sciences, Khorramabad, Iran

Original Article

Abstract

Phenol and its derivatives are pollutant compounds that are present in the wastewater of many industries. The objective of this study was to investigate the photocatalytic degradation of phenol in water containing various concentrations of sodium chloride. A laboratory study was conducted to evaluate the performance of UV/ZnO process on the efficiency of phenol removal from saline water with ZnO nanoparticles fixed on glass using UVC radiation. The effects of pH, contact time, sodium chloride concentrations, and the initial concentration of phenol on the photocatalytic removal of phenol were studied. The photocatalytic degradation of phenol showed suitable efficiency under the absence of sodium chloride (100% phenol removal at a concentration of 5 mg/l and during 120 minutes). However, the removal efficiency decreased in the presence of a concentration of 30 g/l of sodium chloride (92.4%). Additionally, phenol photocatalytic degradation efficiency decreased as a result of an increase in the initial concentration of phenol and the efficiency increased as a result of a decrease in pH (pH = 3). The results obtained from this study indicated that ZnO nanoparticles or ultraviolet rays alone cannot remove phenol fully and have a much lower efficiency in comparison with the photocatalytic degradation of phenol. Thus, the photocatalytic degradation process (UV/ZnO) is an effective method of removing phenol from saline water solutions.

KEYWORDS: Degradation, Phenol, Water Pollution, Nanoparticles

Date of submission: 17 Apr 2015, ***Date of acceptance:*** 22 Jun 2015

Citation: Saeedi S, Godini H, Almasian M, Shams-Khorramabadi Gh, Kamarehie B, Mostafaie P, et al. **photocatalytic degradation of phenol in water solutions using ZnO nanoparticles immobilized on glass.** J Adv Environ Health Res 2015; 3(3): 204-13.

Introduction

Most industrial wastewaters have high concentrations of salt and dangerous organic pollutants. Different industries including petroleum refineries, petrochemical plants, olive oil production, pesticide production, and textile, leather, food, and agricultural industries produce phenolic wastewaters.[1,2] Aromatic pollutants, especially phenol and its derivatives, are frequently found in the environment due to their widespread use.[3] Phenol is a cyclic hydrocarbon which is colorless in pure form and is highly soluble in water, and therefore, it is likely to be present in water sources. Due to their distinct properties, including toxicity, effect on the flavor and odor of water, and adverse effects on human health and living creatures, phenolic compounds are

Corresponding Author:
Hatam Godini
Email: godini_h@yahoo.com

classified as priority pollutants by the US Environmental Protection Agency (USEPA).[4,5] Phenol is quickly absorbed through the skin and can lead to skin and eye burns upon contact. Excessive contact with phenol can lead to coma, seizures, cyanosis, and death.[6] Due to the high toxicity of phenolic compounds, EPA has recommended the permissible level of 1 mg/l in effluents to be released into the environment.[7] Additionally, the World Health Organization (WHO) has considered a concentration of 0.001 mg/l of phenolic compounds in drinking water as the maximum permissible concentration.[8] Biological treatment, extraction from solution, reverse osmosis, chemical oxidation, and electrochemical methods are the most important methods of removal of phenol and phenolic compounds from saline wastewaters. High costs, low efficiency, and the generation of dangerous and toxic byproducts are among the factors which limit the use of some of these methods of removal.[9]

Recently, another technique called advanced oxidation has been used for the removal of contaminants which involves the generation of very strong oxidation agents such as hydroxyl radicals.[10] The photocatalytic degradation process is considered as a novel treatment method, because the catalyst can be easily activated under normal temperature and pressure.[11] This method is a possible technique for the removal of organic and non-organic pollutants from the air and water.[12] In photocatalytic degradation, pollutants are degraded under the radiation of UV rays and in the presence of metal oxide particles like ZnO and TiO_2.[13] One of the advantages of ZnO over TiO_2 is that ZnO can absorb the higher ultraviolet (UV) spectrum, and this is due to the absorption threshold of this compound which is at the 425 nm wavelength.[14] Additionally, ZnO is less toxic, is cheaper, and in some cases it is more active than TiO_2.[15]

Many researchers have studied the removal of various refractory organic pollutants using photocatalytic processes. However, few articles have investigated the efficiency of this technique in saline environments. In a study on the photocatalytic degradation of phenol via UV/TiO_2 in solutions with various salt concentrations, Azevedo et al. were able to obtain a removal efficiency of 90% for a phenol concentration of 50 mg/l and a pH of 7.[16] In a study on the photocatalytic degradation (UV/TiO_2) of humic acid in saline water, Al-Rasheed and Cardin reported that the rate of photocatalytic degradation of humic acid was slower in water with high salinity (46 g/l) in comparison with water with low salinity (2.7 mg/l).[17] Kashif and Ouyang studied the inhibitory effects of some anions on the photocatalytic degradation of phenol.[18] The results of their study showed that chloride ions have a negative effect on the process. In an investigation of the effect of various concentrations of sodium chloride, sulfate, and nitrate on the photocatalytic degradation of 2-phenylphenol, Khodja et al. concluded that these anions have highly negative effects on the degradation of this pollutant.[19]

Due to the higher capability of ZnO in the absorption of the UV spectrum in comparison with TiO_2, ZnO nanoparticles were used in the present study. Additionally, given the difficulty of separating the nanoparticles during their use in the form of a suspension and the need for special equipment for their filtration from the solution, photocatalysts fixed on glass, which are completely neutral substances, were used in the present study.

The objective of this research was to study the performance of the photocatalytic UV/ZnO process in the removal of phenol in four saline concentrations (0, 10, 20, and 30 g/l), taking into account the effects of other parameters such as solution pH, initial concentration of phenol, and contact time.

Materials and Methods

This research was discontinuously conducted

on a laboratory scale in a plexiglass reactor with a capacity of 1 l. This reactor consists of two segments. The first segment functioned as a media on which ZnO fixed on glass and the solution containing the pollutant (a combination of various concentrations of phenol and NaCl) were placed. The second segment functioned as the cover of the reactor which allowed 5 lamps to be installed on its walls. UV_c lamps and their electrical transformers were placed in a wooden case in the cover segment with a distance of 1 cm from the reactor media in order to prevent the dissemination of the rays into the environment. This reactor has an entry orifice and an exit orifice which are situated on its two sides and the entry orifice is lower than the exit orifice. The entry and exit orifices are connected by a special tube to a peristaltic pump with a maximum rotational speed of 120 rpm so that complete mixing occurs inside the reactor. Figure 1 shows a diagram and figure of this reactor.

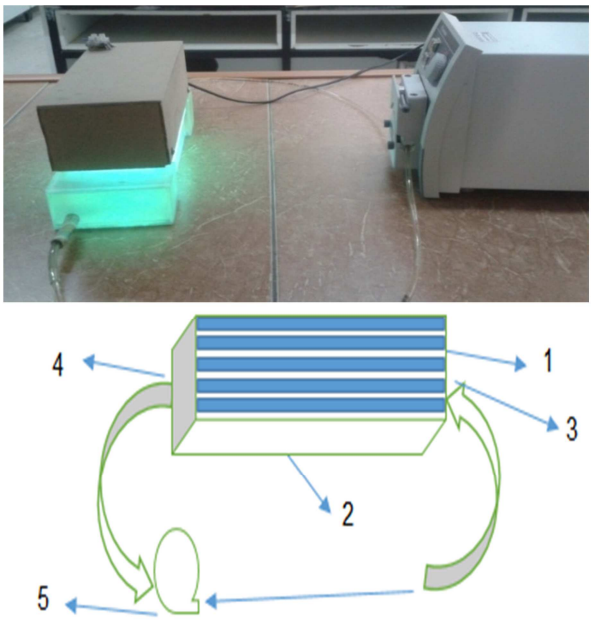

Figure 1. A figure and diagram of the noncontinuous rotational reactor

1. The reactor cover and the lamps attached to it; 2. The glass bed containing fixed zinc oxide nanoparticles; 3. Entry orifice; 4. Exit orifice; and 5. Peristaltic pump

To fix ZnO nanoparticles, the thermal fixing method was used.[20] First, sandblasted glass surfaces suited to the size of the reactor were prepared. Then, the pieces of glass were placed in a 50% solution of sodium hydroxide for 24 hours. After removal from the solution, they were washed with distilled and tap water. In the next stage, a 3% suspension of ZnO nanoparticles was prepared and mixed using a shaker (Behdad Co., Iran) for half an hour. Moreover, to distribute the ZnO nanoparticles homogeneously in the solution, it was placed in an ultrasonic bath (SONER 203 H, Rocker Scientific Co., Taiwan) machine with a frequency of 50 KHz under the influence of ultrasonic waves. Then, 5 cc of this suspension in which the nanoparticles were completely separated was spread evenly on each piece of glass, each of which had been dried and weighed. The pieces of glass were placed in a hot air oven (DSL 60, Texcare Instrument Co., India) at a temperature of 40 to 50 ^{o}C for 6 hours so that they would dry slowly. Then, the temperature of the hot air oven was raised to 110 ^{o}C for one hour, and in the final stage, the pieces of glass were placed in an electric furnace (FT 1200, Meta Therm Furnace Pvt. Ltd., India) at a temperature of 450 ^{o}C for 1 hour.[20] Ultimately, to set aside the pieces of glass on which nanoparticles were poorly fixed and were not stable enough, they were rinsed with distilled water along the reactor flow.

In the present study, phenol with a purity of 99% was purchased from Merck & Co., Germany. ZnO nanoparticles with laboratory level purity were purchased from the British DPH Company. X-ray diffraction (XRD) tests were performed using a Philips PNA analytical diffractometer and scanning electron microscope (SEM) equipped with an energy-dispersive X-ray spectroscopy (EDX) system using Seron AIS2300C on the nanoparticles powder and on the nanoparticles fixed on the glass. All chemicals used in this study including chloridric acid and sodium

hydroxide (used to adjust the pH), sodium chloride (for the preparation of the saline solution), and the reagents used in the colorimetry of phenol including potassium ferricyanide, phosphate buffer, and ammonium hydroxide were bought from Merck & Co. Other equipment used in this study included 5 ultraviolet 6 watt lamps (Philips), UV meter (UVc-254, Luetern, Germany), pH meter (Hana-211, Germany), UV/vis spectrophotometer (2100 Unico, US), and peristaltic pump (Heidolph pump drive 5001, Germany).

First, a stock phenol solution (1 g phenol in 1000 cc distilled water) was prepared. Next, in order to produce the calibration curve, various concentrations were prepared from this solution. Additionally, in later stages of the experiment, the same solution was used to prepare the desired samples of phenol with the concentrations required for the experiments via dilution with distilled water. To determine the concentration of phenol in unknown and standard samples, the direct colorimetry method was used with 4-aminoantpyrine as the reagent at a wave length of 500 nanometers, using the 5530D colorimetry method as presented in the standard methods for the examination of water and wastewater.[21] To make the concentration of phenol in the studied samples similar to the amount found in industrial wastewaters, the phenol solutions were prepared in five concentrations of 5, 10, 20, 40, and 80 mg/l. Moreover, four concentrations of sodium chloride (0, 10, 20, and 30 g/l) were mixed with various concentrations of phenol to obtain saline wastewater. To determine the optimum pH in photocatalytic degradation, the experiments were carried out in five amounts of pH (i.e., 3, 5, 7, 9, and 11). To adjust the pH, 0.1 normal hydrochloridric acid and sodium hydroxide solutions were used. During each process and at time intervals of 30, 60, 90, 120, 150, and 180 minutes, samples were taken from the solution content of the reactor. It is also necessary to state that after each stage of the experiments, the used glass surfaces were heated at a temperature of 450 ^{o}C in the furnace to reactivate them and make sure that the performance of the fixed nanoparticles was acceptable. To compare the results, the samples were exposed to UV rays alone, ZnO nanoparticles alone, or both UV rays and ZnO nanoparticles in separate stages. It should also be mentioned that all experiments were carried out at laboratory temperatures. All experiments were conducted in triplicate.

To analyze the data, repeated measures model and longitudinal models (generalized linear models) were used in SPSS software (version 21, SPSS Inc., Chicago, IL, USA).

Results and Discussion

The X-ray diffraction result of ZnO nanoparticles used in the present research is presented in Figure 2. In figures 3 and 4, the nanoparticles fixed on glass surfaces, and the physical properties, size, degree of purity, and the composition of the particles are illustrated.

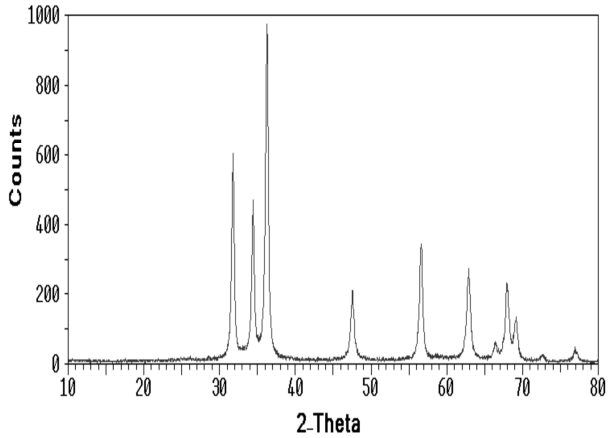

Figure 2. X-ray diffraction results of ZnO nanoparticles

The results obtained from XRD patterns indicate that the ZnO nanoparticles used had a hexagonal structure and were of a high degree of purity. Additionally, sharp peaks indicate

good crystallization of the ZnO nanoparticles. The results obtained from SEM micrographs also showed that the size of the ZnO nanoparticles used in this study was less than 100 nm. Furthermore, after fixing them on glass, porosity rates remained at a desirable level and the dimensions of the nanoparticles was still at the nano level. In addition, considering the EDX spectrum, only ZnO nanoparticles could be observed on the glass surfaces and there were no other impurities.

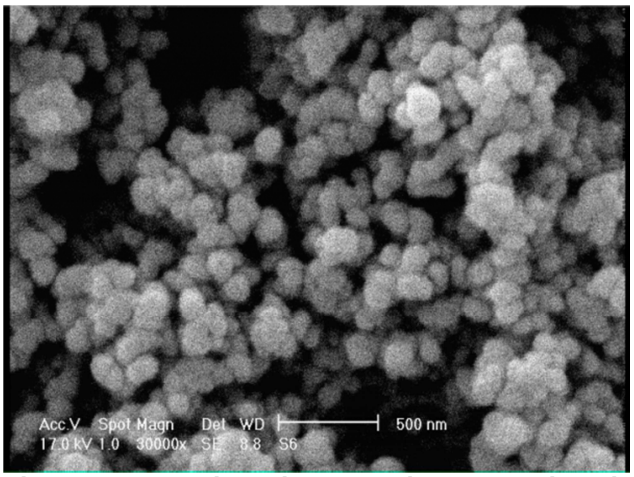

Figure 3. Scanning electron microscope (SEM) micrograph of ZnO nanoparticles fixed on glass with a magnitude of 30000

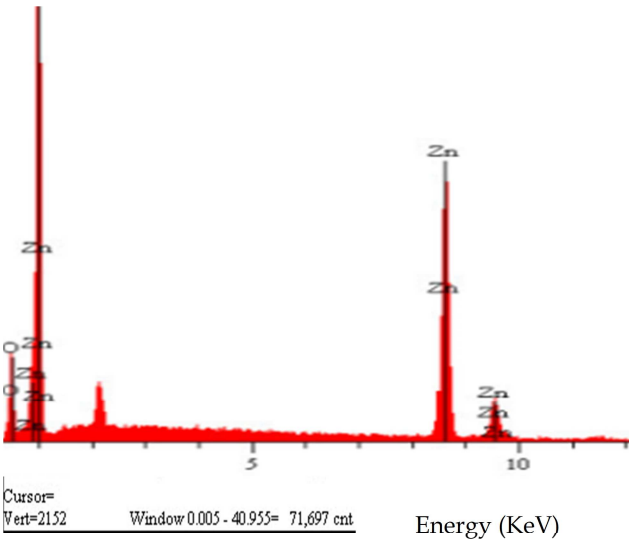

Figure 4. The results of X-ray spectroscopy (EDX) analysis of ZnO nanoparticles fixed on glass

The results of the adsorption of phenol on the surface of ZnO nanoparticles are presented in figure 5. In this figure, it can be observed that the adsorption of phenol on the surface of the nanoparticles is negligible if compared with the photocatalytic degradation of phenol in the UV/ZnO process. A survey of the effect of the separate contact of the synthetic wastewater containing the pollutant with ZnO nanoparticles, as shown in figure 5, showed that phenol removal rates were negligible after 180 minutes of contact time. Gaya et al., in a study on the effect of ZnO alone on the removal of 4-chlorophenol with a concentration of 50 mg/l, observed no considerable change in the concentration of the pollutant after 300 minutes.[22]

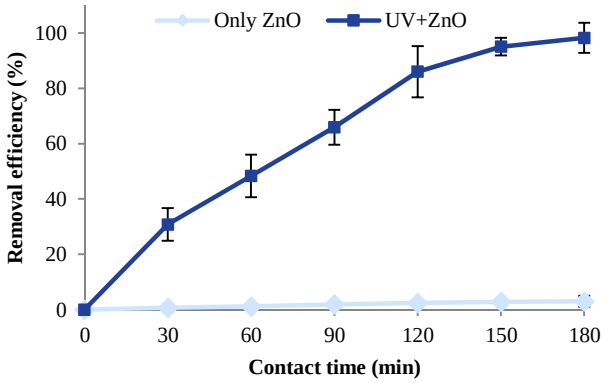

Figure 5. Comparison of the efficiency of ZnO nanoparticles alone and the UV/ZnO process in the removal of phenol (pH = 3, Phenol = 20 mg/l, and NaCl = 10 g/l)

The results of the effect of UV radiation alone on the removal of phenol are presented in figure 6 (A and B). Results show that although the use of UV rays alone can be effective in the removal of lower concentrations of phenol, in higher concentrations, the removal efficiency is reduced considerably. Moreover, it is less effective in comparison with the photocatalytic process of UV/ZnO. Phenol removal efficiency was higher at the lowest studied concentration (5 mg/l), but, at higher concentrations (80 mg/l), the removal

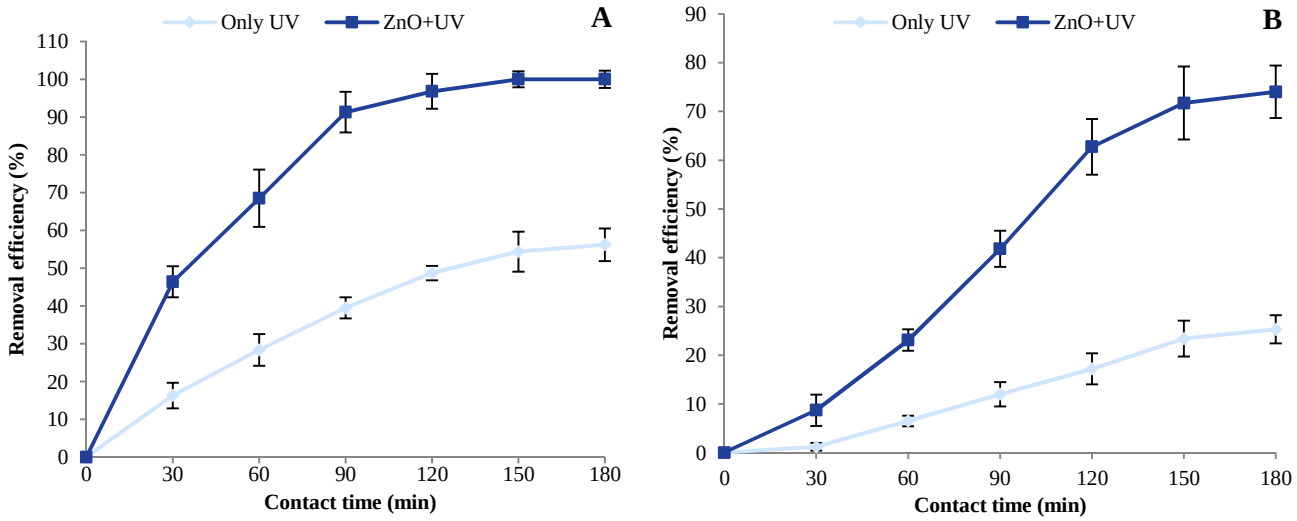

Figure 6. Comparison of the use of UV rays alone and the UV/ZnO process in the removal of phenol (pH = 3, NaCl = 10 g/l, radiation intensity = 3950 µw/cm^2, and (a) C_{phenol} = 5 mg/l, (b) C_{phenol} = 80 mg/l)

efficiency decreased because not enough hydroxyl radicals (the main factor for pollutant degradation) were generated.[23] Given the above-mentioned issues, it can be said that the use of these processes alone is not highly effective in the removal of phenol. Thus, it is necessary to modify the process and use the nano-photocatalytic process UV/ZnO in order to achieve higher removal efficiencies.

The results obtained from the study of the effects of pH variation in the UV/ZnO process with 5 amounts of pH are presented in figure 7. As seen in figure 7, the phenol removal efficiency was higher under acidic conditions than under basic conditions; the highest removal efficiency for the studied concentrations of phenol was at pH of 3 (90.2%) and the lowest removal efficiency was at pH of 11 (71.3%).

Two reasons can be mentioned for this phenomenon. The first reason may be the fact that higher numbers of H^+ ions are present in the acidic environment which leads to the formation of $H^\cdot$ radicals which also form $HO_2^\cdot$ radicals with the oxygen present in the solution, which finally convert to $OH^\cdot$ radicals.[23] Electrostatic reactions between phenol and the surface of the catalyst are known as another factor affecting the pH. This phenomenon can be explained by the surface properties of ZnO.

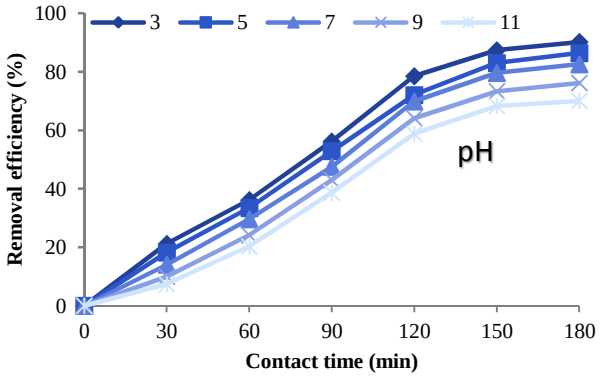

Figure 7. The effect of pH on the removal of phenol in the UV/ZnO process (the initial concentration of phenol = 40 mg/l, NaCl = 10 g/l, and radiation intensiy = 3950 µw/cm^2)

In this study, the pH_{zpc} (point of zero charge) of the ZnO nanoparticles was about 8.60. At pH levels higher than this, the surface charge of the ZnO nanoparticles was negative, while at pH levels lower than this, the particles had a positive surface charge.[24] Many ionic compounds like phenols have negative charges (anionic compounds) which can be easily attracted to the surface of ZnO particles at pH

levels less than pH_{zpc}. However, at pH levels higher than pH_{zpc}, ZnO nanoparticles repel each other because they have negative charges.[25] The results obtained from the statistical analysis also showed that the difference in the mean phenol removal rates was significant at various pH levels (P< 0.001). In their investigation of the effect of pH (2.5 to 12.5) on the removal of phenol and benzoic acid using the UV/ZnO photocatalytic process, Mrowetz and Selli reported that the highest removal efficiency was obtained at the pH of 2.5.[26]

The results of the phenol removal efficiency at various concentrations of sodium chloride (0, 10, 20, 30 g/l) are shown in figure 8. As can be seen in figure 8, an increase in the concentration of sodium chloride (NaCl) leads to a reduction in the removal efficiency. The highest removal efficiency (92.4%) was obtained in the absence of sodium chloride, and the lowest removal efficiency (81.12%) was obtained for the 30 g/l concentration of sodium chloride at the same contact time (180 minutes).

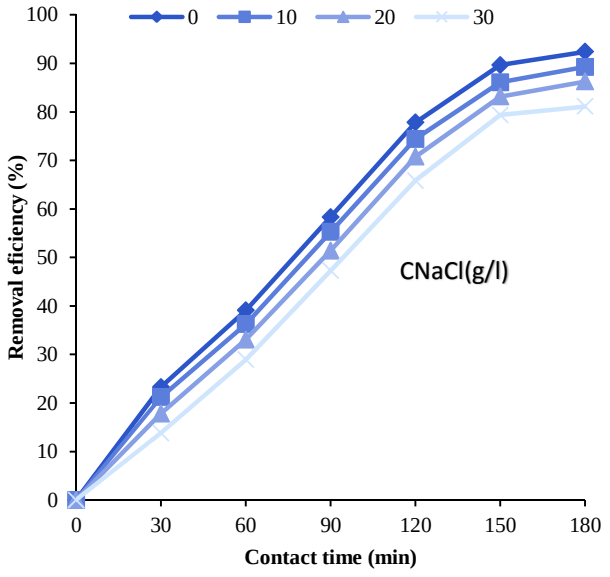

Figure 8. The effect of various concentrations of sodium chloride on the removal of phenol in the UV/ZnO process (pH = 3, phenol = 40 mg/l, and radiation intensity = 3950 µw/cm^2)

Regarding the negative effect of the various concentrations of NaCl on the photocatalytic degradation of phenol and the reduction of removal efficiency with the increase in saline concentration (NaCl) in the studied solution (Figure 8), it can be said that the reduction in the efficiency of the process can be attributed to the presence of chloride ions, because chloride ions are able to adsorb hydroxyl radicals.[27] Additionally, it seems that the inhibitory effect of sodium chloride is due to the joining of the chloride ions to electrons and optical cavities. The chloride ions, which have been adsorbed to these cavities and have been oxidized, are converted to chlorine atoms, and then, again are reduced as chloride ions by the electrons.[16] The results obtained from the repeated measures model statistical analysis also indicated a significant difference in the mean phenol removal efficiency at various NaCl concentrations (P = 0.004). Moreover, the results suggest that sodium chloride has a negative effect on the oxidation of phenol. Papadam et al.[28] and LAmour et al.[29] obtained similar results in their studies.

The study of the effect of initial concentration of phenol on photocatalytic degradation (for the optimum pH obtained in the previous stage) has shown that as the initial concentration of phenol increased, the photocatalytic degradation rates decrease (Figure 9).

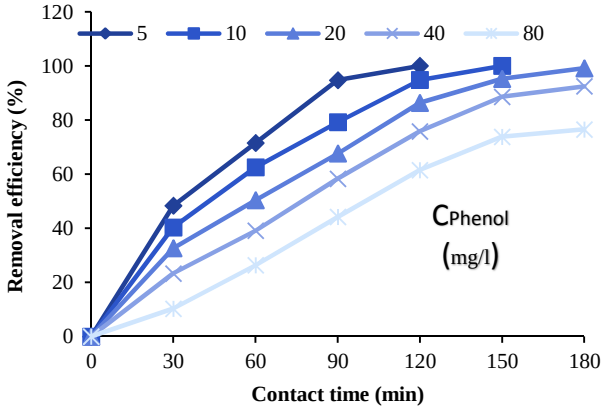

Figure 9. The effect of the initial concentration of phenol and contact time on the removal of phenol in the UV/ZnO process (pH = 3, and radiation intensity = 3950 µw/cm^2)

Therefore, removal efficiency has an inverse relationship with the initial concentration of phenol. Additionally, the time needed to achieve a desirable removal efficiency increased as the initial concentration of phenol was raised. After 120 minutes and at an acidic pH, the highest removal efficiency (100%) was achieved at the lowest concentration (5 mg/l), and the lowest removal rate at a concentration of 80 mg/l and a contact time of 180 minutes was 76.5%.

In investigating the effect of the initial concentration of phenol and contact time on photocatalytic degradation, as can be seen in figure 9, as the initial concentration of phenol increased, the photocatalytic degradation rates decreased. In explaining this issue, it can be stated that, in the photocatalytic process, as a result of the increase in the amount of influent pollutant, the likelihood of collision of the pollutant particles with the oxidizing agent (i.e., hydroxyl) is reduced, which leads to a reduction in the efficiency of the removal system at higher concentrations. Another reason for this issue is the generation of byproducts which are more reactive than phenol and which react with the present radicals or are adsorbed onto the surface of the photocatalyst; therefore, these byproducts compete with phenol in adsorption onto active sites on the ZnO surface and in reacting with hydroxyl radicals.[26,30] The results obtained from statistical analysis have demonstrated the significant difference between mean phenol removal efficiencies at its various concentrations ($P < 0.001$). Pardeshi and Patil[31] and Chiou et al.[32] have also reached similar results in their studies. Moreover, Zamankhan et al.[33], in a study on the removal of phenol using the photocatalytic method and ZnO nanoparticles, concluded that an increase in contact time leads to an increase in the removal efficiency of phenol.

Kinetics results of phenol removal through the photocatalytic process are shown in figure 10. Two models, the pseudo-first-order and the pseudo-second-order, were used to determine a possible mechanism involved in the degradation. The R^2 for pseudo-first-order kinetics ($R^2 = 0.93$) was higher than the pseudo-second-order ($R^2 = 0.75$).

The removal of phenol in the UV/ZnO process fit the pseudo-first-order reaction patterns well ($R^2 = 0.93$). The photocatalytic oxidation kinetics of many organic compounds have often been modeled with the Langmuir–Hinshelwood equation, which also covers the adsorption properties of the substrate on the photocatalyst surface.[14] The results of this study are in agreement with that of the studies by Behnajady et al.[14] and Alalm and Tawfik [34]

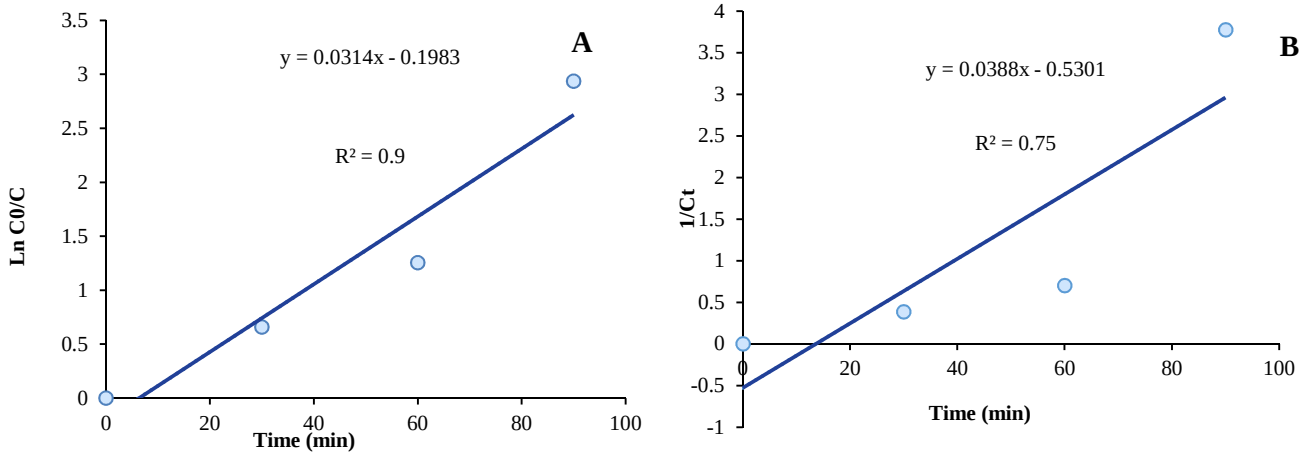

Figure 10. Phenol removal kinetics in the UV/ZnO process: (A) the pseudo-first-order and (B) the pseudo-second-order (pH = 3, retention time = 90 minutes, and phenol concentration = 5 mg/l)

Conclusion

In this study, the removal of phenol from saline wastewaters using the UV/ZnO photocatalytic process was investigated. In general, the results obtained from this study show that the use of the UV/ZnO process even in wastewaters containing anions like chloride, which is a scavenger of hydroxyl radicals and has an inhibitory effect on the process, was an effective method in removing phenol. However, at higher concentrations of sodium chloride (30 g/l), the time needed for achieving the desirable treatment levels increased. Additionally, ZnO nanoparticles alone or UV rays alone have a lower efficiency in the removal of phenol in comparison with the UV/ZnO photocatalytic process.

Conflict of Interests

Authors have no conflict of interests.

Acknowledgements

We would like to extend our gratitude to the experts and people in charge of the research laboratories of the School of Health and the Razi Herbal Medicines Research Center of the Lorestan University of Medical Sciences, Iran.

References

1. Juang RS, Huang WC, Hsu YH. Treatment of phenol in synthetic saline wastewater by solvent extraction and two-phase membrane biodegradation. J Hazard Mater 2009; 164(1): 46-52.
2. Moussavi G, Khavanin A, Alizadeh R. The investigation of catalytic ozonation and integrated catalytic ozonation/biological processes for the removal of phenol from saline wastewaters. J Hazard Mater 2009; 171(1-3): 175-81.
3. Martinkova L, Kotik M, Markova E, Homolka L. Biodegradation of phenolic compounds by Basidiomycota and its phenol oxidases: A review. Chemosphere 2016; 149: 373-82.
4. Sen BK, Deshmukh DK, Deb MK, Verma D, Pal J. Removal of phenolic compounds from aqueous phase by adsorption onto polymer supported iron nanoparticles. Bull Environ Contam Toxicol 2014; 93(5): 549-54.
5. Vlastos D, Antonopoulou M, Konstantinou I. Evaluation of toxicity and genotoxicity of 2-chlorophenol on bacteria, fish and human cells. Sci Total Environ 2016; 551-552: 649-55.
6. Busca G, Berardinelli S, Resini C, Arrighi L. Technologies for the removal of phenol from fluid streams: a short review of recent developments. J Hazard Mater 2008; 160(2-3): 265-88.
7. Balasubramanian A, Venkatesan S. Removal of phenolic compounds from aqueous solutions by emulsion liquid membrane containing Ionic Liquid [BMIM]+[PF6] in Tributyl phosphate. Desalination 2012; 289: 27-34.
8. Mukherjee S, Kumar S, Misra AK, Fan M. Removal of phenols from water environment by activated carbon, bagasse ash and wood charcoal. Chemical Engineering Journal 2007; 129(1-3): 133-42.
9. Bazrafshan E, Amirian P, Mahvi AH, Ansari-Moghaddam A. Application of adsorption process for phenolic compounds removal from aqueous environments: a systematic review. Global NEST Journal 2016; 18(1): 146-63.
10. Carra I, Sanchez Perez JA, Malato S, Autin O, Jefferson B, Jarvis P. Performance of different advanced oxidation processes for tertiary wastewater treatment to remove the pesticide acetamiprid. J Chem Technol Biotechnol 2016; 91(1): 72-81.
11. Lee KM, Lai CW, Ngai KS, Juan JC. Recent developments of zinc oxide based photocatalyst in water treatment technology: A review. Water Research 2016; 88: 428-48.
12. Xu Yh, Liang Dh, Liu Ml, Liu Dz. Preparation and characterization of Cu2O TiO2: Efficient photocatalytic degradation of methylene blue. Materials Research Bulletin 2008; 43(12): 3474-82.
13. Eydivand S, Nikazar M. Degradation of 1,2-dichloroethane in simulated wastewater solution: a comprehensive study by photocatalysis using Tio_2 and Zno nanoparticles. Chem Eng Commun 2015; 202(2): 102-11.
14. Behnajady MA, Modirshahla N, Hamzavi R. Kinetic study on photocatalytic degradation of C.I. Acid Yellow 23 by ZnO photocatalyst. J Hazard Mater 2006; 133(1-3): 226-32.
15. Sobana N, Swaminathan M. Combination effect of ZnO and activated carbon for solar assisted photocatalytic degradation of Direct Blue 53. Solar Energy Materials and Solar Cells 2007; 91(8): 727-34.
16. Azevedo EB, de Aquino Neto FR, Dezotti M. TiO2-photocatalyzed degradation of phenol in saline media: lumped kinetics, intermediates, and acute toxicity. Applied Catalysis B: Environmental 2004; 54(3): 165-73.
17. Al-Rasheed R, Cardin DJ. Photocatalytic degradation

of humic acid in saline waters. Part 1. Artificial seawater: influence of TiO_2, temperature, pH, and air-flow. Chemosphere 2003; 51(9): 925-33.
18. Kashif N, Ouyang F. Parameters effect on heterogeneous photocatalysed degradation of phenol in aqueous dispersion of TiO2. J Environ Sci (China) 2009; 21(4): 527-33.
19. Khodja AA, Sehili T, Pilichowski JF, Boule P. Photocatalytic degradation of 2-phenylphenol on TiO2 and ZnO in aqueous suspensions. Journal of Photochemistry and Photobiology A: Chemistry 2001; 141(2-3): 231-9.
20. Masoumbeigi H, Rezaee A, Khataee A, Hashemian SH. Effect of UV radiation intensity on photocatalytic removal of E. coli using immobilized ZnO nanoparticles. Trauma Mon 2009; 14(3): 149-53.
21. Eaton AD, Franson MA. Standard Methods for the Examination of Water & Wastewater. Washington, DC: American Public Health Association; 2005.
22. Gaya UI, Abdullah AH, Zainal Z, Hussein MZ. Photocatalytic treatment of 4-chlorophenol in aqueous ZnO suspensions: intermediates, influence of dosage and inorganic anions. J Hazard Mater 2009; 168(1): 57-63.
23. Hemmati Borji S, Nasseri S, Nabizadeh Nodehi R, Mahvi A, Javadi A. Photocatalytic degradation of phenol in Aqueous Solutions by Fe(III)-doped TiO2/UV Process. Iran J Health Environ 2011; 3(4): 369-80.
24. Wang J, Jiang Z, Zhang Z, Xie Y, Wang X, Xing Z, et al. Sonocatalytic degradation of acid red B and rhodamine B catalyzed by nano-sized ZnO powder under ultrasonic irradiation. Ultrason Sonochem 2008; 15(5): 768-74.
25. Benhebal H, Chaib M, Salmon T, Geens J, Leonard A, Lambert SD, et al. Photocatalytic degradation of phenol and benzoic acid using zinc oxide powders prepared by the solgel process. Alexandria Engineering Journal 2013; 52(3): 517-23.
26. Mrowetz M, Selli E. Photocatalytic degradation of formic and benzoic acids and hydrogen peroxide evolution in TiO_2 and ZnO water suspensions. Journal of Photochemistry and Photobiology A: Chemistry 2006; 180(1-2): 15-22.
27. Maciel R, Sant'Anna GL, Dezotti M. Phenol removal from high salinity effluents using Fenton's reagent and photo-Fenton reactions. Chemosphere 2004; 57(7): 711-9.
28. Papadam T, Xekoukoulotakis NP, Poulios I, Mantzavinos D. Photocatalytic transformation of acid orange 20 and Cr(VI) in aqueous TiO_2 suspensions. Journal of Photochemistry and Photobiology A: Chemistry 2007; 186(2-3): 308-15.
29. LAmour RJA, Azevedo EB, Leite SGF, Dezotti M. Removal of phenol in high salinity media by a hybrid process (activated sludge + photocatalysis). Separation and Purification Technology 2008; 60(2): 142-6.
30. Parida KM, Dash SS, Das DP. Physico-chemical characterization and photocatalytic activity of zinc oxide prepared by various methods. J Colloid Interface Sci 2006; 298(2): 787-93.
31. Pardeshi SK, Patil AB. A simple route for photocatalytic degradation of phenol in aqueous zinc oxide suspension using solar energy. Solar Energy 2008; 82(8): 700-5.
32. Chiou CH, Wu CY, Juang RS. Photocatalytic degradation of phenol and m-nitrophenol using irradiated TiO2 in aqueous solutions. Separation and Purification Technology 2008; 62(3): 559-64.
33. Zamankhan H, Ayati B, Ganjidoust H. Photocatalytic Degradation of Phenol by Immobilized Nano ZnO on Concrete Surface. Iranian Journal of Chemistry & Chemical Engineering 2012; 31(3-4): 9-20.
34. Alalm MG, Tawfik A. Solar Photocatalytic Degradation of Phenol in Aqueous Solutions Using Titanium Dioxide. International Journal of Chemical, Molecular, Nuclear, Materials and Metallurgical Engineering 2014; 8(2): 136-9.